ISSN 1340－9662

日本医科大学

先端医学研究所紀要

第１巻 平成27年度

Institute for Advanced Medical Sciences
Nippon Medical School
Year Book

Vol. 1 (2015)

日本医科大学

先端医学研究所紀要

第１巻 平成２７年度

Institute for Advanced Medical Sciences
Nippon Medical School
Year Book

Vol. 1 (2015)

平成27年５月14日　中庭にて

目　　次

紀要第１巻の発刊によせて

所長　南　　史朗

先端医学研究所紀要第１巻をお送り申し上げます。本紀要は、平成 27 年度の本研究所の研究業績を中心にまとめたものです。

平成 27 年 4 月 1 日より、老人病研究所から名称を変更し、「先端医学研究所」となりました。

当研究所は、1954 年に老年医学の研究施設として発足しました。その後、時代とともに内容も変遷し、発生から老化までの加齢科学の研究をはじめ、分子・細胞レベルから個体に至る生命科学の研究へと発展してきました。最近の医学研究の進歩に伴い、病態が細胞・分子レベルで解析されるようになり、疾病の治療も対症療法から根本治療へと変わりつつあります。医学研究のめざましい発展と技術革新を背景に、2015 年 4 月に歴史ある老人病研究所を改組するとともに、名称を先端医学研究所としました。医学博士課程を担当する 5 つの分野を含む 6 つの部門によって構成されています。本研究所の基本テーマを「細胞代謝 Cellular metabolism」とし、部門の枠を超え、互いに協力して、医学の広い領域にわたる研究を遂行してゆく体制を作りました。

医学研究の進歩がめざましい今日、研究所の機能強化と社会のニーズに答えることを目的とし、「自由な研究活動の場」、開かれたラボとして広範な医学研究ができるようにしてゆく所存です。また、病院と一体化した研究所の特徴を生かし、研究の成果がきっと臨床に還元できるように、トランスレーショナル研究を推進するように、研究所員ともども努力してゆきたいと思います。

皆様のご指導、ご鞭撻をお願い申し上げます。

Ⅰ．病態解析学部門

Department of Molecular Pathophysiology

病態解析学部門
（大学院　分子細胞構造学部門）

【研究概要】

老人病研究所病理部門では、１）ケロイド発生機序の研究、２）血管形成メカニズムの解析など、形態に主眼をおいた特色のある研究を行っている。

１）ケロイド発生機序の研究

武蔵小杉病院形成外科と無瘢痕創傷を目的に肥厚性瘢痕とケロイド発生の解析を行っている。これまでケロイド発生に関与する遺伝子解析で IL－6 及び c－Abl 遺伝子の発現上昇を見いだし IL－6 シグナルのケロイド発生への関与を明らかにした。ケロイドでは TGF－ß や PDGF が過剰発現を示すことからこれらのシグナル伝達を同時に抑制する小分子標的治療薬 STI571 のケロイド線維芽細胞への投与によるプロコラーゲン産生とタイプⅠコラーゲン mRNA の発現の低下を目的にケロイド新薬としての可能性の解析を進めている。さらに、TGF－ß と PDGF シグナル伝達の抑制に関与する microRNA 遺伝子を解析しケロイド線維化調節に関わる COLIA2 プロモーターに関する研究にも着手している。

２）血管形成メカニズムの解析

血管の構築メカニズムは未だ不明な点が多い。特に血管の形態は多様性に富んでおり、大動脈から毛細血管まで様々なものが存在する。我々はこれらの形態の多様性がどのように生じるのか、血管の多様な形態を規定する機構についての研究を行っている。これまでに、アフリカツメガエルのオタマジャクシを用い、発生時にみられる血管のダイナミックな形態学的変化が「いつ」・「どこで」生じるのかを明らかにしてきた。本年度は live cell imaging によってリアルタイムで血管の構築過程を解析できるトランスジェニックカエルを作製した。このトランスジェニックカエルは VEGFR2 のプロモーター・エンハンサーによって血管内皮細胞に GFP や mCherry を特異的に発現させており、血管内皮細胞の挙動を細胞レベルで明らかにすることができる。今後は長期間の観察を可能とする循環システムの条件検討を行っていく必要がある。血管の形態は疾患と直接関わっていることが多いことから、血管の形態を制御することによって疾患を治療する新たな方法が開発されることが期待される。

【研究業績】
〈英文著書〉

〈学会発表〉
（国際学会）
（一般演題）

（国内学会）
（一般演題）

1．藤原正和：アフリカツメガエルによる血管の形態に関わる因子の機能解析 . 第２３回日本血管生物医学会学術集会 , 2016. 3.（神戸）
2．藤原正和：アフリカツメガエルによる血管形成イメージング解析 . 第４回日本比較病理学研究会 , 2016. 2.（東京）

【代表的研究論文】
Shimizu, H., Yamagish S., Chiba H., Ghazizadeh M.: Methionine aminopeptidase 2 as a potential therapeutic target for human non-small-cell lung cancers. Adv Clin Exp Med. 2016; 25:117-128.

ORIGINAL PAPERS

Adv Clin Exp Med 2016, **25**, 1, 117–128
DOI: 10.17219/acem/60715

ISSN 1899–5276

Hajime Shimizu[1, 3, A–D, F], Shigeki Yamagishi[2, B, C, E], Hideki Chiba[3, E, F], Mohammad Ghazizadeh[1, A, C–F]

Methionine Aminopeptidase 2 as a Potential Therapeutic Target for Human Non-Small-Cell Lung Cancers

[1] Department of Molecular Pathology, Institute of Gerontology, Nippon Medical School, Japan
[2] Department of Surgery, Division of Thoracic Surgery, Aizu Chuo Hospital, Fukushima, Japan
[3] Department of Basic Pathology, Fukushima Medical University, Fukushima, Japan

A – research concept and design; **B** – collection and/or assembly of data; **C** – data analysis and interpretation; **D** – writing the article; **E** – critical revision of the article; **F** – final approval of article

Abstract

Background. Methionine aminopeptidase 2 (MetAP2) is a bi-functional protein that plays a critical role in the regulation of post-translational processing and protein synthesis.
Objectives. We studied whether MetAP2 is activated and expressed in human non-small-cell lung cancer (NSCLC) tissues and whether inactivation of MetAP2 activity, with its specific inhibitor fumagillin, potentially inhibits proliferation of NSCLC cells.
Material and Methods. The expression and function of MetAP2 were evaluated in NSCLC tissues, primary cell cultures and cell lines using immunohistochemistry, RT-PCR, Western blot, aminopeptidase activity assay and flow cytometry. MetAP2 expression was also studied in relation to clinicopathological factors.
Results. MetAP2 expression in NSCLS, including adenocarcinoma (ADC) and squamous cell carcinoma (SCC), showed a moderate to strong positive reaction while normal appearing bronchial epithelium showed weak staining and normal alveolar epithelial cells were widely negative. A high MetAP2 mRNA and protein expression was found in NSCLC tissues. The aminopeptidase activity in NSCLC was 2-fold higher than that in normal lung tissues. In a series of 41 ADC patients, MetAP2 expression was significantly correlated with patient's outcome or survival time. Inhibition of MetAP2 by fumagillin in SCC cell lines revealed a significant increase in caspase-3 activity as compared to the control ($p = 0.001$).
Conclusions. Our results indicate that MetAP2 is involved in NSCLC and is an important regulator of proliferative and apoptotic targets. Thus inhibition of MetAP2, such as by fumagillin, may be a potential therapeutic modality for prevention of tumor cell growth, development and progression in NSCLC patients (**Adv Clin Exp Med 2016, 25, 1, 117–128**).

Key words: apoptosis, methionine aminopeptidase 2 (MetAP2), myristoylation, fumagillin, non-small-cell lung cancer (NSCLC).

Non-small-cell lung cancer (NSCLC) is one of the most difficult malignancies to treat. Despite years of research, the prognosis for patients with lung cancer remains poor, with a five-year survival rate of 14%. Nevertheless, lung cancer may be curable in its early stages and most patients derive some benefit from treatment, such as longer survival or amelioration of symptoms [1]. DNA ploidy analysis may be efficient to estimate malignant potential in lung ADCs [2]. Recently, clinical application of molecular targeted therapy such as epidermal growth factor receptor (EGFR) has improved prognosis. Accordingly, the overall survival of patients with metastatic NSCLC evidencing EGFR mutations has improved to 27–30.5 months when treated with EGFR [3]. Therefore, molecular targeted therapy for the appropriate population, using good predictive markers, is indispensable.

The gene expression profile analysis of human esophageal cell carcinoma cell lines after early

response to ionizing irradiation using cDNA microarray screening disclosed MetAP2 genes that were modulated in irradiation [4]. The MetAP2 gene may be useful in understanding the molecular basis of radiotherapy and in developing strategies to augment its effect or establish novel, less hazardous alternative adjuvant therapies. Overexpression of MetAP2 in immortalized bronchial epithelial cell line NL20 accelerated growth and was reversed using treatment with MetAP2 inhibitors. Thus MetAP2 plays an important role in tumor cell growth and may contribute to tumorigenesis [5, 6].

Protein synthesis starts with an initiator methionine in both prokaryotes and eukaryotes. The translational process on ribosomes starts with methionine. In order for the newly synthesized protein to be transported to its exact intracellular location, the methionine at the NH2-terminal is removed. After the removal of methionine *via* MetAP, protein myristoylation takes place by the enzyme *N*-myristoyl-transferase (NMT). NMT is a cytosolic enzyme in eukaryotic cells [7]. The process is essential for further amino terminal modifications (e.g. acetylation by N-α acetyltransferase and myristoylation of glycine by N-myristoyl-transferase). The structural alterations from these modifications are essential in cell proliferation [8].

In eukaryotes, two isoforms of MetAP have been identified as MetAP1 and MetAP2 [9]. Both MetAP1 and MetAP2 are essential components of the cell growth machinery. In yeasts and humans, two proteins are known to possess MetAP2 activity and are known as MetAP1 and MetAP2. Downregulation of either MetAP1 or MetAP2 protein expression by small interfering RNA (siRNA) significantly inhibited the proliferation of human endothelial cells [10].

MetAP2 has attracted much more attention than MetAP1 due to the discovery of MetAP2 as a target molecule of the anti-angiogenic compounds, fumagillin and ovalicin [11]. Identification of MetAP2 as the cellular target of fumagillin class molecules, and the significant growth inhibition observed in cells sensitive to MetAP2 inhibition suggested the direct involvement of MetAP2 in the regulation of cell proliferation [12, 13].

Targeting the angiogenesis process has become an important strategy for inhibiting tumor growth. Fumagillin and its derivatives have been known to exert their inhibitory effects by specifically and covalently binding to MetAP2 [14, 15]. Inhibitors of angiogenesis can be classified into 2 groups, specific and nonspecific factors. Non-specific inhibitors, angiostatin, a tissue inhibitor of metalloproteinases-2 (TIMP-2), and endostatin have attracted interest because of their strong antitumor effect. Recently, much research has focused on TNP-470, a synthetic analog of fumagillin, and its derivatives (IDR-803, IDR-804, IDR-805, CKD-732) [16].

High expression of MetAP2 has been demonstrated in breast, colorectal and cholangio-carcinoma [17–19]. Suppression of hepatoma growth and angiogenesis by fumagillin has also been reported [20]. As for NSCLC, moderate-to-high MetAP2 staining was identified only in lung carcinoma cell lines not lung cancer tissues [5]. Here we demonstrate the first description of increased MetAP expression in NSCLC tissues, primary cell cultures from NSCLC and cell lines. Our findings strongly suggest that the inhibition of MetAP2 by fumagillin or its analogs may be a potential target for tumor cell growth, development and progression in NSCLC patients.

Material and Methods

Material

We investigated 41 cases of NSCLC histologically classified as ADC [21], ranging in age from 45 to 80 years (mean, 67 years). The age, gender, tumor size, histological grading, nodal metastasis, staging and patient outcome were evaluated by reviewing the medical and pathologic records. Tumor size was evaluated using the greatest perpendicular diameter of each lung lesion. In addition, we studied surgical tissues from 8 cases of histologically classified primary NSCLC including 4 cases of ADC and 4 cases of SCC in order to evaluate MetAP2 aminopeptidase enzyme activity, mRNA expression, immunohistochemical localization and protein expression. Ten cases of normal lung tissues freshly obtained from resected benign lesions served as control. The other tissue samples were fixed in neutral-buffered formaldehyde and processed for histological and immunohistochemical evaluation. Furthermore, we studied cell cultures from RERF-LC-AI (well differentiated) and LC-1/sq (moderately differentiated) human SCC cell lines for MetAP2 inhibition assay by a novel inhibitor of MetAP2, fumagillin.

Methods

Cell Lines and Culture Condition

RERF-LC-AI (well differentiated) and LC-1/sq (moderately differentiated) human SCC cell lines were purchased from Riken BioResource Center (Tsukuba, Japan). The tumor cells were cultured in Dulbecco's modified Eagle's Medium (DMEM) containing 10% fetal bovine serum, 100 IU/mL

penicillin, 100 ug/mL streptomycin, and 0.25% amphotericin B at 37°C in a humidified atmosphere in a 5% CO_2 incubator. The cells were treated with trypsin (0.25%), harvested and processed for secondary cultures in the same culture medium until they reached 80% confluence.

In this study, tumor cells obtained at the low-passage cultures (passages at 4–5) were used.

Preparation of Tissues

The tissue samples (mean weight, 300 mg) were homogenized in 10 volumes of 0.01 mol/L phosphate-buffered saline (PBS) pH 7.4 and sonicated at 40 amplitudes for 2 min to obtain the soluble fraction. After centrifugation at 4°C, the supernatants were used to measure MetAP2 aminopeptidase activity and proteins in triplicate. For caspase-3 activity assay, primary cell cultures from NSCLC and normal lung tissues were harvested by centrifugation at 10,000 rpm for 5 min at 4°C and counted. For each case, 1×10^6 cells re-suspended in ice cold cell lysis buffer, and sonicated at 40 amplitudes for 30 s.

The cell lysates were centrifuged at 10,000 rpm for 3 min, and the supernatants were transferred to a microcentrifuge tube for caspase-3 activity assay.

MetAP2 Aminopeptidase Activity Assay

MetAP2 aminopeptidase activity was determined by hydrolysis of methionine L-Leu-*p*-nitroanilide as a substrate, described elsewhere [22]. For MetAP2 activity, an assay mixture (500 μL) containing 50 mM Tris-HCl at pH 7.5 and 0.25 mM methionine L-Leu-p-nitroanilide as a substrate with an appropriate concentration of the enzyme was used. The reaction mixtures were incubated at 37°C for 30 min, left for 15 min on ice, and followed by spectrophotometric determination at 405 nm. The amount of aminopeptidase activity that released one micromole of L-Leu-p-nitroanilide per minute under assay conditions was defined as one unit.

Semi-Quantitative RT-PCR Analysis of MetAP2 mRNA Expression

The total RNA was extracted using an RNeasy mini kit (Quiagen, Hilden, Germany), according to the manufacturer's instructions. Before cDNA synthesis, the RNA was incubated with DNase and then precipitation was done using 95% ethanol. The precipitated RNA was then electrophoresed on 2.0% agarose-ethidium bromide (EtBr) gels to verify the RNA quantity. Subsequently, RNA concentration was determined by UV spectrophotometry. Total RNA (1.5 μg) was then reversely transcribed utilizing the specific primers. The following PCR amplification was carried out in a Thermal Cycler (Takara, Tokyo, Japan). In each case, the PCR cycles were optimized to confirm amplification within the linear phase. For each sample, the relative mRNA level was normalized using glyceraldehyde 3-phosphate dehydrogenase (GAPDH). The following primer pairs were used: MetAP2 sense, 5'ATGGCGGGTGTGGAGGAGGTAGCGGCCT-3' (nucleotides 135-162) and anti-sense 5'TTAATAGTCATCTC CTCTGCTGACAACT-3' (nucleotides 1544–1571). The expected PCR product for MetAP2 was 1440 bp. The internal control was GAPDH. For quantification of the PCR bands, we used densitometry with Quantity One Software (Bio-Rad Labs, Hercules, CA, USA) relative to GAPDH. The results were considered as the mean ± SE of three experiments.

Immunostainings for MetAP2

Primary cultures of RERF-LC-AI and LC--1/sq human SCC cell lines were stained using an indirect immunofluorescence method. Cells (2.5 × 104) in chamber slides (Nalge Nunc Int., Naperville, Illinois) were cultured overnight. Two chamber slide sets from LSCC were prepared, one of which received 1 ug/mL fumagillin (BIOMOL Research Lab, Inc, USA) treatment. After 24 h culture, we fixed the cells in cold acetone, washed in PBS, and treated for 30 min with 10% normal horse serum to eliminate non-specific reaction. The cells were treated with 1 : 50 dilution of polyclonal anti-human MetAP2 antibody overnight followed by PBS washes and reaction with FITC--conjugated goat anti-rabbit IgG at 1 : 100 dilution. Immunoperoxidase reaction for metAP2 was done using frozen or deparaffinized sections and a streptavidin-biotin peroxidase complex method. In brief, endogenous peroxidase was blocked by 10% normal goat serum and the sections were reacted with 1 : 50 polyclonal rabbit anti-human MetAP2 antibody (Zymed Lab Inc, CA) overnight. After PBS washes, the sections were treated with biotinylated goat anti-mouse or anti-rabbit IgGs, washed and processed using a streptavidin-biotin-peroxidase kit (Histofine, Nichirei, Japan). The chromogenic reaction was with diaminobenzidine. Counterstaining was done with hematoxylin. For negative control, the primary antibody was omitted or substituted with non-immune rabbit serum.

MetAP2 Expression in Lung Adenocarcinomas

We studied the relationships between MetAp2 expression and pathological and clinical features (tumor grade, tumor stage, tumor size and nodal metastasis). MetAP2 staining was graded by the

percentage of staining area of tumor cells as follows: 0: 0%, 1: 1~25%, 2: 26~50%, 3: 51~75% and 4: 76~100%. Staining intensity was graded 0: negative, 1: mild, 2: moderate and 3: strong staining. The staining score (0 to 12) was estimated by multiplying the staining area 0 to 4 (%) by the staining intensity 0 to 3. We set the low expression of MetAP2 intensity as a score of 0 to < 6 and high expression as a score of 6 to 12.

Western Blot Analysis

We extracted proteins from the primary cultures of three cases each of adenocarcinoma and SCC of the lung. Each protein sample (20 ug/lane) was run on SDS gels, transferred onto Immobilon polyvinylidene difluoride membranes (Bio-Rad Lab, Hercules, CA, USA) in a transfer buffer consisting of 0.02% SDS, 25 mM Tris-HCl, pH 8.3, 192 mM glycine, and 20% v/v methanol, then incubated overnight at 4°C with a blocking buffer (5% nonfat dry milk, 50 mM Tris-HCl, pH 7.5, 0.1% Tween-20, 150 mM NACI). Two sets of membranes were made and incubated with 1 : 500 polyclonal rabbit anti-human MetAP2 antibodies (Zymed Lab Inc, CA, USA) overnight at room temperature. Proteins were extracted from the primary cultures of three cases of ADC and SCC of the lung and normal lung tissues. The samples were washed with 50 mM Tris-HCl, pH 7.5, containing 150 mM NaCI and 0.1% Tween 20 and then were treated with corresponding secondary antibodies conjugated with alkaline phosphatase. The reaction was developed with the ProtoBlot NBT and BICP System (Promega, Madison, WI, USA).

Caspase-3 Fluorometric Measurement

Caspases-3 production requires that the active enzymes undergo folding from their large and small subunit constituents after expressing separately in *Escherichia coli*. The methodological details have been described previously [23]. The active enzyme was obtained under optimal conditions for each enzyme; each subunit from the purified inclusion bodies were solubilized in 6 M guanidine HCl and subsequently diluted to a 100 μg/mL final concentration at room temperature.

Measurement of the fluorescence counts in the wells was done with a 400 nm excitation filter and 505 nm emission filter. The levels of released 7-amino-4-trifluoromethyl coumarin were measured with a BioLumin 960 spectrofluorometer (Molecular Dynamics Japan, Tokyo, Japan). The specific activity of caspase-3 present was calculated in each sample. The relative absorbance was calculated as described according to the manufacturer's instructions (MBL, Co, LTD, Nagoya, Japan).

Flow Cytometric Assay

RERF-LC-AI and LC-1/sq human SCC cells obtained from the low-passage cultures (passages at 4–5) were utilized in this study. To measure propidium iodide (PI) staining, lung cancer cells (1×10^4) were harvested and stained with FITC--labeled PI (Molecular Probes, Eugene, OR, USA) as specified by the supplier. Briefly, cancer cells (1×10^4) in 1 mL of medium were cultured as indicated for 21h, washed and then stained with PI-FITC in a binding buffer and analyzed with CellQuest software (BD Bioscience, San Jose, CA, USA) with FACSCalibur within 1 h. The data was expressed as the mean of three experiments before and after treatment.

Statistical Analysis

Statistical analyses for comparisons between the clinicopathological findings were performed using Fisher's exact test and Kaplan-Meier survival analyses. The difference between two related groups was examined for statistical significance using the Student's *t*-test for paired data. A $p < 0.05$ was recorded as statistically significant.

Results

MetAP2 Expression in Normal Lung and NSCLC Tissues

Immunoperoxidase staining for MetAP2 in a paraffin section of normal alveolus showed negative staining (Fig. 1A). Sections from bronchial epithelium showed a weak degree of staining (Fig. 1B). ADC (well differentiated) and SCC cells showed moderate to strong intensity (Fig. 1C, D). The intensity of MetAP2 expression was greater in carcinoma cells as compared to bronchial epithelial tissues. SCC tissues showed stronger staining than ADC tissues.

Pathological Features of Lung Adenocarcinoma Patients and Expression of MetAP2

We studied paraffin-embedded lung tissue sections of 41 cases of histologically classified ADCs. The relationships between pathological and clinical features are shown in Table 1. A comparison between the low expression of MetAP2 intensity and high expression of MetAP2 intensity in ADCs showed that 21 cases had low expression and 20 cases had high expression of MetAP2. There was

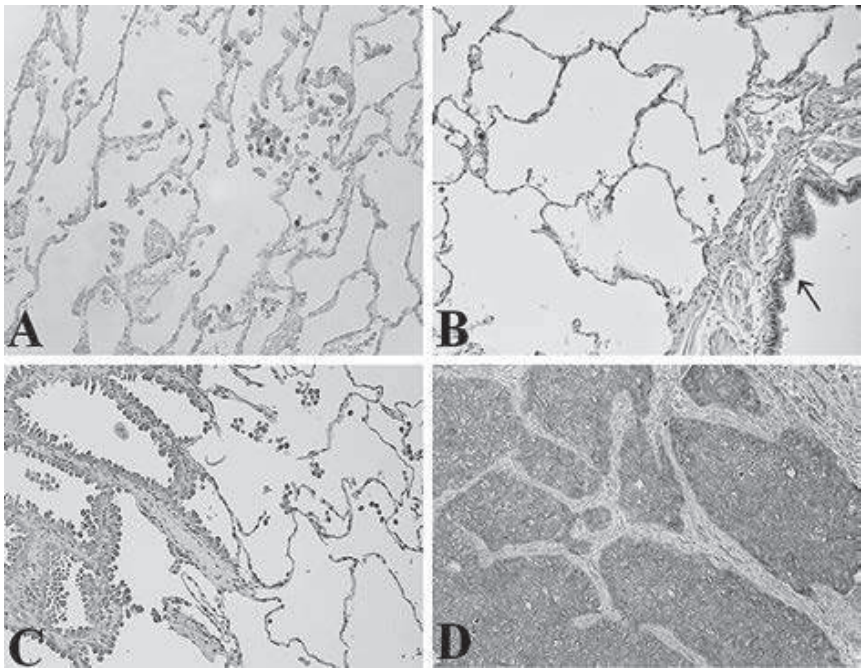

Fig. 1. Immunohistochemical analysis of human normal lung and cancer tissues (A-D, magnification ×100). MetAP2 in paraffin section from normal alveolus showed negative staining (Fig. 1A). Bronchial epithelium showed a weak degree of staining (Fig. 1B, arrow). ADC (well-differentiated) and SCC cells showed moderate to strong intensity (Fig. 1C, D)

Table 1. Pathological features of lung adenocarcinoina patients and expression of MetAP2

Variables	No.	MetAP2 expression		
		low	high	p-value
Age				
≤ 70	24	13	11	0.756
> 70	17	8	9	
Gender		15		
male	30	6	15	1.000
female	11		5	
Tumor size				
≤ 30 mm	16	9	7	0.751
> 30 mm	25	12	13	
Tumor differentiation				
w/d & m/d	28	14	14	1.000
p/d	13	7	6	
Node metastasis				
negative	27	16	11	0.197
positive	14	5	9	
Pathological stage				
stage I	28	14	10	0.350
stage II & III	13	7	10	
Patient outcome				
alive	10	3	9	0.043
dead	31	18	11	

* w/d & m/d – well differentiated & moderately-differentiated; ** p/d – poorly differentiated.

no significant association between the low and high expression of MetAP2 and clinical features (tumor size, tumor differentiation, nodal metastasis and staging), but patient outcome revealed a significant difference between low and high MetAP2 expressing patients (Table 1; $p < 0.04$).

MetAP2 Activities in Normal Lung and NSCLC Tissues

Using methionine-*p*-nitroanilide as a substrate, we measured the spectrophotometric determination of the hydrolysis of methionine *p*-nitroanilide in their soluble and membrane-bound forms in surgically removed lung carcinoma tissues and normal lung tissues freshly obtained from resected benign lesions, serving as the control. The mean aminopeptidase activity was 80.6 ± 13.4 in normal lung tissue vs. 156.9 ± 20.8 in lung carcinoma tissue. Compared to normal lung tissue, carcinoma tissue had a remarkably higher activity (Table 2). In 4 cases of ADC, each case showed a significantly higher aminopeptidase activity than an unaffected normal tissue counterpart (Fig. 2A) and overall, ADC cases had 2 times higher activity than normal tissue counterparts (97.3 ± 16.51 vs. 45.4 ± 8.6; $p < 0.03$, Fig. 2B). Likewise, 6 cases of SCC tissues had 196.7 ± 20.1 aminopeptidase activity vs. 104.2 ± 15.2 activity in unaffected adjacent normal lung tissues (Fig. 2C) with an overall significant difference ($p < 0.04$; Fig. 2D).

Table 2. Aminopeptidase activities in normal lung and NSCLC* tissues

Case**	Age/Sex	Aminopeptidase activity (unit/L)	
		normal	tumor
1	82 / M	29.311.8	73.3 ± 3.3
2	77 / F	38.7+1.8	129.3 ± 5,2
3	65 / F	69.7± 1.5	122 ± 5.3
4	71 / M	43.7± 2.0	64.7+3.2
5	77 / M	102.7± 5.5	115.7± 5.S
6	64 / M	149.7 ± 2.6	174 ± 3.5
7	78 / M	50± 1.7	247 ± 7.8
8	76 / M	102 ± 3.6	226.7± 9.5
9	60 / M	141 ± 3.8	182.3 ± 4.6
10	74 / M	79.7 ± 2.0	234.3 ± 7.4

* NSCLC – non-small cell lung cancer; ** cases 1–4 – adenocarcinoma and 5–10 – squamous cell carcinoma (SCC); the data presented as mean ± S.E.

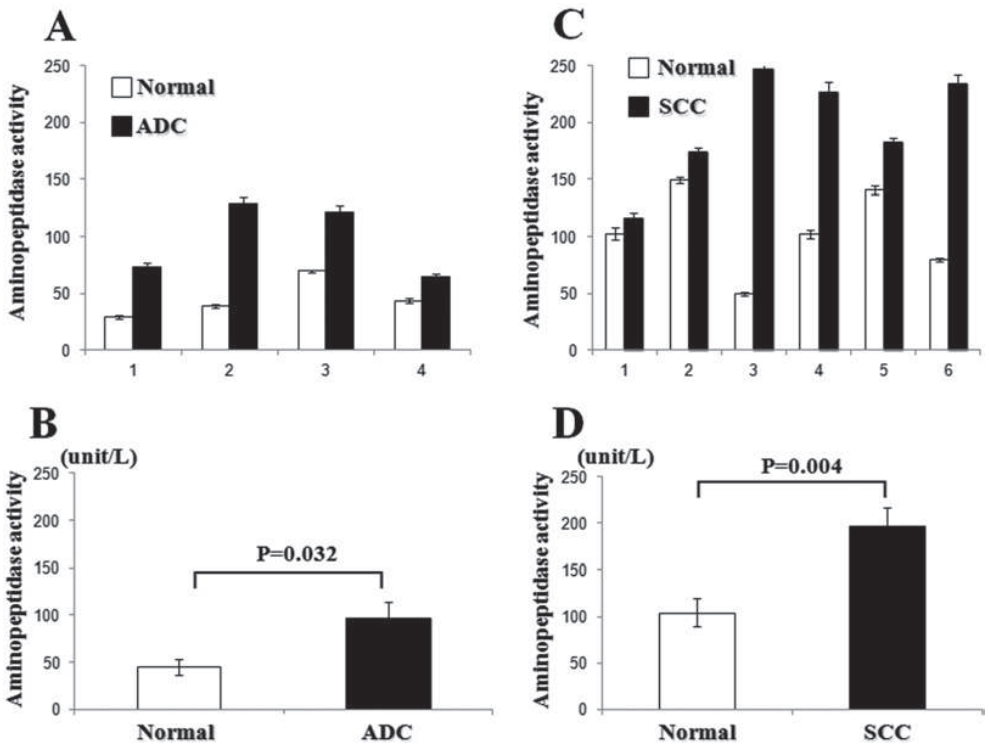

Fig. 2. Spectrophotometric determination of hydrolysis of methionine *p*-nitroanilide in their soluble and membrane-bound forms in surgically-removed lung carcinoma tissues and unaffected adjacent surrounding tissues. Comparison of the expression level of MetAP2 between 4 cases of ADC and 4 cases of normal lung tissues separately (A) and in combination (B). Comparison of the expression level of MetAP2 between 6 cases of SCC and 6 cases of unaffected adjacent normal lung tissues separately (C) and in combination (D)

Semi-Quantitative RT-PCR and Western Blot Analysis of MetAP2 in Normal Lung and NSCLC Tissues

To assess the mRNA expression levels of MetAP2, we studied surgical operating tissues from 7 cases of histologically classified primary NSCLC as 4 ADC and 3 SCC patients. Normal lung tissues were obtained from surgically resected benign lesions.

The mRNA levels of MetAP2 in the four cases of ADC were significantly different compared to normal lung tissues (Fig. 3A; $p < 0.008$). Also, the three cases of SCC had a significant upregulation of the MetAP2 gene as compared to normal lung tissues (Fig. 3B; $p < 0.002$).

Proteins were extracted from subconfluent primary cultures of three representative cases of ADC and SCC and normal lung tissue counterparts. The levels of MetAP2 in the three cases of ADC (Fig. 3C) and three cases of SCC (Fig. 3D) showed a significant difference in the quantitative measurement of the protein expression compared to normal lung tissues ($p < 0.05$; respectively).

MetAp2 Immunofluorescence Intensity, Caspase-3 Activity and Cell Death Effect of Fumagillin in Cultured SCC Cell Lines

We assessed the effect of fumagillin as an inhibitor of MetAP2 on cell proliferation activity and cell death population using caspase-3 fluorometric and PI (propidium iodide) flow cytometric analysis. We used the primary cultures of RERF-LC-AI (well differentiated) and LC-1/sq (moderately differentiated) human SCC cell lines.

The immunofluorescence intensity of MetAP2 in moderately differentiated SCC cells was decreased after fumagillin (1 μg/mL) treatment for 24 h (Fig. 4A). Also, caspase-3 activity was markedly

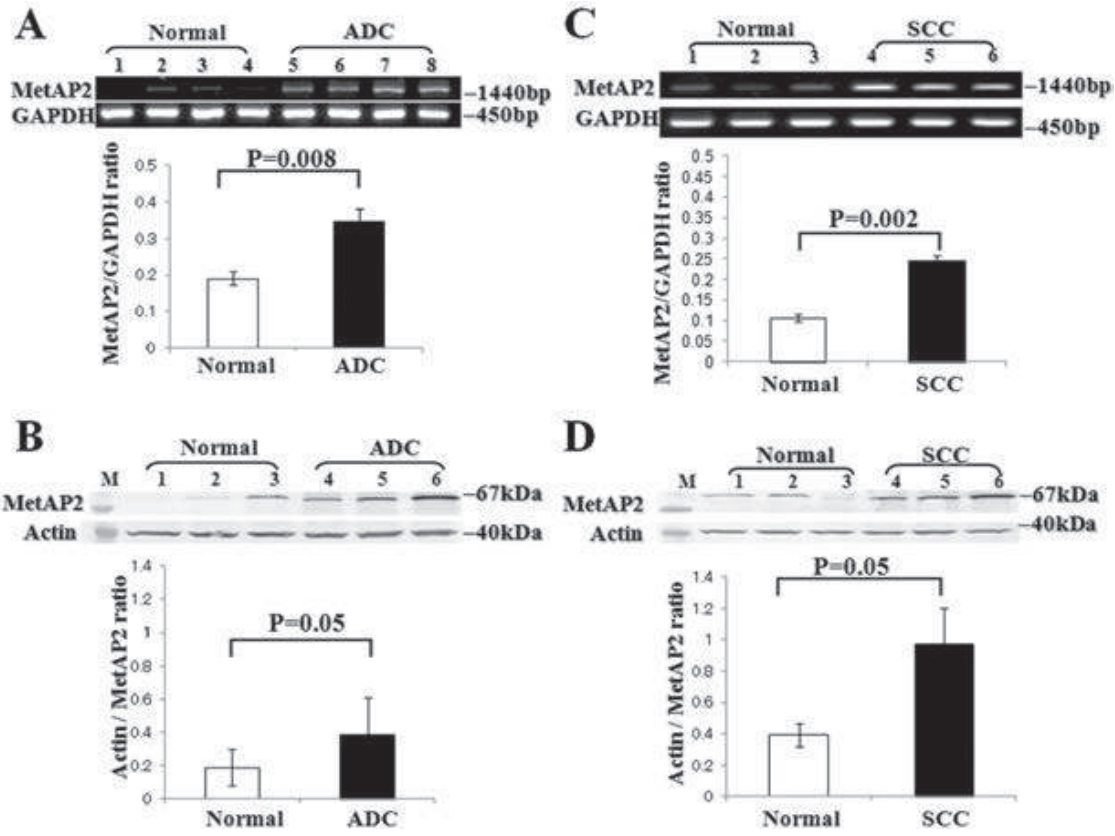

Fig. 3. MetAP2 mRNA and protein expression in ADC and SCC. (A) The mRNA levels of MetAP2 by RT-PCR in 4 cases of ADC compared to 4 cases of normal lung tissues showed significant increase in ADC ($p < 0.008$). (B) The protein levels of MetAP2 by Western blot in 3 cases of ADC compared to 3 cases of normal lung tissues showed significant increase in ADC ($p < 0.05$). (C) The mRNA levels of MetAP2 by RT-PCR in 3 cases of SCC compared to 3 cases of normal lung tissues showed significant increase in SCC ($p < 0.002$). (D) The protein levels of MetAP2 by Western blot in 3 cases of SCC compared to 3 cases of normal lung tissues showed significant increase in SCC ($p < 0.05$)

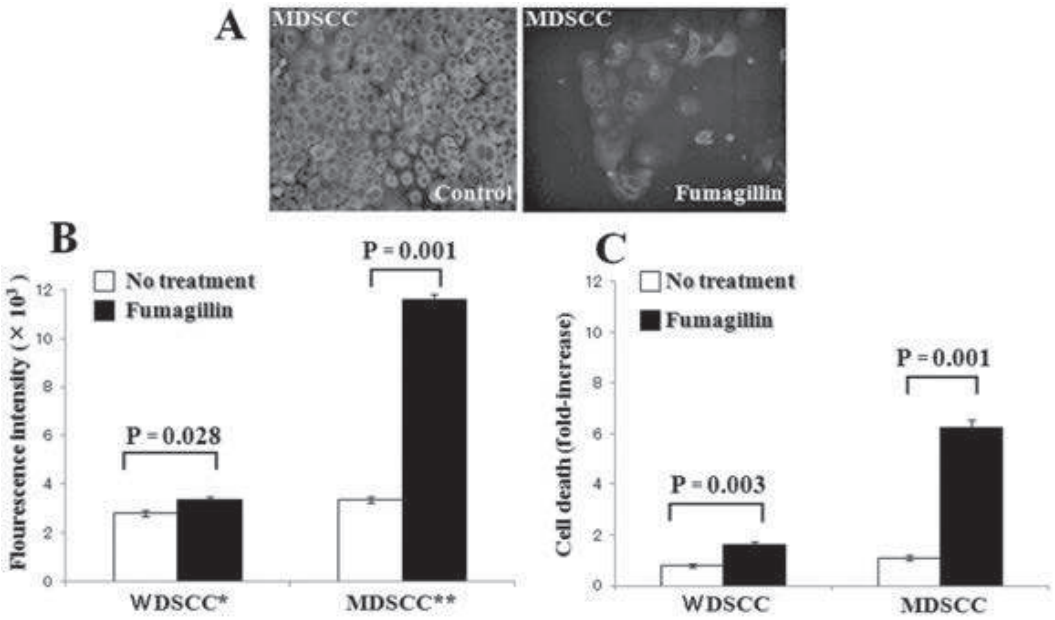

Fig. 4. Inhibition of MetAP2 by addition of fumagillin in WDSCC and MDSCC cell cultures. (A) Immunofluorescence staining of MetAP2 in untreated and treated (plus fumagillin, 1 μg/mL) MDSCC cell culture showed decrease in fluorescence intensity in treated cells (magnification ×200). (B) Caspase-3 fluorometric assay after exposure of MDSCC cells to fumagillin. Both well-differentiated SCC and moderately-differentiated SCC cells showed significantly increased caspase-3 activity. (C) Cell death effect using propidium iodide stain and flow cytometry on MDSCC cells. Both WDSCC and MDSCC cells showed significantly increased cell death by propidium iodide staining

increased in fumagillin-treated well and moderately differentiated SCC cells (Fig. 4B) ($p < 0.028$ and $p < 0.001$, respectively) compared to no-treatment control SCC cells. In the moderately differentiated SCC cells, caspase-3 activity was more increased than in the no-treatment SCC control cells (Fig. 4B). In addition, regarding cell death effect, the fumagillin-treated well and moderately differentiated SCC cells showed significantly increased cell death (Fig. 4C; $p < 0.003$ and $p < 0.001$, respectively).

Discussion

Despite aggressive therapy, patients with advanced stage NSCLC demonstrate a poor survival with significant long-term morbidity in disease survivors. High-risk disease features are strongly correlated with tumor vascularity, suggesting that angiogenesis inhibitors may be a useful addition to current therapeutic strategies [24].

In the past, NSCLCs were seen together without paying attention to the more specific molecular pathological types. This was thought to be appropriate, because different therapeutic procedures were not available for the treatment of the subtypes of NSCLC such as ADC and squamous cell carcinomas. Since the time the first special EGFR mutation was identified, the situation has changed and nowadays this rapidly evolving field provides new results [25]. EGFR mutations have been reported as a predictive factor for favorable prognosis of gefitinib-treated patients with lung ADC. Patient's sex and smoking status were not significantly associated with longer overall survival and progression-free survival according to EGFR mutation status [26]. Patients with advanced NSCLC who were selected on the basis of EGFR mutations improved progression-free survival with acceptable toxicity but those with no EGFR mutation did not.

In all living cells, protein synthesis is initiated with either methionine (in the cytosol of eukaryotes) or formylmethionine. MetAP activity is essential for cellular growth and viability. In yeasts, knockout of either MetAP1 or MetAP2 causes a decrease in growth rates while elimination of both genes is lethal, indicating that the two MetAPs play essential functions and are together essential for yeast proliferation [27, 28]. MetAP2 has attracted more attention than MetAP1 by the discovery of MetAP2 as a target molecule of the anti-angiogenic compounds, fumagillin and ovalicin [13]. A novel MetAP2 inhibitor, fumagillin, strongly inhibits the growth of human colon cancer HT29 cells, melanoma B16F10 cells and neuroblastoma CHP-134 cells [29–31]. MetAP2 is the molecular target of angiogenesis inhibitors, such as fumagillin, which can also inhibit cancer cell proliferation, implying that MetAP2 may play a quite

complex role in tumor progression under which MetAP2 enzyme activity is inactivated through covalent modification [32, 33].

Several studies have demonstrated that the metastasis-associated gene product S100A4 interacts with the angiogenesis-related protein MetAP2. Other studies also support this conclusion [34]. Recently, small molecule protein p67/MetAP2 was shown to have a greater affinity toward ERK1/2 kinases, and its N-terminal p26 segment will mask the phosphorylation sites on ERK1/2 to block the activation and activity of ERK1/2. This will then lead to inhibition of the cell cycle activated through the growth factor-mediated cell signaling pathway and thus cell growth and proliferation [35].

Major components of the cell signaling pathways, the *ras*/mitogen-activated protein kinase (MAPK) systems are altered in lung cancer cells by oncogenes through overexpression or mutation, leading to dysregulated cell signaling and cell proliferation [36]. It has been reported that NCI-H-460 (large cell carcinoma), H1299, A549 (ADC) and Calu6 (anaplastic carcinoma) cell lines cause inhibition of tumor cell growth on three distinct chemical classes of MetAP2 inhibitors as follows: TNP-470, A800141, and A-357300.

This data prompted us to examine the possible new treatment roles of MetAP2 in lung cancers. There was no significant association of low and high expression of MetAP2 and clinical features (tumor size, tumor cell differentiation, nodal metastasis and staging) (Table 1). But median survival time of the low and high expression of MetAP2 disclosed a significant difference (Table 1, $p = 0.043$). Survival rate was more increased in low MetAP2 expression patients (85.7%) than high MetAP2 expression patients (55%). MetAP2 may play quite a complex role in tumor progression, which inactivates MetAP2 enzyme activity through covalent modification [32, 33].

Additionally, we measured the spectrophotometric determination of the hydrolysis of methionine *p*-nitroanilide in their soluble and membrane-bound forms in surgically removed lung carcinoma tissues and unaffected adjacent normal surrounding tissues. Total average aminopeptidase activity was 80.6 ± 13.4 in normal lung tissue versus 156.9 ± 20.8 in lung carcinoma tissue (Table 2). Compared to normal lung tissue, carcinoma tissue had significantly higher activities. Histologically, SCC demonstrated higher MetAP2 activity than ADC. These results were further confirmed by the semi-quantitative RT-PCR analysis of MetAP2 mRNA expression in normal lung and NSCLC tissues. The mRNA levels of MetAP2 in four cases of ADC showed significant differences in the quantitative extent of MetAp2 gene expression as compared to normal lung tissues ($p = 0.008$). Also, three cases of squamous cell carcinomas had significant upregulation of the MetAP2 gene as compared to normal lung tissues ($p = 0.002$). In seven cases of NSCLC, MetAP2 mRNA expression levels were upregulated as compared to normal lung tissues ($p = 0.001$) (data not shown). Also, the levels of MetAP2 in three cases of ADC and three cases of squamous cell carcinomas showed significant differences in the quantitative extent of protein expression compared to normal lung tissues ($p = 0.05$, respectively). MetAP2 proteins were increased in ADC and SCC cases compared to normal lung tissues, according to Western blot analysis. Higher expression of the MetAP2 protein in human cancers further supports the contention that MetAP2 plays a role in cancer development. We saw moderate-to-strong staining of MetAP2 in all ADC cases examined [37]. S100a4 protein is a calcium-binding agent that regulates tumor metastasis and a variety of cellular processes *via* interaction with different target proteins, including MetAP2, a main regulator of the proliferative and apoptotic pathways in mesothelioma cells [33, 34].

Interestingly, the normal bronchial epithelium showed a weak degree of staining; therefore, the frequent MetAP2 expression in NSCLC seems to be categorized as an aberrant expression. This finding correlates to the finding that colorectal normal mucosa far from the cancer shows a mild degree of MetAP2 staining [11].

The frequent and aberrant MetAP2 expressions in biliary epithelial cells might have acquired MetAP2 through their dysplasia-carcinoma sequence. Positive MetAP2 expression was observed in a small population of non-dysplastic biliary epithelial cells. Thus, it has been reported that MetAP2 is a novel biomarker for the early detection of cholangiocarcinoma [19].

In the present study, we asked whether MetAP2 is activated and expressed in human NSCLC tissues or inactivation of MetAP2 activity with fumagillin (an angiogenesis inhibitor) may potentially inhibit proliferation of lung cancer cell lines.

The expression level of MetAP2 was significantly higher in the 6 cases of SCC than 4 cases of ADC. Also, semi-quantitative MetAP2 mRNA and protein levels showed higher expression in SCC than in ADC. Thus, we chose the SCC cell lines to assess the effect of fumagillin as an angiogenesis inhibitor on cell proliferation activity and cell death population using caspase-3 flow cytometric analysis. The immunofluorescence intensity of MetAp2 in the moderately differentiated SCC cell line was decreased after treatment with fumagillin for 24 h (Fig. 4A) and caspase-3 activity was markedly increased (Fig. 4B; $p = 0.001$) as compared to

well-differentiated SCC cells (Fig. 4B; p = 0.028). In addition, the cell death effect was also increased in fumagillin-treated moderately differentiated SCC cells (Fig. 4C; p = 0.001) as compared to well-differentiated SCC cells (Fig. 4C; p = 0.003). These results indicate that fumagillin as an angiogenesis inhibitor has potentially inhibited lung cancer cell proliferation.

The mechanism by which inhibition of MetAP2 might lead to growth inhibition may be through both tumor cell intrinsic and extrinsic mechanisms. A defect in the removal of N-terminal methionine caused by metAP2 inhibition might lead to aberrant levels of proteins important for cell proliferation and apoptosis [33]. In a mechanism that remains to be completely elucidated, inhibition of MetAP2 by small molecule inhibitors led to the transcriptional activation of p53, which in turn activates the expression of p21 that inhibits cycline E/Cdk2, accounting for the cell cycle blockade by these inhibitors [38]. Fumagillin is likewise a eukaryotic initiation factor 2-associated glycoprotein, p67. Fumagillin increases the stability of p67 and affinity to ERKs 1 and 2 and causes the inhibition of the phosphorylation of ERKs 1 and 2 [38, 39]. MetAP2 inhibitors IDR-803, IDR-804, IDR-805 and CDK-732, as well as fumagillin analogs, strongly inhibit the growth of cancers in a model of nude mouse xenograft. Inhibition of angiogenesis is emerging as a promising strategy for the treatment of cancer [41]. Choosing the most appropriate time of day for TNP-470, a synthetic analogue of fumagillin, administration will aid in the treatment of tumors.

The transcription of MetAP2 mRNA is regulated by clock gene proteins of the mCLOCK: mBMAL1 heterodimer in sarcoma180-bearing mice [42]. Interestingly, MetAP2 was expressed in many cell types, including fibroblasts in idiopathic pulmonary fibrosis. In the bleomycin induced acute lung injury in mice, fumagillin attenuated the deposition of collagen [43]. This finding was further confirmed when it was found that PPl--2458, a member of the fumagillin class of irreversible MetAP2 inhibitors, potently inhibits the proliferation of human fibroblast-like synoviocytes derived from rheumatoid arthritis in the late G1 phase of the cell cycle [44]. Further, we report the first study on MetAP2 expression and function in NSCLC tissues and cell lines.

A high MetAP2 mRNA and protein expression as well as activity was found in NSCLC tissues and cell lines and the expression of MetAP2 correlated with patient's outcome. The higher concentration of MetAP2 in NSCLC tissues than the corresponding normal bronchial epithelial cells suggests a greater dependence on this enzyme by malignant cells for their function and proliferation. Hence, a reduction in the enzyme activity may be more harmful to cancer cells than normal epithelial cells. The evaluation of specific inhibitors of MetAP2 in animal models should provide justification for future selection and evaluation of MetAP2 inhibitors in clinical trials for NSCLC patients. MetAP2 is an important regulator of proliferative and apoptotic pathways and its inhibition may provide a potential therapeutic intervention for lung cancer.

Acknowledgements. The authors would like to thank Dr. Kiyoshi Koizumi, Division of Thoracic Surgery, Department of Surgery, Aizu Chuo Hospital, Fukushima, who helped with providing NSCLC patient samples and their medical records data.

References

[1] **Spira A, Ettinger DS:** Multidisciplinary management of lung cancer. N Engl J Med 2004, 350, 379–392.
[2] **Shimizu H, Sugino T, Chiba H:** Interphase cytogenetic analysis of lung adenocarcinomas with bronchioloalveolar pattern. Fukushima J Med Sci 2012, 58, 66–73.
[3] **Maemondo M, Inoue A, Kobayashi K, Sugawara S, Oizumi S, Isobe H:** Gefitinib or chemotherapy for non-small-cell lung cancer with mutated EGFR N Engl J Med 2010, 362, 2380–2388.
[4] **Bo H, Ghazizadeh M, Shimizu H, Kurihara Y, Egawa S, Moriyama Y:** Effect of ionizing irradiation on human esophageal cancer cell lines by cDNA microarray gene expression analysis. J Nippon Med Sch 2004, 71, 172–180.
[5] **Tucker LA, Zhang Q, Sheppard GS, Lou P, Jiang F, McKeegan E:** Ectopic expression of methionine aminopeptidase-2 causes cell transformation and stimulates proliferation. Oncogene 2008, 26, 3967–3976.
[6] **Selvakumar P, Lakshmikuttyamma A, Kanthan R, Kanthan SC, Dimmock JR, Sharma RK:** High expression of methionine aminopeptidase 2 in human colorectal adenocarcinomas. Clin Cancer Res 2004, 10, 2771–2775.
[7] **Walsh CT, Garneau-Tsodikova S, Gatto GJ Jr:** Protein posttranslational modifications: The chemistry of proteome diversifications. Angew Chem Int Ed Engl 2005, 44, 7342–7372.
[8] **Sawanyawisuth K, Wongkham C, Pairojkul C, Saeseow OT, Riggins GJ, Araki N:** Methionine aminopeptidase 2 over-expressed in cholangiocarcinoma: potential for drug target. Acta Oncol 2007, 46, 378–385.
[9] **Walker KW, Bradshaw RA:** Yeast methionine aminopeptidase I. Alteration of substrate specificity by site-directed mutagenesis. J Biol Chem 1999, 274, 13403–13409.
[10] **Bernier SG, Taghizadeh N, Thompson CD, Westlin WF, Hannig G:** Methionine aminopeptidases type I and type II are essential to control cell proliferation. J Cell Biochem 2005, 95, 1191–1203.

[11] **Selvakumar P, Lakshmikuttyamma A, Dimmock JR, Sharma RK:** Methionine aminopeptidase 2 and cancer. Biochim Biophys Acta 2006, 1765, 148–154.
[12] **Turk BE, Griffith EC, Wolf S, Biemann K, Chang YH, Liu JO:** Selective inhibition of amino-terminal methionine processing by TNP-470 and ovalicin in endothelial cells. Chem Biol 1999, 6, 823–833.
[13] **Griffith EC, Su Z, Niwayama S, Ramsay CA, Chang YH, Liu JO:** Molecular recognition of angiogenesis inhibitors fumagillin and ovalicin by methionine aminopeptidase 2. Proc Natl Acad Sci USA 1998, 95, 15183–15188.
[14] **Ingber D, Fujita T, Kishimoto S, Sudo K, Kanamaru T, Brem H:** Synthetic analogues of fumagillin that inhibit angiogenesis and suppress tumour growth. Nature 1990, 6, 555–557.
[15] **Liu S, Widom J, Kemp CW, Crews CM, Clardy J:** Structure of human methionine aminopeptidase-2 complexed with fumagillin. Science 1998, 282, 1324–1327.
[16] **Chun E, Han CK, Yoon JH, Sim TB, Kim YK, Lee KY:** Novel inhibitors targeted to methionine aminopeptidase 2 (MetAP2) strongly inhibit the growth of cancers in xenografted nude model. Int J Cancer 2005, 10, 124–130.
[17] **Martínez JM, Prieto I, Ramírez MJ, Cueva C, Alba F, Ramírez M:** Aminopeptidase activities in breast cancer tissue. Clin Chem 1999, 45, 1797–1802.
[18] **Selvakumar P, Lakshmikuttyamma A, Kanthan R, Kanthan SC, Dimmock JR, Sharma RK:** High expression of methionine aminopeptidase 2 in human colorectal adenocarcinomas. Clin Cancer Res 2004, 10, 2771–2775.
[19] **Sawanyawisuth K, Wongkham C, Pairojkul C, Saeseow OT, Riggins GJ, Araki N:** Methionine aminopeptidase 2 over-expressed in cholangiocarcinoma: potential for drug target. Acta Oncol 2007, 46, 378–385.
[20] **Yoshida T, Kaneko Y, Tsukamoto A, Han K, Ichinose M, Kimura S:** Suppression of hepatoma growth and angiogenesis by a fumagillin derivative TNP470: possible involvement of nitric oxide synthase. Cancer Res 1998, 58, 3751–3756.
[21] **Travis WD, Brambilla E, Noguchi M:** International association for the study of lung cancer/American thoracic society/European respiratory society international multidisciplinary classification of lung adenocarcinoma. J Thorac Oncol 2011, 6, 244–285.
[22] **Nirasawa S, Nakajima Y, Zhang ZZ, Yoshida M, Hayashi K:** Intramolecular chaperone and inhibitor activities of a propeptide from a bacterial zinc aminopeptidase. Biochem J 1999, 341, 25–31.
[23] **Thornberry NA, Rano TA, Peterson EP, Rasper DM, Timkey T, Garcia-Calvo M:** A combinatorial approach defines specificities of members of the caspase family and granzyme B. Functional relationships established for key mediators of apoptosis. J Biol Chem 1997, 272, 17907–17911.
[24] **Shusterman S, Maris JM:** Prospects for therapeutic inhibition of neuroblastoma angiogenesis. Cancer Lett 2005, 228, 171–179.
[25] **Bittner N, Ostoros G, Géczi L:** New treatment options for lung adenocarcinoma – in view of molecular background. Pathol Oncol Res 2013, 5. (Epub ahead of print).
[26] **Toyooka S, Takano T, Kosaka T, Hotta K, Matsuo K, Ichihara S:** Epidermal growth factor receptor mutation, but not sex and smoking, is independently associated with favorable prognosis of gefitinib-treated patients with lung adenocarcinoma. Cancer Sci 2008, 99, 303–308.
[27] **Li X, Chang YH:** Amino-terminal protein processing in *Saccharomyces cerevisiae* is an essential function that requires two distinct methionine aminopeptidases. Proc Natl Acad Sci USA 1995, 92, 12357–12361.
[28] **Chang YH, Teichert U, Smith JA:** Molecular cloning, sequencing, deletion, and overexpression of a methionine aminopeptidase gene from *Saccharomyces cerevisiae*. J Biol Chem 1992, 25, 8007–8011.
[29] **Selvakumar P, Lakshmikuttyamma A, Das U, Pati HN, Dimmock JR, Sharma RK:** NC2213: a novel methionine aminopeptidase 2 inhibitor in human colon cancer HT29 cells. Mol Cancer 2009, 8, 65.
[30] **Hannig G, Lazarus DD, Bernier SG, Karp RM, Lorusso J, Qiu D:** Inhibition of melanoma tumor growth by a pharmacological inhibitor of MetAP-2, PPI-2458. Int J Oncol 2006, 28, 955–963.
[31] **Morowitz MJ, Barr R, Wang Q, King R, Rhodin N, Pawel B:** Methionine aminopeptidase 2 inhibition is an effective treatment strategy for neuroblastoma in preclinical models. Clin Cancer Res 2005, 11, 2680–2685.
[32] **Wang J, Lou P, Henkin J:** Selective inhibition of endothelial cell proliferation by fumagillin is not due to differential expression of methionine aminopeptidases. J Cell Biochem 2000, 77, 465–473.
[33] **Catalano A, Romano M, Robuffo I, Strizzi L, Procopio A:** Methionine aminopeptidase-2 regulates human mesothelioma cell survival: role of Bcl-2 expression and telomerase activity. Am J Pathol 2001, 159, 721–731.
[34] **Endo H, Takenaga K, Kanno T, Satoh H, Mori S:** Methionine aminopeptidase 2 is a new target for the metastasis--associated protein. S100A4. J Biol Chem 2002, 19, 26396–26402.
[35] **Datta B:** Roles of P67/MetAP2 as a tumor suppressor. Biochim Biophys Acta 2009, 1796, 281–292.
[36] **Dy GK, Adjei AA:** Novel targets for lung cancer therapy: part I. J Clin Oncol 2002, 15, 2881–2894.
[37] **Tucker LA, Zhang Q, Sheppard GS, Lou P, Jiang F, McKeegan E:** Ectopic expression of methionine aminopeptidase-2 causes cell transformation and stimulates proliferation. Oncogene 2008, 27, 3967–3976.
[38] **Lu J, Chong CR, Hu X, Liu JO:** Fumarranol, a rearranged fumagillin analogue that inhibits angiogenesis *in vivo*. J Med Chem 2006, 49, 5645–5648.
[39] **Datta B, Majumdar A, Datta R, Balusu R:** Treatment of cells with the angiogenic inhibitor fumagillin results in increased stability of eukaryotic initiation factor 2-associated glycoprotein, p67, and reduced phosphorylation of extracellular signal-regulated kinases. Biochemistry 2004, 43, 14821–14831.
[40] **Datta B:** Roles of P67/MetAP2 as a tumor suppressor. Biochim Biophys Acta 2009, 1796, 281–292.
[41] **Chun E, Han CK, Yoon JH, Sim TB, Kim YK, Lee KY:** Novel inhibitors targeted to methionine aminopeptidase 2 (MetAP2) strongly inhibit the growth of cancers in xenografted nude model. Int J Cancer 2005, 10, 124–130.

[42] Nakagawa H, Koyanagi S, Takiguchi T, Kuramoto Y, Soeda S, Shimeno H: 24-hour oscillation of mouse methionine aminopeptidase2, a regulator of tumorprogression, is regulated by clock gene proteins. Cancer Res 2004, 64, 8328–8333.

[43] Kass D, Bridges RS, Borczuk A, Greenberg S: Methionine aminopeptidase-2 as a selective target of myofibroblasts in pulmonary fibrosis. Am J Respir Cell Mol Biol 2007, 37, 193–201.

[44] Bernier SG, Lazarus DD, Clark E, Doyle B, Labenski MT, Thompson CD, Westlin WF, Hannig G: A methionine aminopeptidase-2 inhibitor, PPI-2458, for the treatment of rheumatoid arthritis. Proc Natl Acad Sci USA 2004, 101, 10768–10773.

Address for correspondence:

Hajime Shimizu
Department of Molecular Pathology
Institute of Gerontology
Nippon Medical School
Nakahara-ku
Kosugi-cho
Kawasaki
Japan 211-8533
Tel.: +81 44 733 1823
E-mail: hirstone@nms.ac.jp

Conflict of interest: None declared

Received: 1.12.2014
Revised: 24.03.2015
Accepted: 24.11.2015

Ⅱ．細胞生物学部門

Department of Biochemistry and Cell Biology

細胞生物学部門
（大学院　細胞生物学部門）

教授　太田　成男

【研究概要】

研究室の特色

大学院医学研究科細胞生物学分野（先端医学研究所細胞生物学部門）では最新のバイオテクノロジーを駆使して、老化や病気の原因を細胞の中から分子レベルで探り、それを応用できるところまで到達しようとしている。細胞内小器官のミトコンドリアはエネルギー産生だけでなく様々なプラスの機能を持ち、一方、マイナス面としては、活性酸素を発している。エネルギー代謝を促進し、活性酸素の弊害を抑制することで、多くの疾患の予防と治療に貢献し、ひいては老化の抑制に貢献できるものと考えている。さらに、研究を発展させて、分子状水素を様々な疾患の予防と治療に貢献しようとしている。

研究が本当の意味で社会に役立つためには、しっかりとした基礎が必要である。また、科学は人間の知的欲求を満たしてくれる。そして、科学の成果は私たちの生活の質を向上させる。科学は「知」と「実」を与えてくれる。研究成果を実用化されるよう努めることも私たちの責務である。

今年度の主な研究成果は以下のようである。

(1) 分子状水素はフリーラジカル連鎖反応で生じる脂質メディエーターを調節して遺伝子発現を制御する

Iuchi, K., Imoto A., Kamimura N., Ichimiya H., Yokota T., Ohta S.: Molecular hydrogen regulates gene expression by modifying the free radical chain reaction-dependent generation of oxidized phospholipid mediators. Sci Rep. 2016 Jan 7;6:18971. doi: 10.1038/srep18971.

分子状水素が、遺伝子発現を制御するメカニズムを初めて解明した。分子状水素は脂質フリーラジカル連鎖反応に干渉し、脂質メディエーターを改変し、その脂質メディエーターがカルシウムシグナリングを制御し、遺伝子発現を制御するものである。

(2) 水素分子は、脂肪酸代謝を向上させるために、転写活性化補助因子 PGC-1α の遺伝子の発現を刺激する

Kamimura N, Ichimiya H, Iuchi K, Ohta S.: Molecular hydrogen stimulates the gene expression of transcriptional coactivator PGC-1α to enhance fatty acid metabolism. npj Aging and Mechanisms of Disease. 2016;2:16008 DOI:10.1038/npjamd.2016.8

分子状水素は、脂質代謝を促進するメカニズムを解明した。分子状水素は、脂質ラジカル連鎖反応を抑制し、過酸化脂質を低下させる。過酸化脂質から生成させる４―ヒドロキシノネナール（4-HNE）を低下させる。4-HNE がシグナル分子として機能して、PGC-1α を増加させ、脂質代謝関連遺伝子発現を亢進させるというものである。

(3) ラットの網膜における一酸化窒素由来ペルオキシナイトライトによって引き起こされる酸化ストレスに対する水素分子の保護効果

Yokota T, Kamimura N, Igarashi T, Takahashi H, Ohta S, Oharazawa: Protective effect of molecular hydrogen against oxidative stress caused by peroxynitrite derived from nitric oxide in rat retina. Clin Experiment Ophthalmol. 2015 Aug;43(6):568-77.

(4) 文脈性恐怖条件付後の急性拘束ストレスによる恐怖記憶の低減：タイミングの重要性

Uwaya A, Lee H, Park J1, Lee H, Muto J, Nakajima S, Ohta S, Mikami T: Acute immobilization stress following contextual fear conditioning reduces fear memory: timing is essential. Behav Brain Funct. 2016 Feb 24;12(1):8. 10.1186/s12993-016-0092-1.

学会・社会活動

ミトコンドリア学会機関誌である国際誌「Mitochondrion」の編集委員も引き続き務めている。また、Nature Partner Journal Aging and Mechanism of Disease が発刊され、Editorial Board となった。今年度は分子状水素医学シンポジウムから、日本分子状水素医学生物学会を設立し、初代の理事長を務めている。日本ミトコンドリア学会は理事、日本 Cell Death 学会では評議員も務めている。

〈原著論文〉

1. Nicolson, GL.[1)], Mattos, GF.[2)], Settineri, R.[3)], Costa, C.[2)], Ellithorpe, R.[4)], Rosenblatt, S.[5)], Valle, JL.[6)], Jimenez, A.[7)], Ohta, S. ([1)]Dept. Mol. Pathol,, The Inst. Mol. Med., Huntington Beach, USA., [2)]Lab. Ion Channels, Sch. Med., Univ. de la República, Montevideo, Uruguay., [3)]Sierra Res., Irvine, USA., [4)]Tustin Longevity Ctr., Tustin, USA., [5)]Saint John's Health Ctr., Santa Monica, USA. [6)]Progressive Med. Ctr., Orange, USA., [7)]Hope Cancer Inst., Playas de Tijuana, Mexico.): Clinical Effects of Hydrogen Administration:From Animal and Human Diseases to Exercise Medicine. Int J Clin Med.2016;7:32-76.

2. Iuchi, K., Imoto, A., Kamimura, N., Ichimiya, H., Yokota, T., Ohta, S.: Molecular hydrogen regulates gene expression by modifying the free radical chain reaction-dependent generation of oxidized phospholipid mediators. Sci Rep. 2016; 6:18971.

3. Kamimura, N., Ichimiya, H., Iuchi, K., Ohta, S.: Molecular hydrogen stimulates the gene expression of transcriptional coactivator PGC-1 α to enhance fatty acid metabolism. npj Aging and Mechanisms of Disease. 2016;2:16008.

4. Hayashida, K.[1)], Sano, M.[1)], Kamimura, N., Yokota, T., Suzuki, M.[2)], Ohta, S., Fukuda, K.[1)], Hori, S.[2)]. ([1)]Dept. Cardiol., Sch. Med., Keio Univ., [2)]Dept. Emergency and Critical Care Med., Sch. Med., Keio Univ.): Response to Letter Regarding Article, "Hydrogen Inhalation During Normoxic Resuscitation Improves Neurological Outcome in a Rat Model of Cardiac Arrest Independently of Targeted Temperature Management". Circulation. 2015;132(11):e148.

5. Yokota, T., Kamimura, N., Igarashi, T.[1)], Takahashi, H.[1)], Ohta, S., Oharazawa, H.[2)]. ([1)]Dept. Ophthalmol., [2)]Dept. Ophthalmol., Musashikosugi Hosp.): Protective effect of molecular hydrogen against oxidative stress caused by peroxynitrite derived from nitric oxide in rat retina. Clin Experiment Ophthalmol. 2015;43(6):568-77.

6. Kanamaru, T., Kamimura, N., Yokota, T., Nishimaki, K., Iuchi, K., Lee, H., Takami, S.[1)], Akashiba, H.[1)], Shitaka, Y.[1)], Ueda, M.[2)], Katsura, K.[2)], Kimura, K.[2)], Ohta, S. ([1)]Pharmacol. Res. Lab., Astellas Pharma Inc., [2)]Dept. Neurological Sci.): Intravenous transplantation of bone marrow-derived mononuclear cells prevents memory impairment in transgenic mouse models of Alzheimer's disease. Brain Res. 2015;1605:49-58.

7. Uwaya, A., Lee, H., Park, J.[1)], Lee, H.[2)], Muto, J.[3)], Nakajima, S.[4)], Ohta, S., Mikami, T.[5)]. ([1)]Dept. Lab. Med., The Jikei Univ. Sch. Med., [2)]Dept. Cell Biol. Neurosci., Juntendo Med. Sch., [3)]Grad. Sch. Health and Sport Sci., Nippon Sport Sci. Univ., [4)]Kyoritsu Women's Junior College, [5)]Dept. Health and Sport Sci.) : Acute immobilization stress following contextual fear conditioning reduces fear memory: timing is essential. Behav Brain Funct. 2016;12(1):8.

8. Iuchi, K., Yagura, T.[1)]. ([1)]Dep. Biosci., Sch. Sci. Technol., Kwansei Gakuin Univ.) : DNA binding activity of Ku during chemotherapeutic agent-induced early apoptosis. Exp Cell Res. 2016;342(2):135-44.

〈総説〉

1. Ohta, S.: Molecular hydrogen as a novel antioxidant: overview of the advantages of hydrogen for medical applications. Methods Enzymol. 2015;555:289-317.
2. 太田成男：分子状水素医学：広範な疾患治療と予防医学の応用へ向かって　臨床麻酔 2015:39(6):832-9.
3. 太田成男：ミトコンドリアとエイジング(老化)　アンチエイジング医学の基礎と臨床・第3版　メジカルルレビュー　編集：日本抗加齢医学会　専門医指導子認定委員会　2015; 80-81.
4. 太田成男：水素医学の創始、展開、今後の可能性：広範な疾患に対する分子状水素の予防ならびに治療の臨床応用へ向かって　生化学　2015;87(1)82-90.
5. 太田成男：医療への水素利用　ケミカルエンジニアリング　化学工業社 2015;60(3)42(206)-8(12).
6. 早坂理恵（太田成男：監修）水素美容のひみつ　産学社　2015. 5:1-112.

〈海外講演〉

1. Ohta, S.: Molecular Hydrogen as a Novel Antioxidant: Overviews of the Advantages of Hydrogen for Medical Applications. European Pharma Global Congress 2015. Valencia, Spain　2015. 08. 25-27.
2. Kamimura, N., Nishimaki, K., Ichimiya, H., Ohta, S.: Molecular hydrogen improves obesity and diabetes by regulating hepatic gene expression and stimulating energy metabolism in db/db mice. The 2015 Gordon Research Conference on Biology of Aging, Sunday River, USA, 2015. 07. 19-24.
3. Nishimaki, K., Yokota, T., Kamimura, N., Ohsawa, I., Ohta, S.: Drinking effect of hydrogen water prevents progression of Alzheimer's disease. The 2015 Gordon Research Conference on Biology of Aging, Sunday River, USA, 2015. 07. 19-24.

〈一般学会講演〉

1. 上村尚美，Wolf Alexander，一宮治美，井内勝哉，西槙貴代美，横田隆，太田成男：糖尿病モデルマウスの *in vivo* 酸化還元状態の測定と分子状水素の効果．日本分子生物学会年会（第38回）日本生化学会大会（第88回）合同大会．2015.12.1-4.
2. 井内勝哉，井本明美，西槙貴代美，一宮治美，Lee Hyunjin，横田隆，上村尚美，太田成男：分子状水素はフリーラジカル連鎖反応で生じる脂質メディエーターを調節して遺伝子発現を制御する．日本分子生物学会年会（第38回）日本生化学会大会（第88回）合同大会．2015.12.1-4.
3. 横田隆，上村尚美，五十嵐勉，高橋浩，小原澤英彰，太田成男：ペルオキシナイトライト産生酸化ストレス傷害に対する水素分子（H2）のラット網膜保護効果．日本分子生物学会年会（第38回）日本生化学会大会（第88回）合同大会．2015.12.1-4.
4. 上村尚美、Alexander M Wolf、一宮治美、井内勝哉、西槙貴代美、横田隆、太田成男：糖尿病モデルマウスにおけるミトコンドリアの in vivo 酸化還元状態の測定と分子状水素の効果　第15回日本ミトコンドリア学会　福井(福井県国際交流会館)　2015.11.19—20.

5. 井内勝哉，井本明美，西槙貴代美，一宮治美，Lee Hyunjin，横田隆，上村尚美，太田成男：TBHP を用いた酸化ストレス誘導性の細胞死に対する分子状水素の保護作用，第 24 回日本 CellDeath 学会学術集会，2015.7.11-12.
6. 中嶋裕也、太田成男、Wolf Alexander: ブルーライト照射による皮膚内での酸化ストレス誘導　第 40 回日本香粧品学会　東京（有楽町朝日ホール）2015.6.19（会期 6.18-19）
7. 太田成男：水素医学研究の最新情報　アンチエイジング歯科学会 2015.5.16（会期 5.16-17）

SCIENTIFIC REPORTS

OPEN

Molecular hydrogen regulates gene expression by modifying the free radical chain reaction-dependent generation of oxidized phospholipid mediators

Received: 13 July 2015
Accepted: 02 December 2015
Published: 07 January 2016

Katsuya Iuchi[1,*], Akemi Imoto[1,*,†], Naomi Kamimura[1,*], Kiyomi Nishimaki[1,*], Harumi Ichimiya[1], Takashi Yokota[1] & Shigeo Ohta[1,2]

We previously showed that H_2 acts as a novel antioxidant to protect cells against oxidative stress. Subsequently, numerous studies have indicated the potential applications of H_2 in therapeutic and preventive medicine. Moreover, H_2 regulates various signal transduction pathways and the expression of many genes. However, the primary targets of H_2 in the signal transduction pathways are unknown. Here, we attempted to determine how H_2 regulates gene expression. In a pure chemical system, H_2 gas (approximately 1%, v/v) suppressed the autoxidation of linoleic acid that proceeds by a free radical chain reaction, and pure 1-palmitoyl-2-arachidonyl-*sn*-glycero-3-phosphocholine (PAPC), one of the major phospholipids, was autoxidized in the presence or absence of H_2. H_2 modified the chemical production of the autoxidized phospholipid species in the cell-free system. Exposure of cultured cells to the H_2-dependently autoxidized phospholipid species reduced Ca^{2+} signal transduction and mediated the expression of various genes as revealed by comprehensive microarray analysis. In the cultured cells, H_2 suppressed free radical chain reaction-dependent peroxidation and recovered the increased cellular Ca^{2+}, resulting in the regulation of Ca^{2+}-dependent gene expression. Thus, H_2 might regulate gene expression via the Ca^{2+} signal transduction pathway by modifying the free radical-dependent generation of oxidized phospholipid mediators.

Molecular hydrogen (H_2) was originally thought to behave as an inert gas in mammalian cells; however, our previous studies showed that this is not always the case[1], demonstrating that H_2 neutralizes the hydroxyl radical (·OH) and peroxynitrite ($ONOO^-$) inside cells and acts as a novel antioxidant to protect the cells against oxidative stress[1,2]. Inhalation of 1%–4% (v/v) H_2 gas is effective for the treatment of ischemia/reperfusion injuries[1,3,4]. Recently, inhalation of 1.3% H_2 gas from a premixed gas was shown to protect neurons in a cardiac arrest model[5]. However, the mechanism of how such a low concentration of H_2 exerts the positive effects is not known.

Numerous studies have strongly suggested that H_2 has the potential for a variety of therapeutic and preventive applications[6,7]. In addition to extensive animal experiments, more than 10 clinical studies examining the efficacy of H_2 have been reported[6,7], including double-blinded clinical studies in patients with Parkinson's disease and rheumatism[8,9]. Based on these studies, the field of hydrogen medicine is rapidly growing.

Subsequently, H_2 was shown to exhibit multiple functions, including anti-inflammatory, anti-apoptotic, anti-allergic, and antioxidant activities, as well as regulation of differentiation and energy metabolism[6,7]. To exert multiple functions in addition to anti-oxidative roles, H_2 regulates various signal transduction pathways and the expression of many genes[6,7]. For examples, H_2 protects neural cells and stimulates energy metabolism by

[1]Department of Biochemistry and Cell Biology, Graduate School of Medicine, Nippon Medical School, 1–396 Kosugi-machi, Nakahara-ku, Kawasaki-city, Kanagawa 211–8533, Japan. [2]Department of Neuroregenerative Medicine, Juntendo University Graduate School of Medicine, 2-1-1 Hongo, Bunkyo-ku, Tokyo 113–8421, Japan. *These authors contributed equally to this work. †Present address: Department of Clinical Chemistry, School of Allied Health Sciences, Kitasato University, 1-15-1 Kitasato, Minami-ku, Sagamihara-city, Kanagawa 252-0373, Japan. Correspondence and requests for materials should be addressed to S.O. (email: ohta@nms.ac.jp)

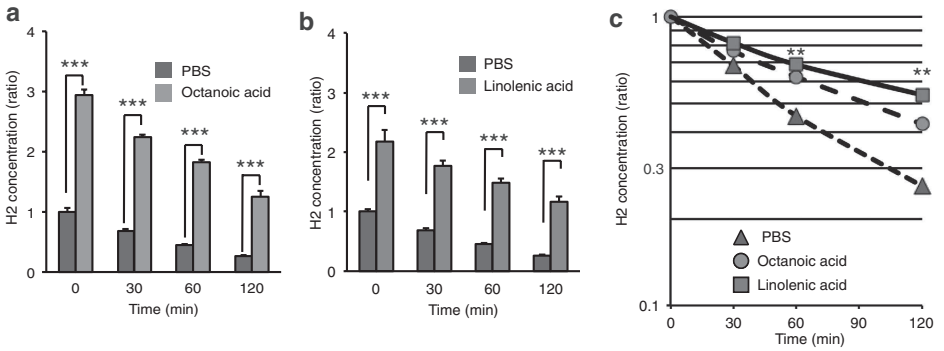

Figure 1. Solubility of H_2 in fatty acids in the presence of an aqueous solvent. H_2-saturated phosphate-buffered saline (PBS) was mixed with the same volume (75 mL) of saturated fatty acid (octanoic acid) (**a**) or unsaturated fatty acid (linolenic acid) (**b**) and maintained for 16 h in a closed aluminum bag as described in Methods. The same volume (3 mL) of each phase was transferred to each open tube (ϕ13 mm), followed by measurement of H_2 at the indicated time ($n = 4$). The experiments were performed at 25 °C. ***$P < 0.001$ *vs.* PBS. (**a**,**b**) Significance was calculated using an unpaired two-tailed Student's t-test. (**c**) Time courses of retention times of H_2 in each phase in the open vessels. **$P < 0.01$, *vs.* octanoic acid ($n = 4$).

stimulating the hormonal expression of ghrelin[10] and fibroblast growth factor 21 (FGF21)[11], respectively. In contrast, H_2 relieves inflammation by decreasing pro-inflammatory cytokines[12]. However, it is difficult to explain the molecular mechanisms by which H_2 exerts these functions by conventional concepts alone. To understand the molecular mechanisms by which H_2 exerts these multiple functions, it is essential to identify the primary targets of H_2 that modulate signal transduction and gene expression.

Therefore, in this study, we aimed to elucidate one of the molecular mechanisms by which H_2 mediates signal transduction and gene expression. Our results suggested that low concentrations of H_2 modulated Ca^{2+} signal transduction and regulated gene expression by modifying the production of oxidized phospholipid species.

Results

H_2 accumulated in the lipid phases. To understand the difference between intracellular conditions and aqueous solutions, we focused on the lipid phases to determine the intracellular localization of H_2 accumulation at room temperature. H_2 incorporation was two- or three-fold higher in the liquid fatty acid phases than in the aqueous phase in the presence of both water and fatty acids, and was retained longer in the fatty acid phases than in the aqueous phase in open vessels (Fig. 1a,b). In particular, H_2 seemed to be retained significantly longer in the unsaturated fatty acid (linolenic acid) than in the saturated fatty acids (octanoic acid) (Fig. 1c), although this difference in retention time might be attributed to the difference in the number of carbons. Since unsaturated fatty acids are the primary targets for initiating a free radical chain reaction, we assumed that H_2 could efficiently suppress this reaction in biomembranes, even at low concentrations.

Autoxidation of unsaturated fatty acids was suppressed by low concentrations of H_2 gas. Autoxidation of unsaturated fatty acids proceeds by a free radical chain reaction in air[13]. Thus, we measured autoxidation of a filmy di-unsaturated fatty acid (linoleic acid: R-CH = CH-CH_2-CH = C-R') at 37 °C for 20 h in the dark in the presence of various concentrations of H_2 gas. A conjugated diene, which should be formed by autoxidation, was estimated by the absorption at 234 nm (Fig. 2a). The absorption at 234 nm was increased depending on the formation of the conjugated diene [R-CH = CH-CH = CH-CH(-OOH)-R' or R-CH(-OOH)-CH = CH-CH = CH-R'] accompanied by peroxidation in a pure chemical system (H_2, O_2, and N_2 were supplied from gas cylinders) (Fig. 2b). O_2 was essential for autoxidation (Fig. 2c). As a result, even only approximately 1% H_2 gas significantly suppressed autoxidation of linoleic acid at 37 °C, even in the absence of any catalysts in the dark in a pure chemical system (Fig. 2c).

Ca^{2+} signal transduction by H_2-dependent chemical oxidation of phospholipids. Phospholipids are converted into oxidized mediators that modulate various signal transduction pathways by not only enzymatic reactions, but also by chemical oxidation[14,15]. Oxidized phospholipids, including 1-palmitoyl-2-(5-oxovaleroyl)-*sn*-glycero-3-phosphocholine (POVPC) and 1-palmitoyl-2-glutaroyl-*sn*-glycero-3-phosphocholine (PGPC), are present in oxidatively modified low-density lipoproteins (oxLDLs) and have been found in atherosclerotic lesions[15]. These compounds are important as inducers of different cellular responses, including inflammation, proliferation, and cell death. Moreover, autoxidation of 1-palmitoyl-2-arachidonyl-*sn*-glycero-3-phosphocholine (PAPC) leads to the chemical production of various bioactive phospholipid species, such as POVPC, PGPC, 1-palmitoyl-2-(5-hydroxy-8-oxooct-6-enoyl)-*sn*-glycero-3-phosphocholine (HOOA-PC), and 5-hydroxy-8-oxo-6-octenedioic acid (HOdiA-PC)[14,15].

We assumed that low concentrations of H_2 would influence some chemical reactions leading to the production of putative oxidized lipid mediators for the modulation of signal transduction. Because PAPC is one of the major phospholipids in mammalian biomembranes, the role of H_2 in the chemical production of oxidized phospholipid

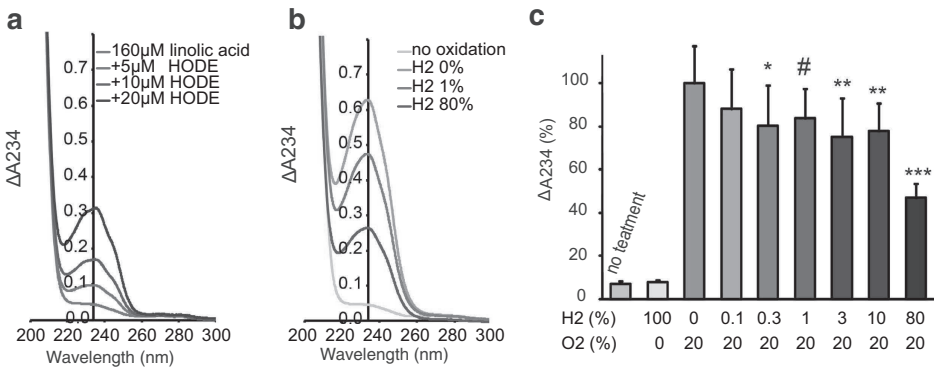

Figure 2. Suppression of autoxidation of linoleic acid-film by H_2 gas. (**a**) Profile of ultraviolet absorption of 9-hydroxyoctadecadienoic acid; $CH_3(CH_2)_4$-CH = CH-CH = CH-CH(-OH)-$(CH_2)_7$-COOH) (9-HODE) in cyclohexane, shown as a standard conjugated diene. (**b**) Linoleic acid-film was autoxidized at 37 °C for 20 h in a glass tube placed in a closed aluminum bag in the presence of various concentrations of H_2 and O_2 as described in Methods. Representative profiles of ultraviolet absorption of the cyclohexane solution of H_2-dependent autoxidized linoleic acid are shown. (**c**) Linoleic acids autoxidized with various concentrations of H_2 were evaluated by measuring absorption at 234 nm. $^*P = 0.034$ (0.3% H_2), $\#P = 0.069$ (1% H_2), $^{**}P < 0.01$ (3% H_2, 10% H_2), and $^{***}P < 0.001$ (80% H_2) *vs.* 0% H_2 ($n = 15$).

mediators was determined by conducting autoxidation of pure PAPC (resulting in OxPAPC) in the absence of any catalysts in the dark. The peroxidation of PAPC in air was confirmed by an increase in the signal for the fluorescent dye specific to lipid peroxides, Liperfluo (Fig. 3a). A previous study indicated that OxPAPC activates transcription factors involved in Ca^{2+} signaling[16]. Indeed, when THP-1 cells (a human monocytic cell line derived from a patient with acute monocytic leukemia) were exposed to OxPAPC, a transient increase in cellular Ca^{2+} was observed when a Ca^{2+}-sensitive fluorescent dye, Fluo4-AM was used (Fig. 3b). This Ca^{2+} signaling depended on OxPAPC in an oxidation time-dependent manner (Fig. 3c).

Next, the H_2-dependent production of OxPAPC, which leads to the activation of Ca^{2+} signaling, was investigated by autoxidizing PAPC for 3 days at 25 °C in air at various concentrations of H_2 (designated as H_2OxPAPC, and the notation of H_2[x%]OxPAPC was used when autoxidized in the presence of x% H_2). H_2 suppressed the generation of total peroxides as revealed by Liperfluro fluorescence intensity (Fig. 3d). Ca^{2+} signaling was observed when PAPC was autoxidized with less than 0.3% H_2, whereas more than 1.3% H_2 significantly disrupted this signaling (Fig. 3e).

In order to investigate the molecule(s) influenced by H_2, we analyzed H_2OxPAPCs by using mass spectrometry on autoxidation day 3. In all, 209 bands were detected, with molecular masses ranging from 126.3754 to 991.6494 Da; this was consistent with the findings of a previous report[15] (Supplementary Fig. 1). The differences in the production of H_2OxPAPC and OxPAPC species were presented using a heat map (Supplementary Fig. 1i). The levels of many bands were increased or decreased with differences in concentrations of H_2. For examples as the relatively increased species, the levels of the Ca^{2+} signaling inducers POVPC[16], HOOA-PC, HOdiA-PC, and hydroxyeicosatetraenoic acid-3-phosphocholine (HETE-PC)[17] were slightly increased in response to H_2 (Supplementary Fig. 1i).

Because the reduced form of POVPC was reported to function as an antagonist[18], it is possible that increased levels of the reduced form(s) of some OxPAPC species, rather than the decreased levels of putative agonists (such as POVPC), might have disrupted Ca^{2+} signaling as a putative antagonist(s). Further studies are warranted to identify the H_2-dependent bioactive mediator(s).

Comprehensive analysis of H_2-dependent regulation of gene expression. Next, we investigated how H_2OxPAPC influences gene expression. PAPC was autoxidized in the absence or presence of various concentrations of H_2 for 3 days and then administered to cultured THP-1 cells. In a preliminary experiment, the change in the expression level of tumor necrosis factor (TNF)-α gene in response to OxPAPC from that to H_2OxPAPC peaked at 4 h. Thus, by using microarray analysis, we comprehensively analyzed the change in gene expression in response to the H_2-dependent mediators at 4 h in three samples under each condition. In all, 86 genes were selected according to the following criteria as described in the legend of Fig. 4a: a significant increase in OxPAPC (*vs.* PAPC), and a significant decrease in H_2[1.3%]OxPAPC and H_2[5%]OxPAPC (*vs.* OxPAPC) (Supplementary Table 1). The gene expression profile was presented in a heat map (Fig. 4a). The selected genes were validated by semi-quantitative real-time polymerase chain reaction (RT-PCR), and marginal changes in the expression levels of some genes were confirmed (Supplementary Fig. 2).

In addition, the regulatory expression of TNF-α and IL-8 by H_2OxPAPC was investigated using THP-1 and a different cell type (human aortic endothelial cells: HAEC), respectively (Fig. 4b,c).

According to the Kyoto Encyclopedia of Genes and Genomes (KEGG) Pathway Database (http://www.genome.jp/kegg/pathway.html), the functions of 7,143 genes were identified and classified (Fig. 4d, upper). We

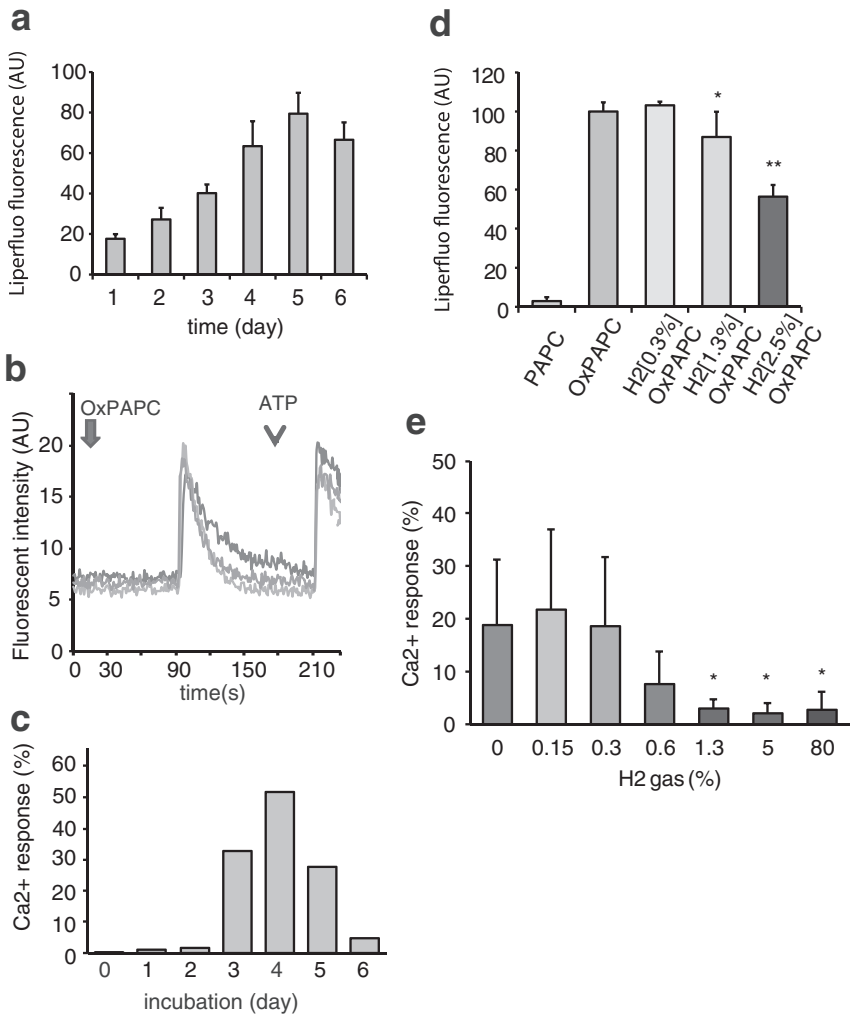

Figure 3. PAPC autoxidized with H_2 modulated Ca^{2+} signaling. (**a**) Chemically pure PAPC was autoxidized in air with 100% humidity at 25 °C in a closed aluminum bag for the indicated periods, and time-dependent production of peroxides in air from chemically pure PAPC was estimated using Liperfluo fluorescence, where wavelengths of excitation and emission were set at 488 and 535 nm, respectively, as described in Methods. (**b**) Representative responses in THP-1 by OxPAPC with the fluorescent Ca^{2+} indicator Fluo4-AM are shown as described in Methods. The arrow and arrowhead indicate the addition of OxPAPC and ATP, respectively. ATP (a ligand of the Ca^{2+} channel P2X7) was used as a positive control. (**c**) PAPC was autoxidized for the indicated periods at 25 °C, and subjected to the Ca^{2+}-signaling assay in THP-1 cells. The OxPAPC-induced Ca^{2+} response depended on autoxidizing period of OxPAPC. (**d**) PAPC was autoxidized in air for 3 days in the absence or presence of the indicated concentrations of H_2 (H_2OxPAPC), and the peroxide of OxPAPC or H_2OxPAPC was estimated using Liperfluo as described in (**a**) ($n = 3$-6). $^*P = 0.044$, $^{**}P < 0.01$. (**e**) PAPC was autoxidized in air for 3 days with the indicated concentrations of H_2 (H_2OxPAPC) and then subjected to Ca^{2+} signaling assays as described in Methods ($n = 6$). $^*P = 0.021$ (1.3%H_2), $^*P = 0.022$ (5% H_2), and $^*P = 0.030$ (80% H_2) *vs.* no H_2.

classified the 86 selected genes (Fig. 4e, lower). Of these 86 genes, 46.5% belonged to those involved in signaling pathways (Fig. 4d, upper), whereas 25.8% of the total number of 7,143 genes is involved in signaling pathways (Fig. 4d, lower). Genes encoding factors involved in signal transduction and transcription factors are indicated by blue and black, respectively, on the right in the heat map (Fig. 4a).

Among the genes involved in signaling pathways, the proportion of those belonging to Ca^{2+} signaling were lower in the selected genes than in those in the entire genome, indicating that H_2 regulates fewer components of the Ca^{2+} signaling pathways (Fig. 4e, lower). This was consistent with the finding that H_2OxPAPC decreased Ca^{2+} signaling. In contrast, the proportion of genes belonging to the mitogen-activate protein kinase (MAPK)

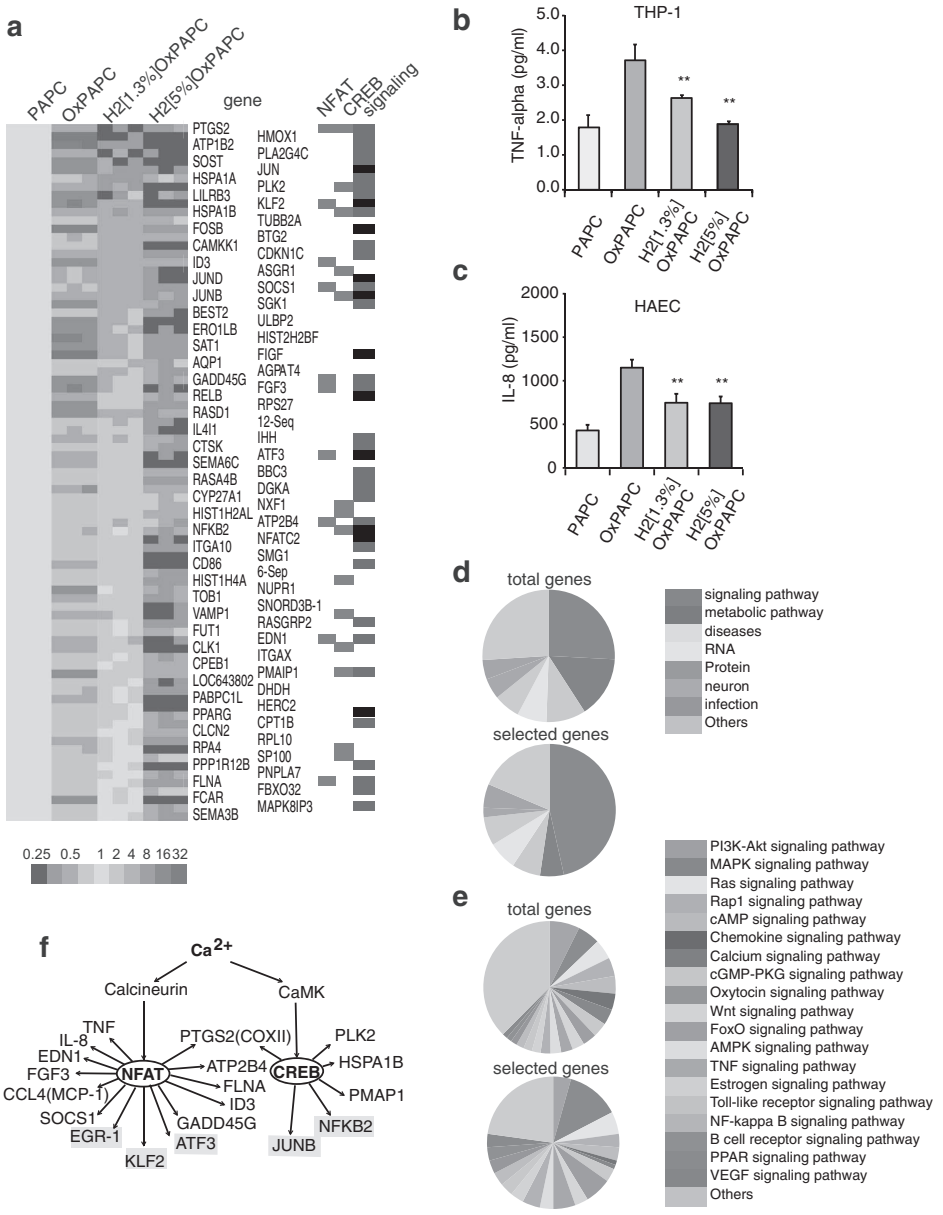

Figure 4. Changes in gene expression regulated by H_2OxPAPC. (**a**) Three samples of PAPC, OxPAPC, and H_2OxPAPC were exposed to THP-1 cells for 4 h , and the gene expression was comprehensively analyzed using microarray. Eighty-six genes were selected according to the following criteria; genes up-regulated by OxPAPC (more than 2.5-fold, *vs.* PAPC) and those down-regulated by H_2[1.3%]OxPAPC and H_2[5%]OxPAPC (less than 0.75-fold and 0.5-fold, respectively, *vs*. OxPAPC) are shown in a heat map (red and green indicate the up-regulation *vs.* PAPC treatment, and the down-regulation *vs.* OxPAPC treatment, respectively, as shown in the color gradient). Possible target genes of NFAT and CREB are marked with red on the right. Genes encoding factors involved in signal transduction and transcription are indicated by blue and black, respectively, on the right. The release of TNF-α (**b**) (from THP-1) and IL-8 (**c**) (from HAEC) was investigated using ELISA as described in Methods. (**d**, upper) Ratio of genes belonging to each category for a total of 7,142 genes identified by the KEGG database. (**d**, lower) Ratio of genes belonging to each category in the 86 selected genes listed in a. (**e**, upper) Ratio of genes belonging to each signaling pathway identified by the whole KEGG database. (**c**, lower) Ratio of genes belonging to each signaling pathway in the selected genes listed in (**a**). (**f**) The H_2OxPAPC-dependent expression of genes transcribed by CREB and NFAT. Transcription factors are indicated in yellow.

signaling was higher (Fig. 4e, lower), indicating that H_2 regulates more components of MAPK signal transduction pathways (Fig. 4e, lower).

The signal transduction pathways that were regulated by H_2 are shown in Supplementary Table 1 according to the KEGG Pathway Database. These data suggested the possibility that low concentrations of H_2 contribute to various signal transduction pathways via oxidized phospholipid species.

cAMP response element binding protein (CREB)-target genes were selected according to the CREB Target Gene Database (http://natural.salk.edu/CREB/), and nuclear factor of activated T cells (NFAT) target genes were selected by referring to Medline, as shown in Supplementary Table 1. The target genes of CREB and NFAT are marked by red on the right in the heat map panel as NFAT or CREB (Fig. 4a). A considerable number of the selected genes were targets of CREB or NFAT (Fig. 4f). These data are consistent with the findings of previous studies showing the Ca^{2+}-dependent regulation by these transcription factors: CREB is activated via phosphorylation by a calmodulin-dependent kinase (CaMK)[19] in a Ca^{2+}-dependent manner, and NFAT is dephosphorylated by calcineurin (CN) in a Ca^{2+}-dependent manner, translocates to the nucleus, and then functions as a transcription factor with its partner proteins, e.g., activator protein 1 (AP-1), CREB, or nuclear factor-kappa B (NF-κB)[20]. Indeed, exposure of THP-1 to OxPAPC, but not to H_2OxPAPC, stimulated the nuclear translocation of NFAT (Supplementary Fig. 3).

Thus, H_2-dependent oxidized mediators or putative antagonists could be associated with transcriptional regulation via Ca^{2+} signaling.

Free radical inducers contributed to the NFAT pathway in cultured cells. Autoxidation of unsaturated fatty acids, including PAPC, proceeds by a free radical chain reaction[13], and·OH is the primary trigger for this reaction[13,21,22]. We previously showed that H_2 reduces ·OH levels inside cultured cells by using the spin trapping method and a specific fluorescent indicator[1]. Thus, in this study, we investigated the effects of H_2 on the lipid free radical chain reaction by using cultured cells. To initiate a free radical chain reaction inside the cells, we used 2,2′-azobis(2-methylpropionamidine)dihydrochloride (AAPH)[23], which is not affected by H_2 (Supplementary Fig. 4) and is suitable for the slow generation of free radicals by a spontaneous chemical reaction. The lipid free radical chain reaction results in the production of lipid peroxides (LPOs)[21,24], which can be detected using the fluorescent dye Liperfluo[25]. Thus, we exposed cultured THP-1 cells to AAPH and estimated LPO production based on the Liperfluo signal. The Liperfluo signal significantly decreased in the presence of low levels of H_2 gas (e.g., 1.3%; Fig. 5a,b). Thus, even at such low concentrations, H_2 has the potential to reduce the generation of LPOs by suppressing the initiation and/or propagation of free radical chain reactions in cultured cells.

Next, we determined whether the responses induced by chemically produced H_2OxPAPC (Figs 3 and 4) could simulate the effects induced by the free radicals in cultured cells. When THP-1 cells were exposed to AAPH, the cellular Ca^{2+} levels increased (Fig. 5c) in a time-dependent manner (Fig. 5d), as shown by the analysis of Fluo-3, and the Ca^{2+} signaling was suppressed by H_2 (Fig. 5c,e). NFAT was also activated, as shown by the translocation of NFAT into the nucleus (Fig. 5f,g), and the nuclear translocation of NFAT were recovered by H_2 (Fig. 5f,g). Moreover, the free radical inducer stimulated the expression of some target genes of NFAT, including *TNF-α*, early growth response protein 1 (*EGR1*), and activating transcription factor 3 (*ATF3*), which have been shown in Supplementary Table 1, and H_2 decreased their expressions (Fig. 5h), suggesting that H_2 regulates these genes via the NFAT pathway.

In contrast, AAPH-mediated activation of CREB was not observed (Supplementary Fig. 5) in this cultured cell line, regardless of the stimulation of cellular Ca^{2+}. In particular, the expression of the CREB-target gene *NFKB2* (NF-κB, subunit 2 gene) was not affected by AAPH (Fig. 5i), and the expression of *HMOX1* (Heme Oxygenase 1 gene), a nuclear factor-E2-related factor 2 (Nrf2)-target, was slightly but not significantly increased by H_2 (Fig. 5i). This result was consistent with those of a previous study[26]. Thus, the NFAT pathway could mainly contribute to the H_2-dependent transcriptional response induced by free radicals at least in THP-1 cells.

Taken together, these cellular responses, at least partly, are in agreement with those obtained using the *in vitro* H_2-dependent products of OxPAPC species (Figs 3, 4). Therefore, we proposed a model in which H_2 is linked to the modulation of Ca^{2+} signal transduction and the NFAT pathway via oxidized phospholipid species, as illustrated in Fig. 6.

Discussion

While the biological effects of H_2 have been evaluated in more than 300 animal studies and 10 clinical analyses in humans[6,7], the molecular mechanisms by which H_2 at low concentrations exerts its multiple effects on signal transduction remained unknown. Therefore, in this study, we aimed to examine how H_2 regulates signal transduction pathways that mediate gene expression. Our results suggested that low concentrations of H_2 modulated Ca^{2+} signal transduction and regulated gene expression by modifying the production of oxidized phospholipid species. Hence, these data provide important insights into one of the molecular mechanisms by which H_2 mediates gene expression.

H_2 can be ingested via several methods. Drinking of H_2-infused water (H_2-water) has been shown to be efficacious in the treatment of various diseases in animal models and humans[6,7]; however, H_2 can be infused up to only 0.8 mM under atmospheric pressure, and drinking saturated H_2-water provides a blood concentration up to only ~10 μM, with a short dwelling time in the body[11,27]. Moreover, inhaling 1%–4% (v/v) H_2 gas was shown to be effective, reaching concentrations of 8–32 μM H_2 in the blood[1,4,5]. However, initiation of cellular signals by these low concentrations of H_2 may be difficult to be explained because H_2 should be too inert to react with most molecules. To activate H_2 for reaction with the other molecules, a sufficient level of a putative catalyst must be present; however, it is unlikely that such a putative catalyst would be abundant inside cells. Moreover, H_2 is very small and is unlikely to bind to a putative H_2-binding receptor because its intra-molecular fluctuation would be

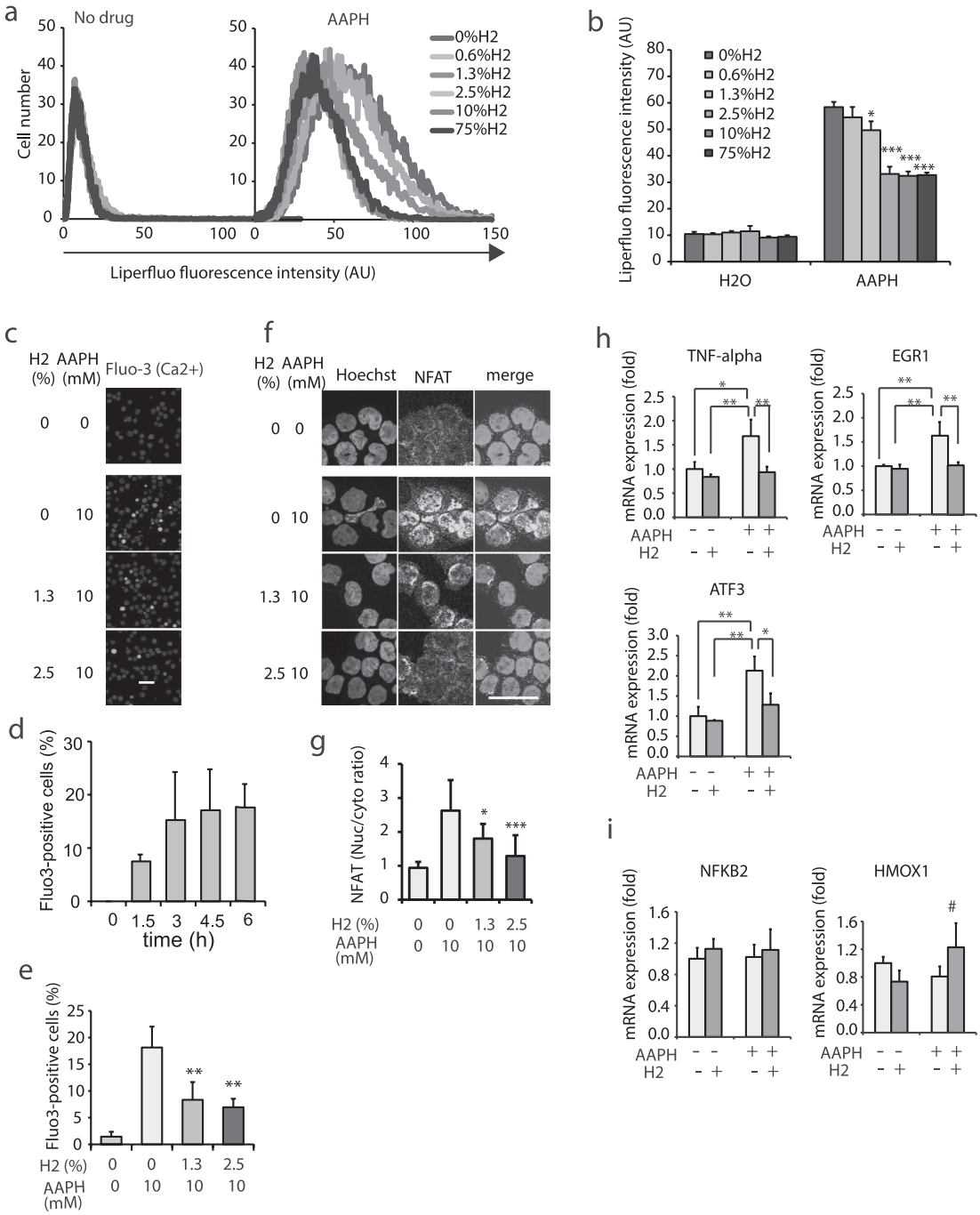

Figure 5. H_2 suppressed free radical inducer-dependent fatty acid peroxidation and Ca^{2+} and NFAT signaling. (**a**) THP-1 was exposed to a free radical inducer (10 mM AAPH) in the absence or presence of the indicated concentrations of H_2 for 4.5 h. Representative flow cytometric profiles are shown to demonstrate lipid peroxides with Liperfluo signals. (**b**) The Liperfluo signals were quantified. $^{*}P = 0.015$, $^{***}P < 0.001$ *vs.* 0% H_2 ($n = 6$). (**c**) THP-1 cells were treated with 10 mM AAPH for 3 h in the presence of the indicated concentrations of H_2. Intracellular Fluo-3 fluorescence intensity was observed using a laser scanning confocal microscope. Scale bar: 50 μm. (**d**) THP-1 cells were treated with 10 mM AAPH for the indicated periods in the absence of H_2 and then time dependent increase in Ca^{2+}-signal was monitored by intracellular Fluo-3 fluorescence intensity as described in (**c**). (**e**) Fluo3-positive cells were semi-quantified after the treatment with 10 mM AAPH for 3 h in the absence or presence of the indicated concentrations of H_2. $^{**}P < 0.01$ *vs.* no H_2 ($n = 3$). (**f**) THP-1 was

treated with 10 mM AAPH for 3 h in the presence of the indicated concentrations of H_2. The translocation of NFAT into the nucleus was examined as described in Methods and shown by immunostaining in yellow. The nucleus was counter-stained with Hoechst 33342 as shown in blue. Scale bar: 50 μm. (**g**) The NFAT-expressing areas were semi-quantified and shown by the ratio of NFAT in the nucleus with that in cytosol. $^{*}P = 0.023$ and $^{**}P < 0.01$ *vs.* no H_2 ($n = 10$). (**h**,**i**) The expressions of the NFAT-target genes (*TNF-α*, *EGR1*, and *ATF3*) (**h**) and non-NFAT target gens (*NFKB2* and *HMOX1*) (**i**) were estimated using RT-PCR coupled with a TaqMan probe (the probes are listed in Supplementary Table 2). The names of the genes are described in Supplementary Table 1. $^{*}P = 0.015$ (for *ATF3*) (+AAPH and +H_2 *vs.* +AAPH and –H_2). #$P = 0.14$ (for *HMOX1*) (+AAPH and –H_2 *vs.* +AAPH and + H_2), and $^{**}P < 0.01$ ($n = 3$)

expected to lead to instability in terms of thermodynamics, as previously discussed[28]. Thus, it was unknown how low concentrations of H_2 regulate signal transduction and gene expression.

Since increased oxidative stress involving ·OH triggers free radical chain reactions, we assumed that the chemically produced mediators derived from phospholipids could contribute to various pathogenic conditions. In the present study, we verified that a small amount of H_2 (as low as 1.3%) affected free radical-dependent lipid peroxidation, from which oxidized lipid mediators should be derived[22].

Generally, H_2 hydrogenates unsaturated fatty acids at higher temperatures with a palladium catalyst. To the best of our knowledge, no studies have examined autoxidation-dependent hydrogenation at approximately 1% (v/v) H_2 gas at 37 °C without any catalysts. Although H_2 was thought to be inert in the absence of a catalyst at body temperature, we demonstrated that approximately 1% (v/v) H_2 suppressed autoxidation of an unsaturated fatty acid in a chemically pure system in this study; thus, our data provided insights into the biological activities of H_2.

There are two possibilities: the effects of oxidized phospholipid species on Ca^{2+} signaling may be explain by decreased levels of a putative agonist that induces Ca^{2+} signaling or by increased levels of a putative antagonist that disturbs Ca^{2+} signaling. Although we could not identify these species in this study, it is likely that H_2 modified the production of reduced forms of oxidized phospholipid species during free radical chain reactions by the following previous findings: POVPC is a bioactive phospholipid-mediator that is produced by chemical oxidation of PAPC, and the reduced form of POPVC has been shown to function as an antagonist for signal transduction[18]. Thus, it is possible that during a lipid free radical chain reaction, H_2 contributes to the generation of a reduced form(s) that function(s) as an antagonist(s). Therefore, we proposed a hypothetic model in which H_2 is linked to the modulation of Ca^{2+} signal transduction and the NFAT pathway via oxidized phospholipid species as illustrated in Fig. 6.

Previous studies have shown that 1%–4% was efficacious in inhaling H_2 gas in various animal experiments[1,3,4,29–31]. Since a mixed gas containing 1.3% H_2, 30% O_2 and 68.7% N_2 is available, the effects of around 1.3% needed to be investigated in further studies, including clinical ones[5]. The effective concentrations of H_2 gas were approximately consistent throughout this study (Figs 2–5).

No receptors involved in Ca^{2+} signaling were identified in the present study; however, a previous study showed that some chemically oxidized phospholipid mediators, such as 9-HODE and 11-HETE, could bind a G-protein coupled receptor (G2A) to induce Ca^{2+} signaling[17]. Thus, putative oxidized phospholipid mediators or antagonists might bind to G-protein coupled receptors to modulate signal transduction.

In addition to the anti-oxidative roles of H_2, it has shown to function as an immunosuppressant in allograft transplantation[32]. This immunosuppressant effect can be explained by the suppression of NFAT activation because an immunosuppressant such as CsA and tacrolimus (FK506) acts through the inactivation of calcineurin. Since pro-inflammatory cytokines are regulated by NFAT-dependent mechanisms[20], the anti-inflammatory effects by H_2 can be explained by the suppression of NFAT. Additionally, the anti-allergic effects of H_2 can be explained by the decrease in Ca^{2+}/NFAT signaling[33].

A considerable number of the multiple functions of H_2, as shown by previous studies, might be explained by the link between H_2 and NFAT because of the numerous multiple functions of NFAT[20,34]. For example, decreased expression of inducible nitric oxide synthase (iNOS) by H_2[35] can be explained by the inactivation of NFAT[36]. The suppression of osteoclast differentiation[37] and improvement of hypertension[38,39] by H_2 could involve the NFAT pathway[40,41]. Moreover, the decreased expression of gene products through an NFAT-dependent pathway might be involved in α-synuclein-induced degeneration of midbrain dopaminergic neurons in Parkinson's disease[42]. This NFAT-dependent pathway might explain the beneficial effects of H_2 in these patients[8]. Further studies are needed to elucidate the mechanisms by which H_2 exerts multiple functions in terms of the involvement of the NFAT pathway.

In summary, in this study, we investigated the link among H_2, oxidized phospholipids, and Ca^{2+} signaling. Further studies are warranted to identify the H_2-dependent bioactive mediator(s). Our data provided important insights into one of the mechanisms by which H_2 regulates signal transduction and gene expression; however, H_2 might contribute to other types of signaling pathways as well because H_2 regulates many genes belonging to various signaling pathways. A more detailed understanding of the molecular mechanisms of H_2-dependent signal transduction and gene expression is expected to facilitate the application of H_2 in a wide range of medical applications.

Methods

Measurement of H_2. Gases containing H_2 were prepared by mixing H_2, O_2, N_2, and CO_2 at various concentrations from each gas cylinder equipped with a flow meter. The H_2 concentration in the mixed gas or air was tested in each experiment by using gas chromatography (Breath Gas Analyzer, Model TGA2000; TERAMECS Co. Ltd., Kyoto, Japan) as described previously[1]. For the measurement of H_2 in the solvent, H_2 was transferred to the air phase in a closed aluminum bag, and the concentration of H_2 measured by using gas chromatography

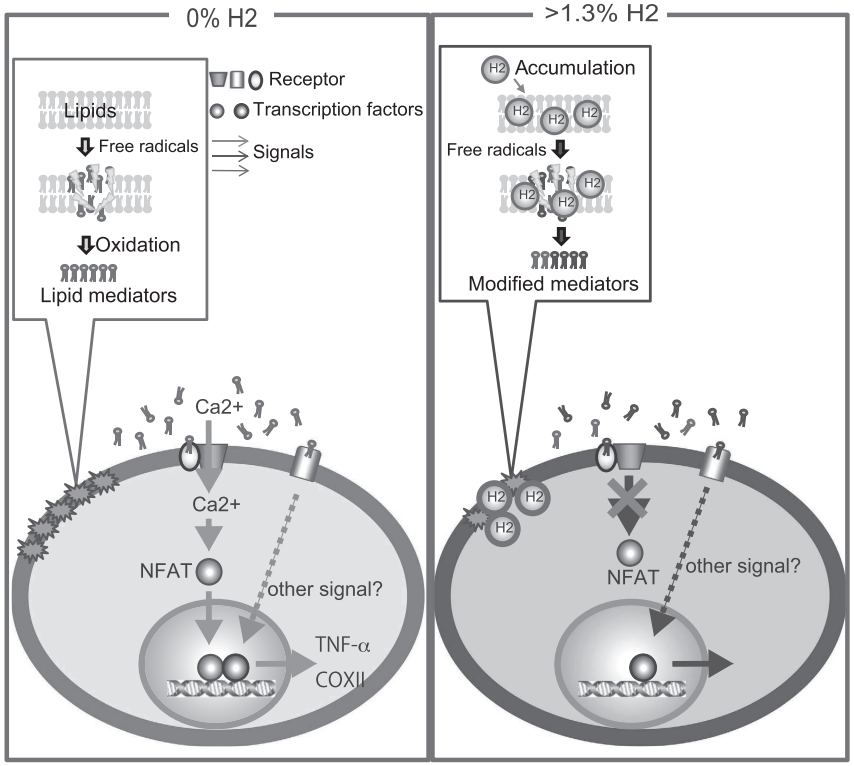

Figure 6. A model of the proposed pathway. When free radical chain oxidation generates oxidized phospholipid mediators, Ca^{2+} signaling is induced, followed by the activation of calcineurin and subsequent induction of the NFAT pathway. On the other hand, H_2 modifies the production of oxidized phospholipids by modulating free radical chain reactions. The putative oxidized phospholipids appear to function as antagonists and lead to a decline in Ca^{2+} signaling.

as described previously[1]. The aluminum used in the bag was covered with a plastic film to avoid any influence of aluminum.

Autoxidation of linoleic acid-film. Linoleic acid and (±)9-HODE were purchased from Nacalai Tesque (Kyoto, Japan) and CAY (MI, USA), respectively. Linoleic acid was dissolved in cyclohexane to 16 mM, and 2 μL was dispensed into each glass tube (ϕ10 × 50 mm) that had been filled with argon gas; it was allowed to dry up to form a linoleic acid-film at the bottom of a glass tube. The glass tubes were placed into a closed aluminum bag, and the gas in the bag was completely replaced with the indicated mixed gas, where pure H_2, O_2, and N_2 were obtained from separate cylinders. The bag was incubated at 37 °C for 20 h for the autoxidation, and 0.2 mL cyclohexane was immediately added to the glass tube to obtain 0.16 mM peroxidized linoleic acid. The concentration of conjugated diene was estimated by measuring the absorption at 234 nm while scanning from 200 to 300 nm.

Autoxidation of pure PAPC in air in the absence or presence of H_2. Chemically synthesized pure PAPC was purchased from Avanti Polar Lipids (Alabaster, AL, USA). PAPC was autoxidized in air as described previously[43]. Briefly, 0.5 mg of PAPC in 50 μL of chloroform was transferred to a ϕ10 × 50 mm glass tube and dried up under a gentle stream of nitrogen. The lipid residue was allowed to autoxidize in air with 100% humidity at 25 °C in the presence or absence of the indicated concentrations of H_2 gas in a closed aluminum bag for the indicated periods, and then suspended in PBS at a concentration of 0.5 mg/mL.

Estimation of OxPAPC with Liperfluo. OxPAPC was assayed in ethanol with Liperfluo as described previously[25]. Five min after adding OxPAPC to 1 μM Liperfluo at room temperature, the fluorescence was measured using a fluorescence spectrophotometer (RF-5300PC; Shimadzu Corporation, Kyoto, Japan), where wavelengths of excitation and emission were set at 488 and 535 nm, respectively.

Measurement of Ca^{2+} signaling. Intracellular Ca^{2+} in THP-1 cells treated with OxPAPC was measured using a Calcium Kit-Fluo 4 (CS22; Dojindo, Kumamoto, Japan) according to the manufacturer's protocol. Briefly, THP-1 cells were washed with PBS and incubated with 4.5 μM Fluo 4-AM in recording medium (20 mM HEPES,

115 mM NaCl, 5.4 mM KCl, 0.8 mM $MgCl_2$, 1.8 mM $CaCl_2$, 13.8 mM glucose) containing 0.064% pluronic F-127 and 1.25 mM probenecid for 30 min at 37 °C. The cells were washed with PBS and resuspended in recording medium containing 1.25 mM probenecid. The cells were seeded on 35-mm glass-bottomed dishes and then stimulated with 100 μg/mL OxPAPC or H_2OxPAPC, followed by 25 μM ATP. The changes in Fluo 4-AM fluorescence were monitored using a laser scanning confocal microscope (FV1200; Olympus Corporation, Tokyo, Japan). The strength of each fluorescent signal in 400 cells was examined and judged as positive if there was greater than 30% of the ATP signal.

Intracellular Ca^{2+} of THP-1 cells treated with the free radical inducer AAPH[23] was measured by Fluo-3 (F-23915; Molecular Probes, Eugene, OR, USA). Briefly, THP-1 cells were pre-incubated with 2 μM Fluo 3-AM in HBSS containing 0.02% pluronic F-127 for 30 min at 37 °C, resuspended in RPMI1640 (with 10% FBS) containing 2.5 mM probenecid, seeded in 24-well plates, and then treated with AAPH in the presence or absence of H_2. Changes in Fluo-3 fluorescence signals were observed using a laser scanning confocal microscope (FV1200; Olympus).

Mass spectrometric analysis and presentation of data using heat maps. OxPAPC (dissolved in chloroform at 2.5 mg/mL) was analyzed using by electrospray ionization-mass spectrometry (ESI-MS) by using an LTQ ORBITRAP XL mass spectrometer (Thermo Fisher Scientific, San Jose, CA, USA) equipped with a nitrogen sheath gas flow rate of 40 AU at 300 °C. The sample was directly infused. The scanning range was from *m/z* 250 to 1000 in the positive ion detection mode. The ion spray voltage was set to 4 kV. OxPAPC species were identified according to their *m/z* values and confirmed using mass spectrometric analysis as described previously[14,44,45].

Two independent experiments were performed. The average of the data was used for construction of a heat map and displayed in mass spectrometric profiles. In the heat map, bands were arranged according to molecular mass from small to large, and the strength of each band obtained from H_2OxPAPC was compared with those by OxPAPC. Red and green bands represented increased and decreased levels as compared with those of OxPAPC, respectively. The mass spectrometric display indicates the average band from two experiments. Only when bands were detected by all of 10 experiments (two experiments at 0%, 0.2%, 0.3%, 1.3% and 5% of H_2), they were adopted.

Comprehensive analysis of gene expression. THP-1 cells were exposed for 4 h to PAPC or OxPAPC, H_2[1.3%]OxPAPC, and H_2[5%]OxPAPC that had been autoxidized for 3 days with 0%, 1.3%, or 5% H_2, respectively. Total RNA was extracted using an RNeasy Mini Kit according to the manufacturer's protocol (Qiagen, Valencia, CA, USA) and labeled using a Low-Input QuickAmp Labeling Kit, One-Color (Agilent Technologies, Santa Clara, CA, USA). Gene expression analysis was performed on samples from three independent experiments using a microarray (SurePrint G3 Human GE 8 × 60 K v2 Microarray; Agilent Technologies). The raw microarray data were deposited in the Gene Expression Omnibus (GEO; accession number, GSE62434; http://www.ncbi.nlm.nih.gov/geo/query/acc.cgi?acc=GSE62434). CREB target genes were selected according to the CREB Target Gene Database (http://natural.salk.edu/CREB/), while NFAT target genes were selected by reference to Medline, as listed in Supplementary Table 1. Signal transduction pathways associated with each gene were identified according to the KEGG Pathway Database (http://www.genome.jp/kegg/pathway.html).

Quantitative real-time PCR. To quantify mRNA levels, quantitative real-time PCR was carried out using TaqMan Probe and Premix Ex Taq (Probe qPCR; TaKaRa Bio Inc., Shiga, Japan) in a TaKaRa PCR Thermal Cycler Dice TP960 (TaKaRa Bio) according to the manufacturer's protocols. To normalize mRNA expression levels, glyceraldehyde 3-phosphate dehydrogenase (GAPDH) was used as an endogenous internal control. Primers and probes used for RT-PCR are described in Table 2.

ELISA (Enzyme-linked immuno-sorbent assay) HAEC and THP-1 cells were treated with PAPC, OxPAPC or H_2OxPAPC for 22 h. The IL-8 (HAEC) and TNF-α (THP-1) contents in the culture media were determined using Human CXCL8/IL-8 Quantikine ELISA Kit (R&D Systems, Minneapolis, MN, USA) and Human TNF-α Quantikine ELISA Kit (R&D Systems, Minneapolis, MN, USA), respectively, according to the manufacturer's protocol.

Detection of lipid peroxidation in cultured cells. THP-1 cells (1×10^5 cells/mL) were stained with 5 μM Liperfluo[25] for 30 min and then treated with 10 mM of AAPH[23] for 4.5 h in the absence or presence of the indicated concentrations of H_2 gas in a closed vessel. The cells were analyzed using a Cell Lab Quanta flow cytometer (Beckman Coulter, Miami, FL, USA).

Detection of the translocation of NFAT into the nucleus by immunofluorescence. THP-1 cells (1×10^5 cells/mL) were treated with OxPAPC (0.1 mg/mL), or H_2[2.5%]OxPAPC (0.1 mg/mL) for 1.5 h, which were used for the Ca^{2+} signaling assay, and then the translocation of NFAT was determined using immunofluorescence as follows. The cells were fixed for 20 min with 10% neutral buffered formalin (3.8% formaldehyde), and then permeabilized with 0.2% Triton X-100 in Tris-buffered saline (TBS-T) for 10 min. After the cells were washed, and blocked with 5% nonfat milk in TBS-T, they were incubated with anti-NFAT1 antibodies (1:100 dilution; 25A10.D6.D2; Abcam, Cambridge, MA, USA) overnight at 4 °C, followed by incubation with Alexa Fluor 488-conjugated anti-mouse antibodies (1:400 dilution; A-11029; Life Technologies, Carlsbad, CA, USA) for 1 h at 25 °C. The cells were counterstained with Hoechst 33342. Immunofluorescence was observed using a laser scanning confocal microscope (FV1200; Olympus).

THP-1 cells (1×10^5 cells/mL) were treated with 10 mM AAPH for 3 h in the absence or presence of indicated concentrations of H_2, and the NFAT translocation was investigated using immunofluorescence as described above.

Cell culture. THP-1 cells (ATCC) were cultured in RPMI1640 containing 10% FBS. Human aortic endothelial cells (HAEC) were obtained from Lonza and maintained in endothelial cell growth medium [EBM medium + growth supplements+FCS (Lonza)]. Cells were cultured at 37 °C in a 5% CO_2 humidified atmosphere and were used for experiments from passage 4 to 8.

Statistical analysis. Statistical differences between groups were assessed by one-way analysis of variance (ANOVA) with Tukey-Kramer post hoc analysis unless otherwise mentioned. Statistical analyses were performed with IBM SPSS21 software. Results were considered significant at $P < 0.05$. When $0.01 < P < 0.05$, the actual P values were noted. Data are presented as means ± standard deviations.

References

1. Ohsawa, I. *et al.* Hydrogen acts as a therapeutic antioxidant by selectively reducing cytotoxic oxygen radicals. *Nat. Med.* **13,** 688–694 (2007).
2. Hanaoka, T., Kamimura, N., Yokota, T., Takai, S. & Ohta, S. Molecular hydrogen protects chondrocytes from oxidative stress and indirectly alters gene expressions through reducing peroxynitrite derived from nitric oxide. *Med. Gas Res.* **1,** 18 (2011).
3. Fukuda, K. *et al.* Inhalation of hydrogen gas suppresses hepatic injury caused by ischemia/reperfusion through reducing oxidative stress. *Biochem. Biophys. Res. Commun.* **361,** 670–674 (2007).
4. Hayashida, K. *et al.* Inhalation of hydrogen gas reduces infarct size in the rat model of myocardial ischemia-reperfusion injury. *Biochem. Biophys. Res. Commun.* **373,** 30–35 (2008).
5. Hayashida, K. *et al.* Hydrogen Inhalation During Normoxic Resuscitation Improves Neurological Outcome in a Rat Model of Cardiac Arrest, Independent of Targeted Temperature Management. *Circulation.* **130,** 2173–2180 (2014).
6. Ohta, S. Recent progress toward hydrogen medicine: potential of molecular hydrogen for preventive and therapeutic applications. *Curr. Pharm. Des.* **17,** 2241–2252 (2011).
7. Ohta, S. Molecular hydrogen as a preventive and therapeutic medical gas: initiation, development and potential of hydrogen medicine. *Pharmacol. Ther.* **144,** 1–11 (2014).
8. Yoritaka, A. *et al.* Pilot study of H(2) therapy in Parkinson's disease: a randomized double-blind placebo-controlled trial. *Mov. Disord.* **28,** 836–839 (2013).
9. Ishibashi, T. *et al.* Therapeutic efficacy of infused molecular hydrogen in saline on rheumatoid arthritis: a randomized, double-blind, placebo-controlled pilot study. *Int. Immunopharmacol.* **21,** 468–473 (2014).
10. Matsumoto, A. *et al.* Oral 'hydrogen water' induces neuroprotective ghrelin secretion in mice. *Sci. Rep.* **3,** 3273 (2013).
11. Kamimura, N., Nishimaki, K., Ohsawa, I. & Ohta, S. Molecular hydrogen improves obesity and diabetes by inducing hepatic FGF21 and stimulating energy metabolism in db/db mice. *Obesity* **19,** 1396–1403 (2011).
12. Ishibashi, T. Molecular hydrogen: new antioxidant and anti-inflammatory therapy for rheumatoid arthritis and related diseases. *Curr. Pharm. Des.* **19,** 6375–6381 (2013).
13. Porter, N. A., Caldwell, S. E. & Mills, K. A. Mechanisms of free radical oxidation of unsaturated lipids. *Lipids* **30,** 277–290 (1995).
14. Subbanagounder, G. *et al.* Hydroxy alkenal phospholipids regulate inflammatory functions of endothelial cells. *Vascul. Pharmacol.* **38,** 201–209 (2002).
15. Bochkov, V. N. *et al.* Generation and biological activities of oxidized phospholipids. *Antioxid. Redox Signal.* **12,** 1009–1059 (2010).
16. Bochkov, V. N. *et al.* Oxidized phospholipids stimulate tissue factor expression in human endothelial cells via activation of ERK/EGR-1 and Ca(++)/NFAT. *Blood* **99,** 199–206 (2002).
17. Obinata, H., Hattori, T., Nakane, S., Tatei, K. & Izumi, T. Identification of 9-hydroxyoctadecadienoic acid and other oxidized free fatty acids as ligands of the G protein-coupled receptor G2A. *J. Biol. Chem.* **280,** 40676–40683 (2005).
18. Subbanagounder, G. *et al.* Determinants of bioactivity of oxidized phospholipids. Specific oxidized fatty acyl groups at the *sn*-2 position. *Arterioscler. Thromb. Vasc. Biol.* **20,** 2248–2254 (2000).
19. Bading, H. Nuclear calcium signalling in the regulation of brain function. *Nat. Rev. Neurosci.* **14,** 593–608 (2013).
20. Hogan, P. G., Chen, L., Nardone, J. & Rao, A. Transcriptional regulation by calcium, calcineurin, and NFAT. *Genes Dev.* **17,** 2205–2232 (2003).
21. Niki, E. Biomarkers of lipid peroxidation in clinical material. *Biochim. Biophys. Acta* **1840,** 809–817 (2014).
22. Reis, A. & Spickett, C. M. Chemistry of phospholipid oxidation. *Biochim. Biophys. Acta* **1818,** 2374–2387 (2012).
23. Werber, J., Wang, Y. J., Milligan, M., Li, X. & Ji, J. A. Analysis of 2,2′-azobis (2-amidinopropane) dihydrochloride degradation and hydrolysis in aqueous solutions. *J. Pharm. Sci.* **100,** 3307–3315 (2011).
24. Fruhwirth, G. O., Loidl, A. & Hermetter, A. Oxidized phospholipids: from molecular properties to disease. *Biochim. Biophys. Acta* **1772,** 718–736 (2007).
25. Yamanaka, K. *et al.* A novel fluorescent probe with high sensitivity and selective detection of lipid hydroperoxides in cells. *RSC Advances* **2,** 7894 (2012).
26. Kawamura, T. *et al.* Hydrogen gas reduces hyperoxic lung injury via the Nrf2 pathway *in vivo*. *Am. J. Physiol. Lung Cell. Mol. Physiol.* **304,** L646–656 (2013).
27. Nagata, K., Nakashima-Kamimura, N., Mikami, T., Ohsawa, I. & Ohta, S. Consumption of molecular hydrogen prevents the stress-induced impairments in hippocampus-dependent learning tasks during chronic physical restraint in mice. *Neuropsychopharmacology: official publication of the American College of Neuropsychopharmacology* **34,** 501–508 (2009).
28. Ohta, S. Molecular hydrogen as a novel antioxidant: overview of the advantages of hydrogen for medical applications. *Methods Enzymol.* **555,** 289–317 (2015).
29. Xie, K. *et al.* Hydrogen gas improves survival rate and organ damage in zymosan-induced generalized inflammation model. *Shock* **34,** 495–501 (2010).
30. Buchholz, B. M. *et al.* Hydrogen inhalation ameliorates oxidative stress in transplantation induced intestinal graft injury. *Am. J. Transplant.* **8,** 2015–2024 (2008).
31. Hayashida, K. *et al.* H(2) gas improves functional outcome after cardiac arrest to an extent comparable to therapeutic hypothermia in a rat model. *J. Am. Heart Assoc.* **1,** e003459 (2012).
32. Cardinal, J. S.*et al.* Oral hydrogen water prevents chronic allograft nephropathy in rats. *Kidney Int.* **77,** 101–109 (2010).
33. Motojima, H., Villareal, M. O., Iijima, R., Han, J. & Isoda, H. Acteoside inhibits type Iota allergy through the down-regulation of Ca/NFAT and JNK MAPK signaling pathways in basophilic cells. *J. Nat. Med.* **67,** 790–798 (2013).
34. Musson, R. E., Cobbaert, C. M. & Smit, N. P. Molecular diagnostics of calcineurin-related pathologies. *Clin. Chem.* **58,** 511–522 (2012).

35. Itoh, T. *et al.* Molecular hydrogen inhibits lipopolysaccharide/interferon gamma-induced nitric oxide production through modulation of signal transduction in macrophages. *Biochem. Biophys. Res. Commun.* **411,** 143–149 (2011).
36. Obasanjo-Blackshire, K. *et al.* Calcineurin regulates NFAT-dependent iNOS expression and protection of cardiomyocytes: co-operation with Src tyrosine kinase. *Cardiovasc. Res.* **71,** 672–683 (2006).
37. Li, D. Z., Zhang, Q. X., Dong, X. X., Li, H. D. & Ma, X. Treatment with hydrogen molecules prevents RANKL-induced osteoclast differentiation associated with inhibition of ROS formation and inactivation of MAPK, AKT and NF-kappa B pathways in murine RAW264.7 cells. *J. Bone Miner. Metab.* **32,** 494–504 (2014).
38. He, B. *et al.* Protection of oral hydrogen water as an antioxidant on pulmonary hypertension. *Mol. Biol. Rep.* **40,** 5513–5521 (2013).
39. Kishimoto, Y. *et al.* Hydrogen ameliorates pulmonary hypertension in rats by anti-inflammatory and antioxidant effects. *J Thorac Cardiovasc Surg* **150,** 645–654 (2015).
40. Negishi-Koga, T. & Takayanagi, H. Ca^{2+}-NFATc1 signaling is an essential axis of osteoclast differentiation. *Immunol. Rev.* **231,** 241–256 (2009).
41. Ramiro-Diaz, J. M. *et al.* NFAT is required for spontaneous pulmonary hypertension in superoxide dismutase 1 knockout mice. *Am. J. Physio.l Lung Cell. Mol. Physiol.* **304,** L613–625 (2013).
42. Luo, J. *et al.* A calcineurin- and NFAT-dependent pathway is involved in alpha-synuclein-induced degeneration of midbrain dopaminergic neurons. *Hum. Mol. Genet.* **23,** 6567–6574 (2014).
43. Watson, A. D. *et al.* Structural identification by mass spectrometry of oxidized phospholipids in minimally oxidized low density lipoprotein that induce monocyte/endothelial interactions and evidence for their presence *in vivo*. *J. Biol. Chem.* **272,** 13597–13607 (1997).
44. Spickett, C. M., Reis, A. & Pitt, A. R. Identification of oxidized phospholipids by electrospray ionization mass spectrometry and LC-MS using a QQLIT instrument. *Free Radic. Biol. Med.* **51,** 2133–2149 (2011).
45. O'Donnell, V. B. Mass spectrometry analysis of oxidized phosphatidylcholine and phosphatidylethanolamine. *Biochim. Biophys. Acta* **1811,** 818–826 (2011).

Acknowledgements

We thank Ms. Mayumi Takeda and Ms. Suga Kato for technical assistance and secretarial work, respectively. Financial support for this study was provided by Grants-in-Aid for Scientific Research from the Japan Society for the Promotion of Science (23300257, 24651055, and 26282198 to S.O.; 23500971 and 26350129 to N.K.; and 25350907 to K.N.).

Author Contributions

S.O. conceived of and directed the project, analyzed data, and wrote the manuscript. N.K. planned each experiment. K.I., A.I., N.K., K.N., T.Y. and H.I. performed experiments on cell culture (by K.I.), Ca^{2+} signaling (by A.I.), gene expression (by N.K.), and chemical reactions (by K.N.), supported by H.I. and T.Y.

Additional Information

Supplementary information accompanies this paper at http://www.nature.com/srep

Competing financial interests: S.O. holds the right of a patent regarding a medical use of hydrogen gas.

How to cite this article: Iuchi, K. *et al.* Molecular hydrogen regulates gene expression by modifying the free radical chain reaction-dependent generation of oxidized phospholipid mediators. *Sci. Rep.* **6**, 18971; doi: 10.1038/srep18971 (2016).

Ⅲ. 遺伝子制御学部門

Department of Molecular Oncology

遺伝子制御学部門
（大学院　遺伝子制御学部門）

教授　田中　信之

【研究概要】

我々は、がん抑制因子 p53 の解析を進めることで、がん化及びがん抑制の分子機構を明らかにすることを目的に研究を続けている。この過程で、p53 の誘導遺伝子の同定を行い、Noxa を始めとする様々な p53 の標的遺伝子を発見し解析を進めていると同時に、p53 欠損細胞での様々な細胞応答の変化を解析する過程で、p53 がグルコース代謝を制御していることを発見した。がん細胞がグルコースの代謝を主なエネルギー供給源として増殖していることはワールブルグ効果と呼ばれ、古くから知られているが、その分子制御機構やがん化そのものに対しての役割は明らかではなかった。我々は、p53 欠損細胞では転写因子 NF-κB の転写活性化能が恒常的に高いこと、このことががん化に重要であることを発見し、p53 欠損細胞でのグルコース代謝の上昇が NF-κB の活性化を促すというポジティブフィードバック機構が存在すること、がん細胞が膨大なエネルギーを産生することにこの機構が重要である事を報告している。

これらの p53 の研究に加えて、我々はがん幹細胞の解析を進めている。がんは少数存在する幹細胞様の細胞から発生・進行することが近年明らかとなりつつある。このがん幹細胞は増殖が遅く、抗がん剤に抵抗性のために、がん再発の原因となっており、がん幹細胞をいかにして排除するかが、がん治療の重要な標的となっている。

がんは少数存在する幹細胞様の細胞から発生・進行することが近年明らかとなりつつある。このがん幹細胞は増殖が遅く、抗がん剤に抵抗性のために、がん再発の原因となっており、がん幹細胞をいかにして攻撃するかが、がん治療の重要な標的となっている。安倍が中心となって hedgehog 経路の転写因子 Gli1 が MEP50/PRMT5 アルギニンメチル基転移酵素複合体（メチロソーム）によって活性化されるという新しい機構を発見し、この機構ががんの微小環境でのがん幹細胞の維持に重要である事を明らかにした。更に、EGFR 陽性非小細胞肺がん症例の解析及び肺がん細胞のヌードマウス移植での解析から、この MEP50/PRMT5/Gli1 の活性化経路が肺がんの再発に重要であり、この経路を抑制することががんの再発の予防に重要であることを明らかにし、論文を投稿すると共に、肺癌治療のための抗癌剤の効果の検査法（特願 : 2016-094888 号）の特許を出願した。同時に上原は、がん微小環境で産生される I 型 IFN ががん幹細胞の維持に働いていることを見出した。実際、p53 欠損マウスは生後早期に腫瘍が発生して死亡するが、p53 に加えて I 型 IFN を欠損したマウスは腫瘍の発生が遅れる傾向にあることを見出し、更に I 型 IFN が肺がんや乳がんでのがん幹細胞の維持に重要であることを見出している。更に、清水ががん幹細胞の発生に重要な遺伝子の同定を行い、この遺伝子をゲノム編集により欠損させると、がん化した細胞が腫瘍形成能を失うこと、p53 がこのがん幹細胞の発生を抑制していることを発見している。これらの解析を進めることで、がん幹細胞の発生・維持機構を明らかにすると共に、p53 によるがん化の抑制機構を明らかにしていきたいと考えている。

中嶋は、抗がん剤によるがん細胞のアポトーシス誘導のメカニズムを解析しており、大学院生の松本と共に非小細胞肺がん細胞でのシスプラチンによるアポトーシス誘導の分子機構及びその効果を増強する方法を見出して報告した。更に、抗がん剤で誘導されるオートファジーによるがん細胞の治療抵抗性獲得の機構を解析する過程で、幾つかの非小細胞肺がん細胞が Beclin 1 や ATG5 依存的に起こるマクロオートファジーとは別の、LAMP2A や Hsc70 依存的なシャペロン介在性オートファジーによる

Mcl-1 の分解抑制によって生存していることを、大学院生の鈴木と共に発見し報告しており、がん治療の新たな標的を見出している。同時に岩渕は、EGFR 陽性非小細胞肺がんで、転写因子 HIF-1 が EGFR 特異的分子標的薬ゲフィチニブに対しての耐性の獲得に重要であることを見出すと共に、その分子機構を明らかにしている。

谷村は、炎症組織では p53 の誘導は起こるものの、p53 によるアポトーシスや老化による排除機構が働かないことを見出し、その機構の解析を続けていると共に、Toll 様受容体のシグナル伝達分子 MYD88 が転写因子 NF-κB 依存的に HIF-1 を誘導すること、この経路ががん化に重要であることを見出しており、炎症と発がんの新たな分子機構の解明を目指しており、これらの研究を介して、がん化の分子機構の解析と、効果的ながん治療法の開発を進めている。

【研究業績】

〈原著〉

1）Suzuki J, Nakajima W, Suzuki H, Asano Y and Tanaka N. Chaperone-mediated autophagy promotes lung cancer cell survival through selective stabilization of the pro-survival protein, MCL1. Biochem. Biophys. Res. Commun., http://dx.doi.org/10.1016/j.bbrc.2016.12.037, 2016

2）Matsumoto M, Nakajima W, Seike M, Gemma A and Tanaka N. Cisplatin-induced apoptosis in non-small-cell lung cancer cells is dependent on Bax- and Bak-induction pathway and synergistically activated by BH3-mimetic ABT-263 in p53 wild-type and mutant cells. Biochem. Biophys. Res. Commun., 473:490-496, 2016

3）Nakajima W, Sharma K, Lee JY, Maxim NT, Hicks MA, Vu TT, Luu A, Yeudall WA, Tanaka N and Harada H. DNA damaging agent-induced apoptosis is regulated by MCL-1 phosphorylation and degradation mediated by the Noxa/MCL-1/CDK2 complex. Oncotarget, 14:36353-36365, 2016

〈総説〉

1）Abe Y and Tanaka N. Hedgehog signaling pathway in lung cancer: the mechanisms and roles in tumor progression and implications for cancer therapy. “Cell and Molecular Mechanics in Health and Disease” Biomed Res. Int., in press.

2）W. Nakajima, N. Tanaka, BH3 mimetics: their action and efficacy in cancer chemotherapy, Integr. Cancer Sci. Ther. 3:437e441, 2016

〈学会発表〉

1）田中信之：癌微小環境下での肺癌幹細胞の新たな維持機構の解析とそれを標的とした治療法の検討　第 56 回日本肺癌学会学術集会　シンポジウム、2015、東京

2）阿部芳憲、武内進、田中信之：PRMT5-Gli1 経路の遮断による肺がんの再発および抗がん剤抵抗性腫瘍の抑制効果　第 38 回　日本分子生物学会年会、2015、神戸

3）松本優、中嶋亘、鈴木淳也、田中信之：非小細胞肺癌細胞株におけるシスプラチンによるアポトーシスについての考察　第 38 回　日本分子生物学会年会、2015、神戸

4）鈴木淳也、中嶋亘、田中信之：肺癌の分子標的薬 crizotinib はオートファジーとネクローシスによる細胞死を誘導する　第 38 回　日本分子生物学会年会、2015、神戸

5）上原郁野、田中信之：I 型インターフェロンによる発がんの促進と癌幹細胞維持への関与　第 38 回日本分子生物学会年会、2015、神戸

6）谷村篤子、中里茜、田中信之：マウス繊維芽細胞での内在性活性化 K-ras 発現による癌抑制因子 p53 の下流遺伝子転写調節　第 38 回　日本分子生物学会年会、2015、神戸

〈特許〉

出願

1）阿部芳憲、田中信之、武内進、弦間昭彦、清家正博、清水章、功刀しのぶ : 肺癌治療のための抗癌剤の効果の検査法（特願 : 2016-094888 号）

2）田中信之、林裕史、上原郁野、中嶋亘、鈴木英史：突発性難聴に対する新規の治療法（特願 2016-232704 号）

登録

1）上原郁野、田中信之、谷村篤子、内藤善哉、小暮佳代：炎症性サイトカインの機能を抑制する炎症性疾患治療剤（特許番号：第 6043997 号）

Biochemical and Biophysical Research Communications 473 (2016) 490–496

Contents lists available at ScienceDirect

Biochemical and Biophysical Research Communications

journal homepage: www.elsevier.com/locate/ybbrc

Cisplatin-induced apoptosis in non-small-cell lung cancer cells is dependent on Bax- and Bak-induction pathway and synergistically activated by BH3-mimetic ABT-263 in p53 wild-type and mutant cells

Masaru Matsumoto [a, b], Wataru Nakajima [a], Masahiro Seike [b], Akihiko Gemma [b], Nobuyuki Tanaka [a, *]

[a] Department of Molecular Oncology, Institute for Advanced Medical Sciences, Nippon Medical School, 1-396 Kosugi-cho, Nakahara-ku, Kawasaki 211-8533, Japan
[b] Department of Pulmonary Medicine and Oncology, Graduate School of Medicine, Nippon Medical School, 1-1-5 Sendagi, Bunkyo-ku, Tokyo 113-8603, Japan

ARTICLE INFO

Article history:
Received 4 March 2016
Accepted 14 March 2016
Available online 18 March 2016

Keywords:
Cisplatin
Apoptosis
Bax
Bak
ABT-263
NSCLC

ABSTRACT

Cisplatin is a highly effective anticancer drug for treatment of various tumors including non-small-cell lung cancer (NSCLC), and is especially useful in cases nonresponsive to molecular-targeted drugs. Accumulating evidence has shown that cisplatin activates the p53-dependent apoptotic pathway, but it also induces apoptosis in p53-mutated cancer cells. Here we demonstrated that DNA-damage inducible proapoptotic BH3 (Bcl-2 homology region 3)-only Bcl-2 family members, Noxa, Puma, Bim and Bid, are not involved in cisplatin-induced apoptosis in human NSCLC cell lines. In contrast, the expression of proapoptotic multidomain Bcl-2-family members, Bak and Bax, was induced by cisplatin in p53-dependent and -independent manners, respectively. Moreover, in wild-type p53-expressing cells, cisplatin mainly used the Bak-dependent apoptotic pathway, but this apoptotic pathway shifted to the Bax-dependent pathway by loss-of-function of p53. Furthermore, both Bak- and Bax-induced apoptosis was enhanced by the antiapoptotic Bcl-2 family member, Bcl-X_L knockdown, but not by Mcl-1 knockdown. From this result, we tested the effect of ABT-263 (Navitoclax), the specific inhibitor of Bcl-2 and Bcl-X_L, but not Mcl-1, and found that ABT-263 synergistically enhanced cisplatin-induced apoptosis in NSCLC cells in the presence or absence of p53. These results indicate a novel regulatory system in cisplatin-induced NSCLC cell apoptosis, and a candidate efficient combination chemotherapy method against lung cancers.

1. Introduction

Lung cancer is a leading cause of cancer-related death worldwide in both men and women, and more than 85% of cases are classified as non-small-cell lung cancer (NSCLC), including adenocarcinoma, squamous cell carcinoma and large-cell carcinoma [1]. NSCLCs harboring epidermal growth factor receptor (EGFR) mutations or anaplastic lymphoma kinase (ALK) gene rearrangements have been successfully targeted with tyrosine kinase inhibitors (TKIs) [2,3]. However, the rate of EGFR positive mutation is about 20% and ALK rearrangement is only about 5–7% [4], and thus most NSCLC cases do not respond to these TKIs [1,5]. In such cases, conventional chemotherapy using platinum-based compounds are recommended [6,7]. Cisplatin is the first discovered and most commonly used platinum-based compound [8]. In the cell, cisplatin crosslinks purine bases in DNA, thereby evoking DNA damage responses. The anti-tumor effect of cisplatin is primarily caused by DNA damage induced apoptosis [9]. The tumor suppressor p53 plays an essential role in DNA damage-induced apoptosis through induction of a set of apoptosis inducers [10]. On the other hand, another study showed that cisplatin also induced apoptosis in p53-mutated NSCLC cells and other cancer cells [11]. Therefore, the molecular mechanism underlying cisplatin-induced apoptosis in NSCLC cells has not yet been fully elucidated.

Abbreviations: NSCLC, non-small-cell lung cancer; CDDP, cisplatin [cis-diamminedichloroplatinum (II)]; shRNA, short hairpin RNA; IP, immunoprecipitation; IB, immunoblotting; WCL, whole cell lysate.

* Corresponding author.
E-mail address: nobuta@nms.ac.jp (N. Tanaka).

http://dx.doi.org/10.1016/j.bbrc.2016.03.053
0006-291X/

The Bcl-2 proteins are critical regulators of apoptosis. They possess conserved BH (Bcl-2 homology) domains and are classified into "multidomain" and "BH3-only" proteins. The pro-apoptotic multidomain members Bax and Bak function as apoptosis executers in the mitochondria. Studies on mice lacking both *Bax* and *Bak* showed that Bax and Bak are essential inducers of mitochondrion-mediated apoptosis in response to various stimuli, including DNA damage [12,13]. In contrast, anti-apoptotic multidomain proteins, such as Bcl-2, Bcl-X_L and Mcl-1, inhibit Bax/Bak-mediated apoptosis. BH3-only proteins, which are critical for initiating apoptosis, activate Bax and Bak through direct and/or indirect activation [12,13]. The BH3-only proteins Bim, Bid, Puma and Noxa directly activate Bax and Bak, and also inactivate anti-apoptotic multidomain proteins [14]. Quadruple deficiency of Bim, Bid, Puma and Noxa abrogates apoptosis induced by various stimuli, suggesting the importance of these factors in triggering Bax/Bak-mediated apoptosis induction [14]. In response to DNA damage, the expression of Noxa/Puma and Bim is induced by p53 and FOXO3, respectively, resulting in induction of apoptosis [15–18]. Another study also reported the possible role of Bid in the DNA damage response [19].

Here we examined the mechanism of cisplatin-induced apoptosis of NSCLC cells with the aim of helping develop new approaches for treatment of NSCLC.

2. Materials and methods

2.1. Cells, antibodies and materials

Human NSCLC cell lines A549, H460, LC2/Ad and PC10 were purchased from the American Type Culture Collection (Manassas, VA, USA). Antibodies were purchased from the following manufacturers: Bim (C34C5), Bcl-X_L (54H6), cleaved PARP (D64E10) and cleaved caspase-3 (5A1E) from Cell Signaling Technology (Danvers, MA, USA); Noxa (114C307.1) from Thermo Fisher Scientific (Waltham, MA, USA); Mcl-1 (S-19) and Bax (N-20) from Santa Cruz Biotechnology (CA, USA); alpha-tubulin (DM 1A) from Sigma–Aldrich (Tokyo, Japan); and Bak (06–536) from Millipore (Billerica, MA, USA). Anti-Bak (ab-1; Calbiochem) and anti-Bax (6A7; Sigma–Aldrich) antibodies were used for immunoprecipitation. ABT-263 (Navitoclax) was *purchased from AdooQ BioScience* (Irvine, CA, USA). Cisplatin was purchased from Calbiochem (San Diego, CA, USA).

2.2. Immunoprecipitation and immunoblotting

Immunoprecipitation and immunoblotting analyses were performed as previously described [20].

2.3. RNA interference

Short hairpin RNAs (shRNAs) shNoxa, shBim, shBid, shPuma, shMcl-1 and shBcl-X_L were cloned into the pSuper puro vector (Oligoengine; Seattle, WA, USA). The target sequences were as follows: 5′-GGAAACGGAAGATGGAATA-3′ (shNoxa), 5′-CTACCTCCCTACAGACAGA-3′ (shBim), 5′-GGGATGAGTGCATCACAAA-3′ (shBid), 5′-GGGTCCTGTACAATCTCAT-3′ (shPuma), 5′-GCAAGAGGATTATGGCTAA-3′ (shMcl-1), and 5′-AGGATACAGCTGGAGTCAG -3′ (shBcl-X_L). Retroviral infection was performed as previously described [21]. The lentiviral sh-p53, sh-Bax and sh-Bak-expressing constructs were kindly provided by Dr. Harada (Virginia Commonwealth University, Richmond, VA, USA) [22].

2.4. Quantitative real-time polymerase chain reaction (PCR) analysis

Quantitative real-time PCR (qPCR) analysis was performed as previously described [21]. The primer and probe sets used were predesigned primer/probe sets: *β-actin*, Hs03023880_g1; *Bak*,

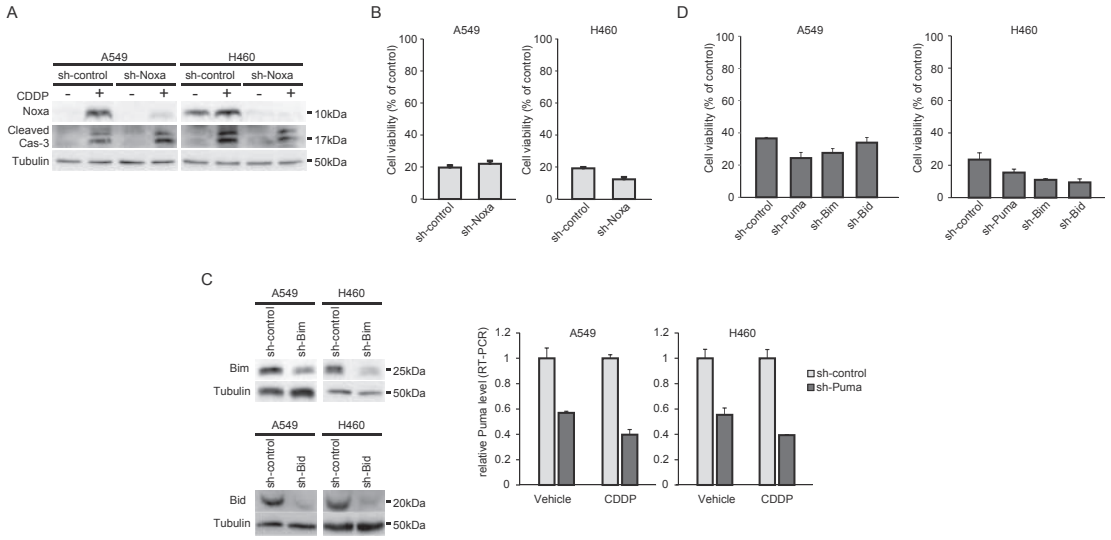

Fig. 1. Effect of Noxa, PUMA, Bim or Bid knockdown on cisplatin (CDDP)-induced apoptosis of NSCLC cells. (A, B) A549 and H460 cells stably expressing sh-Noxa or sh-control were treated with cisplatin (20 μM) for 24 h and analyzed by immunoblot analysis using indicated antibodies (A) and by cell viability assay (B). Results are expressed as the mean ± SEM of at least three independent experiments. P values are relative to the control. $^*P < 0.05$; $^{**}P < 0.01$. (C, D) A549 and H460 cells stably expressing shRNA targeting Bid (sh-Bid) or sh-Bim were subjected to immunoblot analysis using the indicated antibodies (left panel; C). A549 and H460 cells stably expressing sh-Puma or sh-control were treated with cisplatin (20 μM) for 24 h and the expression of Puma was analyzed by qPCR (right panel; C). Data are mean ± SD (n = 3). Cell viability was measured by trypan blue exclusion analysis (D). Results are expressed as the mean ± SEM of at least three independent experiments. P values are relative to the control. $^*P < 0.05$; $^{**}P < 0.01$.

Hs00832876_gl; *Bax*, Hs00180269_ml; and *Puma*, Hs00248075_m1. The mRNA expression levels were normalized to those of *β-actin* levels.

2.5. Cell death assay

NSCLC cell lines were plated in microtiter plates (12 wells, *Greiner Bio-one*, *Frickenhausen*, *Germany*) at a concentration of 1×10^5 cells per well in 500 μl medium and treated with 20 μM cisplatin in the presence or absence of 1 μM ABT-263 for 48 h or 72 h. After treatment, cell viability was measured by the trypan blue dye exclusion method using a VI-Cell image analyzer (Beckman Coulter, Brea, CA, *USA*). The *IC_{50} value* for cisplatin was determined as previously described [20]. The significance of differences between the experimental variables was determined using Student's t-test.

3. Results

3.1. Noxa, PUMA, Bim and Bid do not contribute to cisplatin-induced apoptosis in NSCLC cells

Since a previous study demonstrated that cisplatin induces Noxa-dependent apoptosis in HeLa cells [23], we first analyzed the role of Noxa in cisplatin-induced apoptosis of NSCLC cells. The NSCLC cell lines A549 and H460, which express wild-type p53, were treated with 20 μM cisplatin (IC_{50} was determined as 12 μM and 8 μM, respectively) solved in water to prevent solvent-mediated inactivation [24]. As shown in Fig. 1A, cisplatin induced the expression of Noxa and also the activation of caspase-3, an apoptosis executer. In contrast, shRNA-mediated silencing of Noxa expression did not affect the induction of cleaved caspase-3, a hallmark of caspase-3 activation, and induction of apoptosis (Fig. 1A and B). Silencing of other BH3-only proteins important for triggering apoptosis, Bim, Bid or PUMA, also did not affect cisplatin-induced apoptosis (Fig. 1C and D). Because the expression level of PUMA protein was detected at low levels by immunoblot, we detected the expression of PUMA by qPCR (Fig. 1C, right).

3.2. Cisplatin enhances p53-dependent Bak- and p53-independent Bax-expression

To better examine the mechanism underlying apoptosis induction, we next analyzed the expression of proapoptotic multidomain Bcl-2 family proteins Bax and Bak in response to cisplatin treatment, as a previous study demonstrated that the expression of Bax and Bak is directly regulated by p53 [10,25]. As shown in Fig. 2A and B, the protein and mRNA levels of Bax and Bak were induced by cisplatin. Interestingly, while induction of Bak protein and mRNA by cisplatin was clearly suppressed by silencing of p53 expression, the induction of Bax was not affected, but caspase-3 activation and cleavage of PARP, other hallmarks of apoptosis, were significantly

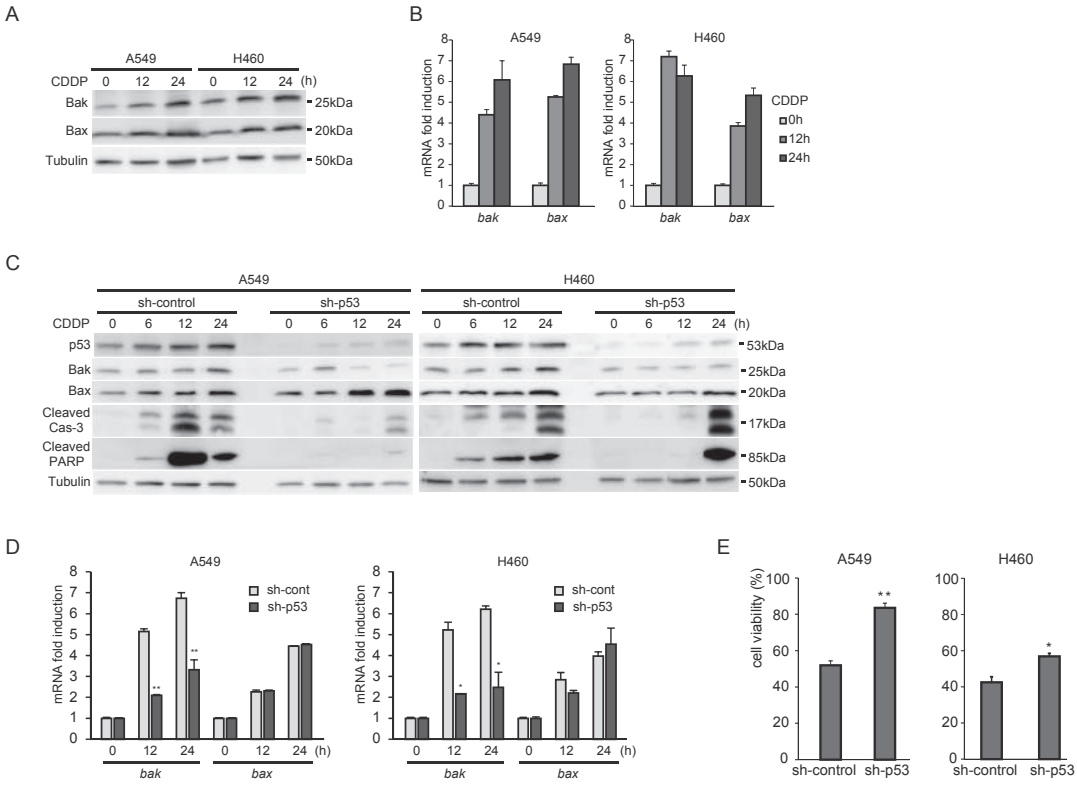

Fig. 2. Role of p53 in the activation of Bax and Bak in cisplatin-treated NSCLC cells. (A, B) A549 and H460 cells were treated with cisplatin (20 μM) for the indicated times and analyzed by immunoblot analysis using indicated antibodies (A), and *Bax* and *Bak* mRNA levels were determined by qPCR. Data are mean ± SD (n = 3). (C, D, E) A549 and H460 cells stably expressing sh-p53 or sh-control were treated with cisplatin (20 μM) for the indicated times, and analyzed by immunoblot analysis using the indicated antibodies (C), and *Bax* or *Bak* mRNA were determined by qPCR (D). Data are mean ± SD (n = 3). Cell viability was measured (E). Results are expressed as the mean ± SEM of at least three independent experiments. Student's *t*-test was used for statistical analysis. P values are relative to the control. $^*P < 0.05$; $^{**}P < 0.01$.

suppressed by silencing p53 (Fig. 2C and D). Induction of apoptosis was also suppressed by shRNA-mediated silencing of p53 expression (Fig. 2E).

3.3. Induction of apoptosis by cisplatin in NSCLC cells lacking p53 function was suppressed by reduced Bax expression

In A549 cells expressing p53 shRNA, the cisplatin-induced activation of Bak (detected by antibodies specific to the activated form of Bak) was suppressed; in contrast, the activation of Bax was still observed (Fig. 3A). Therefore, we next analyzed whether apoptosis induction by cisplatin was also dependent on Bax induction. As shown in Fig. 3B and C, apoptosis induction by cisplatin in A549 cells expressing both p53 shRNA and Bax shRNA was significantly suppressed compared with only p53 shRNA-expressing cells. As expected, in the p53-mutant NSCLC cell lines LC2/Ad and PC10, cisplatin treatment resulted in the induction of Bax but not Bak (Fig. 3D). The expression and induction of Noxa were also suppressed in these cells. Furthermore, cisplatin-induced apoptosis in LC2/Ad cells was suppressed by silencing of Bax but not Bak expression (Fig. 3E).

3.4. Cisplatin-induced apoptosis in NSCLC cells was not affected by reduced expression of Mcl-1 and enhanced by ABT-263

Antiapoptotic multidomain Bcl-2 family proteins, such as Mcl-1 and Bcl-X_L, inhibit apoptosis through direct association with Bax and Bak [12]. As shown in Fig. 4A and B, cisplatin-induced apoptosis in NSCLC cells was enhanced by silencing of Bcl-X_L expression. Although it has been demonstrated that survival of several cancer cell lines completely depend on Mcl-1 [26,27], apoptosis was not affected by silencing of Mcl-1 expression (Fig. 4A and B). BH3-only proteins associate with antiapoptotic multidomain Bcl-2 family proteins via their BH3-domain, resulting in induction of apoptosis [12,13]. Recently, BH3 mimetics have been used for cancer chemotherapy and ABT-263 has proved promising in clinical trials [28,29]. Because ABT-263 is a specific inhibitor of Bcl-2 and Bcl-X_L, but not Mcl-1, we next analyzed the effect of ABT-263 on cisplatin-induced apoptosis. ABT-263 enhanced the cisplatin-induced activation of Bax, Bak, and caspase-3 in A549 cells (Fig. 4C). In contrast, in A549 cells expressing p53 shRNA, cisplatin-induced activation of Bax and Bak was suppressed; however, ABT-263 clearly enhanced the activation of Bax and caspase-3 (Fig. 4C). In correlation with these effects, ABT-263 enhanced apoptosis in A549 cells as well as A549 cells expressing p53 shRNA, especially at early time points (Fig. 4D). Moreover, cisplatin and ABT-263 synergistically enhanced the activation of Bax and caspase-3 and the induction of apoptosis in p53 mutated LC2/Ad and PC10 cells (Fig. 4E and F).

4. Discussion

In the apoptosis regulatory pathways mediated by the Bcl-2 family proteins, induction and/or activation of BH3-only proteins in response to apoptosis-inducing signals result in activation of pro-apoptotic multidomain Bcl-2 families Bax and Bak through direct association and inhibition of anti-apoptotic multidomain Bcl-2 families [12,13]. In this triparticle apoptotic switch, BH3-only proteins function as an initial triggering factor. The importance of

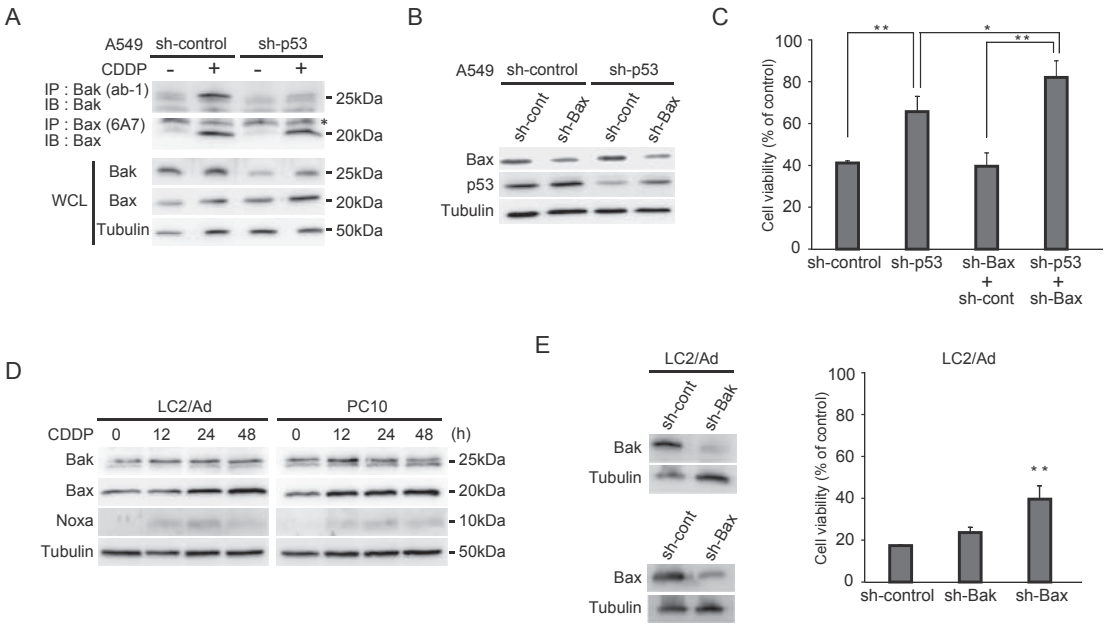

Fig. 3. Bax and Bak activation in cisplatin-treated NSCLC cells lacking p53 function. (A) A549 and H460 cells stably expressing sh-p53 or sh-control were treated with cisplatin (20 μM) for 12 h and analyzed by immunoprecipitation (IP) with conformational change-specific anti-Bak (Ab-1) or conformational change-specific anti-Bax (6A7) antibodies. Immunoblot analyses were carried out on precipitated samples with indicated antibodies (upper panel). The asterisk indicates a nonspecific band. Whole cell lysates (WCLs) were subjected to immunoblot analysis with the indicated antibodies (lower panel). (B, C) A549 and H460 cells stably expressing sh-p53 or sh-control were further infected with lentivirus encoding sh-Bax or sh-control and analyzed by immunoblot analysis using indicated antibodies (B). Cells were treated with cisplatin (20 μM) for 24 h and cell viability was measured (C). Results are expressed as the mean ± SEM of at least three independent experiments. P values are relative to the control. $^{*}P < 0.05$; $^{**}P < 0.01$. (D) LC2/Ad and PC10 cells were treated with cisplatin (20 μM) for the indicated times, and analyzed by immunoblot analysis using indicated antibodies. (E) LC2/Ad and PC10 cells stably expressing sh-Bak, sh-Bax or sh-control were subjected to immunoblot analysis using the indicated antibodies (left panel). The cells were treated with cisplatin (20 μM) for 24 h, and cell viability was measured (right panel). Results are expressed as the mean ± SEM of at least three independent experiments. P values are relative to the control. $^{**}P < 0.01$.

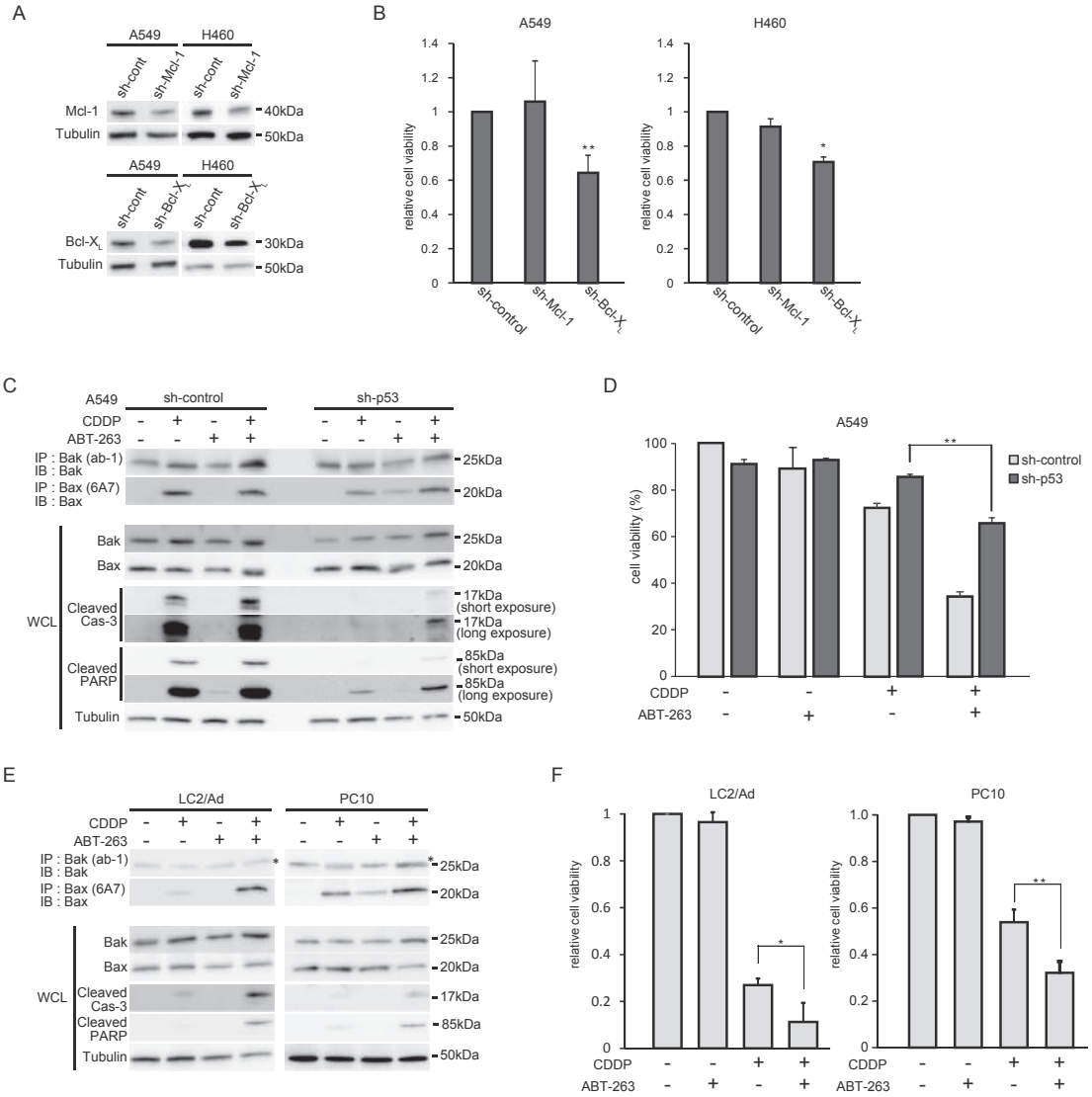

Fig. 4. Effect of ABT-263 on cisplatin-treated p53 mutant NSCLC cells. (A, B) A549 and H460 cells expressing sh-Bcl-X_L, sh-Mcl-1 or sh-control were subjected to immunoblot analysis using the indicated antibodies (left panel). Cells were treated with cisplatin (20 μM) for 24 h and cell viability was measured (B). Results are expressed as the mean ± SEM of at least three independent experiments. P values are relative to the control. $^*P < 0.05$; $^{**}P < 0.01$. (C) A549 cells expressing sh-p53 or sh-control were treated with cisplatin (20 μM) for 12 h, and the active forms of Bax and Bak were detected as described in Fig. 3A (upper panel). WCLs were subjected to immunoblot analysis with the indicated antibodies (under panel). (D) LC2/Ad and PC10 cells were treated with cisplatin (20 μM) in the presence or absence of ABT-263 (1 μM) for 12 h and the active forms of Bax and Bak were detected (upper panel). The asterisk indicates a nonspecific band. WCLs were subjected to immunoblot analysis with the indicated antibodies (lower panel). (E) A549 cells stably expressing sh-p53 or sh-control and LC2/Ad or PC10 cells were treated with cisplatin (20 μM) in the presence or absence of ABT-263 (1 μM) for 12 h and cell viability was measured. Results are expressed as the mean ± SEM of at least three independent experiments. P values are relative to the control. $^*P < 0.05$; $^{**}P < 0.01$.

BH3-only proteins, especially Bim, Bid, Puma and Noxa, was previously demonstrated by the results showing that quadruple deficient cells show almost the same phenotype as Bax and Bak double-deficient cells [14]. However, our present study indicates that the BH3-only proteins do not regulate cisplatin-induced apoptosis in NSCLC cells. In our system, only Noxa was induced by cisplatin, but silencing of Noxa expression and also silencing of Bim, Bid or Puma expression could not affect cisplatin-induced apoptosis. In contrast, we determined that cisplatin induces p53-dependent Bak expression and also p53-independent Bax expression. Moreover, in p53 wild-type cells, cisplatin-induced apoptosis is affected by reduced Bak expression, and in p53 lacking or mutated cells, cisplatin-induced apoptosis is affected by reduced Bax expression. Therefore, although we cannot exclude the possibility that another BH3-only protein regulates this apoptosis or that the other BH3-only proteins compensate for the effect of silencing of single BH3-only protein, our results suggest that Bak- and Bax-induction by cisplatin is important for the induction of apoptosis in NSCLC cells.

MCL-1 is one of the most highly amplified genes in a variety of human cancers, and its expression is often associated with

resistance of chemotherapy and relapse of cancer [30]. Moreover, other studies showed that survival of several cancer cell lines completely depend on Mcl-1 [26,27]. These findings suggest that Mcl-1 is an important factor for cancer cell survival and tumor expansion. However, NSCLC cell lines used in these experiments could not show a protective effect not only in cell survival but also in cisplatin-induced apoptosis. Moreover, the expression of Noxa, a specific inhibitor of Mcl-1, was efficiently induced by cisplatin, but inhibition of the Noxa expression could not affect cisplatin-induced apoptosis, suggesting that the Noxa-Mcl-1 pathway could not effectively regulate cell survival and death in NSCLC. Although Noxa inhibits Mcl-1 by ubiquitin-mediated degradation [31], other studies showed that Noxa, also called APR, is overexpressed in several cancer cell lines [20,32]. Therefore, it is possible that Noxa does not inhibit Mcl-1 through a specific protein modification or expression of other cofactor(s), and also that Mcl-1 cannot function under some conditions.

In several cancers, it has been reported that p53 status is an important determinant of cisplatin sensitivity; however, some studies suggest that cisplatin-induced cell death is independent of p53 status [33,34]. Other studies showed that the absence of p53 does not alter cellular sensitivity to cisplatin [11,34], but the precise mechanism has not been fully elucidated. In the present study, we demonstrate that cisplatin induces apoptosis by the activation of both p53-dependent Bak and p53-independent Bax expression, and inhibition of Bax expression attenuates cisplatin-induced apoptosis in p53 lacking or mutated cells. These results indicate that the induction of Bax is involved in p53-independent apoptosis by cisplatin. A previous study showed that p53 can directly activate the *Bak* promoter [25]. The mechanism of p53-independent Bax induction has not been fully elucidated. However, a previous study showed that p73, a p53-related transcription factor, activates the *Bax* promoter [35], suggesting its possible role in p53-independent Bax induction.

BH3 mimetics, such as ABT-263, are expected to contribute as efficient cancer therapy, but they could not antagonize Mcl-1 [28,29]. In small cell lung cancer, it has been shown that ABT-263 enhances the induction of apoptosis by the HDAC inhibitor, vorinostat [36]. In contrast to its importance in cancer, we observed that Mcl-1 could not affect in cisplatin-induced apoptosis in several NSCLC cell lines. Moreover, ABT-263 synergistically enhances cisplatin-induced apoptosis in these cells, even in mutant p53-expressing cells. These results suggest the possibility that ABT-263 is an efficient therapeutic agent for NSCLC.

Competing financial interests

The authors declare no competing financial interests.

Acknowledgments

We thank Hisashi Harada, Yoshinori Abe, Ikuno Uehara, and Atsuko Tanimura for helpful critical discussions, and Yumi Asano, Miho Kawagoe and Yoshimi Takatera for technical support. This work was supported by Grants-in-Aid from the Ministry of Education, Culture, Sports, Science and Technology of Japan (MEXT) and by a grant from the MEXT-Supported Program for the Strategic Research Foundation at Private Universities.

Transparency document

Transparency document related to this article can be found online at http://dx.doi.org/10.1016/j.bbrc.2016.03.053.

References

[1] Z. Chen, C.M. Fillmore, P.S. Hammerman, C.F. Kim, K.K. Wong, Non-small-cell lung cancers: a heterogeneous set of diseases, Nat. Rev. Cancer 14 (2014) 535–546.
[2] B. Hallberg, R.H. Palmer, Mechanistic insight into ALK receptor tyrosine kinase in human cancer biology, Nat. Rev. Cancer 13 (2013) 685–700.
[3] W. Pao, J. Chmielecki, Rational, biologically based treatment of EGFR-mutant non-small-cell lung cancer, Nat. Rev. Cancer 10 (2010) 760–774.
[4] V. Boolell, M. Alamgeer, D.N. Watkins, V. Ganju, The Evolution of Therapies, in: Non-small Cell Lung Cancer, Cancers (Basel), vol. 7, 2015, pp. 1815–1846.
[5] C.A. Perez, M. Velez, L.E. Raez, E.S. Santos, Overcoming the resistance to crizotinib in patients with non-small cell lung cancer harboring EML4/ALK translocation, Lung Cancer 84 (2014) 110–115.
[6] D.S. Ettinger, W. Akerley, H. Borghaei, A.C. Chang, R.T. Cheney, L.R. Chirieac, T.A. D'Amico, T.L. Demmy, A.K. Ganti, R. Govindan, F.W. Grannis Jr., L. Horn, T.M. Jahan, M. Jahanzeb, A. Kessinger, R. Komaki, F.M. Kong, M.G. Kris, L.M. Krug, I.T. Lennes, B.W. Loo Jr., R. Martins, J. O'Malley, R.U. Osarogiagbon, G.A. Otterson, J.D. Patel, M.C. Pinder-Schenck, K.M. Pisters, K. Reckamp, G.J. Riely, E. Rohren, S.J. Swanson, D.E. Wood, S.C. Yang, M. Hughes, K.M. Gregory, NCCN, Non-small cell lung cancer, J. Natl. Compr. Canc. Netw. 10 (2012) 1236–1271.
[7] A. Rossi, P. Chiodini, J.M. Sun, M.E. O'Brien, C. von Plessen, F. Barata, K. Park, S. Popat, B. Bergman, B. Parente, C. Gallo, C. Gridelli, F. Perrone, M. Di Maio, Six versus fewer planned cycles of first-line platinum-based chemotherapy for non-small-cell lung cancer: a systematic review and meta-analysis of individual patient data, Lancet Oncol. 15 (2014) 1254–1262.
[8] S. Dasari, P.B. Tchounwou, Cisplatin in cancer therapy: molecular mechanisms of action, Eur. J. Pharmacol. 740 (2014) 364–378.
[9] S. O'Grady, S.P. Finn, S. Cuffe, D.J. Richard, K.J. O'Byrne, M.P. Barr, The role of DNA repair pathways in cisplatin resistant lung cancer, Cancer Treat. Rev. 40 (2014) 1161–1170.
[10] K.H. Vousden, C. Prives, Blinded by the light: the growing complexity of p53, Cell 137 (2009) 413–431.
[11] K. Viktorsson, J. Ekedahl, M.C. Lindebro, R. Lewensohn, B. Zhivotovsky, S. Linder, M.C. Shoshan, Defective stress kinase and Bak activation in response to ionizing radiation but not cisplatin in a non-small cell lung carcinoma cell line, Exp. Cell Res. 289 (2003) 256–264.
[12] P.E. Czabotar, G. Lessene, A. Strasser, J.M. Adams, Control of apoptosis by the BCL-2 protein family: implications for physiology and therapy, Nat. Rev. Mol. Cell Biol. 15 (2014) 49–63.
[13] R.J. Youle, A. Strasser, The BCL-2 protein family: opposing activities that mediate cell death, Nat. Rev. Mol. Cell Biol. 9 (2008) 47–59.
[14] H.C. Chen, M. Kanai, A. Inoue-Yamauchi, H.C. Tu, Y. Huang, D. Ren, H. Kim, S. Takeda, D.E. Reyna, P.M. Chan, Y.T. Ganesan, C.P. Liao, E. Gavathiotis, J.J. Hsieh, E.H. Cheng, An interconnected hierarchical model of cell death regulation by the BCL-2 family, Nat. Cell Biol. 17 (2015) 1270–1281.
[15] I. Kamer, R. Sarig, Y. Zaltsman, H. Niv, G. Oberkovitz, L. Regev, G. Haimovich, Y. Lerenthal, R.C. Marcellus, A. Gross, Proapoptotic BID is an ATM effector in the DNA-damage response, Cell 122 (2005) 593–603.
[16] K. Nakano, K.H. Vousden, PUMA, a novel proapoptotic gene, is induced by p53, Mol. Cell 7 (2001) 683–694.
[17] E. Oda, R. Ohki, H. Murasawa, J. Nemoto, T. Shibue, T. Yamashita, T. Tokino, T. Taniguchi, N. Tanaka, Noxa, a BH3-only member of the Bcl-2 family and candidate mediator of p53-induced apoptosis, Science 288 (2000) 1053–1058.
[18] J. Yu, L. Zhang, P.M. Hwang, K.W. Kinzler, B. Vogelstein, PUMA induces the rapid apoptosis of colorectal cancer cells, Mol. Cell 7 (2001) 673–682.
[19] S.S. Zinkel, K.E. Hurov, C. Ong, F.M. Abtahi, A. Gross, S.J. Korsmeyer, A role for proapoptotic BID in the DNA-damage response, Cell 122 (2005) 579–591.
[20] W. Nakajima, M.A. Hicks, N. Tanaka, G.W. Krystal, H. Harada, Noxa determines localization and stability of MCL-1 and consequently ABT-737 sensitivity in small cell lung cancer, Cell Death Dis. 5 (2014) e1052.
[21] K. Kawauchi, K. Araki, K. Tobiume, N. Tanaka, p53 regulates glucose metabolism through an IKK-NF-kB pathway and inhibits cell transformation, Nat. Cell Biol. 10 (2008) 611–618.
[22] A.V. Miller, M.A. Hicks, W. Nakajima, A.C. Richardson, J.J. Windle, H. Harada, Paclitaxel-induced apoptosis is BAK-dependent, but BAX and BIM-independent in breast tumor, PLoS One 8 (2013) e60685.
[23] C. Sheridan, G. Brumatti, M. Elgendy, M. Brunet, S.J. Martin, An ERK-dependent pathway to Noxa expression regulates apoptosis by platinum-based chemotherapeutic drugs, Oncogene 29 (2010) 6428–6441.
[24] M.D. Hall, K.A. Telma, K.E. Chang, T.D. Lee, J.P. Madigan, J.R. Lloyd, I.S. Goldlust, J.D. Hoeschele, M.M. Gottesman, Say no to DMSO: dimethylsulfoxide inactivates cisplatin, carboplatin, and other platinum complexes, Cancer Res. 74 (2014) 3913–3922.
[25] V. Graupner, E. Alexander, T. Overkamp, O. Rothfuss, V. De Laurenzi, B.F. Gillissen, P.T. Daniel, K. Schulze-Osthoff, F. Essmann, Differential regulation of the proapoptotic multidomain protein Bak by p53 and p73 at the promoter level, Cell Death Differ. 18 (2011) 1130–1139.
[26] C.M. Goodwin, O.W. Rossanese, E.T. Olejniczak, S.W. Fesik, Myeloid cell leukemia-1 is an important apoptotic survival factor in triple-negative breast cancer, Cell Death Differ. 22 (2015) 2098–2106.
[27] H. Zhang, S. Guttikonda, L. Roberts, T. Uziel, D. Semizarov, S.W. Elmore,

J.D. Leverson, L.T. Lam, Mcl-1 is critical for survival in a subgroup of non-small-cell lung cancer cell lines, Oncogene 30 (2011) 1963–1968.
[28] C. Billard, BH3 mimetics: status of the field and new developments, Mol. Cancer Ther. 12 (2013) 1691–1700.
[29] M.S. Cragg, C. Harris, A. Strasser, C.L. Scott, Unleashing the power of inhibitors of oncogenic kinases through BH3 mimetics, Nat. Rev. Cancer 9 (2009) 321–326.
[30] R.M. Perciavalle, J.T. Opferman, Delving deeper: MCL-1's contributions to normal and cancer biology, Trends Cell. Biol. 23 (2013) 22–29.
[31] C. Ploner, R. Kofler, A. Villunger, Noxa: at the tip of the balance between life and death, Oncogene 27 (Suppl. 1) (2008) S84–S92.
[32] M. Hijikata, N. Kato, T. Sato, Y. Kagami, K. Shimotohno, Molecular cloning and characterization of a cDNA for a novel phorbol-12-myristate-13-acetate-responsive gene that is highly expressed in an adult T-cell leukemia cell line, J. Virol. 64 (1990) 4632–4639.
[33] P. De Feudis, D. Debernardis, P. Beccaglia, M. Valenti, E. Graniela Sire, D. Arzani, S. Stanzione, S. Parodi, M. D'Incalci, P. Russo, M. Broggini, DDP-induced cytotoxicity is not influenced by p53 in nine human ovarian cancer cell lines with different p53 status, Br. J. Cancer 76 (1997) 474–479.
[34] D. Wang, S.J. Lippard, Cellular processing of platinum anticancer drugs, Nat. Rev. Drug Discov. 4 (2005) 307–320.
[35] M. Stros, T. Ozaki, A. Bacikova, H. Kageyama, A. Nakagawara, HMGB1 and HMGB2 cell-specifically down-regulate the p53- and p73-dependent sequence-specific transactivation from the human Bax gene promoter, J. Biol. Chem. 277 (2002) 7157–7164.
[36] W. Nakajima, K. Sharma, M.A. Hicks, N. Le, R. Brown, G.W. Krystal, H. Harada, Combination with vorinostat overcomes ABT-263 (navitoclax) resistance of small cell lung cancer, Cancer Biol. Ther. 17 (2016) 27–35.

Ⅳ. 生体機能制御学部門

Department of Bioregulation

生体機能制御学部門
（大学院　生体機能制御学部門）

教授　南　　史朗

【研究概要】

生体の個体としての機能とその制御機構の解明をめざし、ホルモン・生理活性物質を対象として生理学的研究を行っている。ホルモンの分泌調節機構、ホルモンの作用機序、ホルモンの細胞内シグナル伝達機構を研究し、病態の解明をめざす。

Ⅰ．栄養状態と細胞内シグナリング（豊島由香、田口雄亮、時田玲子）

動物は、栄養状態に応答して物質代謝を変動し、恒常性を維持する巧妙な仕組みを持つ。体内の様々なホルモン分泌を変化させると共に、組織ごとに細胞内のシグナル伝達因子を変動させることで物質代謝を調節すると考えられる。私たちは、タンパク質・アミノ酸栄養状態に着目し、それによって変動するホルモン（インスリン、インスリン様成長因子、成長ホルモン、アディポネクチンなど）の分泌調節機構、およびこれらホルモンの細胞内シグナル伝達系を介した代謝調節機構の解明を目指している。

1）インスリンシグナル因子の変化がもたらす脂質代謝調節機構の解明

これまでに、低タンパク質栄養状態のラットの肝ではインスリンシグナリングが増強して中性脂肪含量が増加すること、インスリン作用の発揮に重要な IRS-2 および翻訳抑制因子 4E-BP1 の量が増加することを見出してきた。肝臓特異的に 4E-BP1 の発現を抑制したラットを作成して検討した結果、4E-BP1 が低タンパク質栄養状態による脂肪肝の生成に必須な因子であり、肝中性脂肪含量の調節に重要な役割を果たすことを明らかとした。

さらに、IRS-2 の病態生理的意義を明らかにする目的で、ゲノム編集技術の一つである CRISPR/Cas9 法により IRS-2 ノックアウトラットの作出を試み、成功した。

2）インスリンシグナルの増強による脂質合成酵素の変化

単離肝細胞を用いた検討により、低タンパク質栄養状態のラット肝ではインスリンシグナルの増強によって脂質合成酵素 *Acaca* 遺伝子の発現量が増加し、脂質合成亢進の一因と考えられた。

Ⅱ．成長ホルモンの新たな生理作用と作用機序（中田朋子、福島　誠、南　史朗）

成長ホルモン（GH）は雄ラットでは 3 時間ごとに分泌されるのに対し雌では不規則に分泌される。この分泌リズムの違いが様々な遺伝子発現の雌雄差を作っていることが知られているが、その機序や意義はよく解明されていない。私たちは、ラット GH 分泌の雌雄差をマーカーとして GH の新たな生理作用を検討してきた。

1）AKR1D1 はステロイド核の 4 位の二重結合を還元する酵素であり、ステロイドホルモンの代謝や胆汁酸の合成に働く。ラット肝の AKR1D1 の mRNA・タンパク量には雌雄差があり、GH 依存的に変動することを明らかにした。また、AKR1D1 と異物を認識する核受容体 CAR の mRNA 量に相関があることから、GH の肝におけるステロイド代謝調節機序の解明、および異物認識（解毒作用）機序の解明につながると期待される。

Ⅲ．メタボリック症候群の脂肪酸合成酵素 FAS の役割（八木　孝、矢野宏行、南　史朗）

糖尿病や脂肪肝などの代謝異常は、医学的・社会的に重大な問題である。私たちは、栄養状態の変化に対応する肝における糖・脂質代謝異常の機序を解明するために、国際医療センター分子代謝制御研究部（松本道宏博士）と共同研究を行い、脂肪合成酵素 FAS に焦点をあてて研究を進めてきた。

1）肥満・2 型糖尿病における肝 FAS の意義

内性脂肪酸合成（*de novo lipogenesis*：DNL）を触媒するリポジェニック酵素群の活性は食後２型糖尿病肝で亢進している。DNL の鍵となる脂肪酸合成酵素（FAS）は、グルコースからパルミチン酸を合成するリポジェニック酵素であり、その病態生理的意義は不明である。そこで、脂肪肝合併２型糖尿病モデルである ob/ob マウスの遺伝的背景を導入した肝特異的 FAS 欠損マウス (ob/ob LKO) を作製し、検討した。その結果、肥満・糖尿病肝における FAS の発現亢進は、DNL・糖新生・β 酸化・肝糖取り込みの制御を介して絶食－摂食サイクルにおける血糖値の変動、すなわち空腹時の血糖低下や摂食後の高血糖を軽減し、血糖の恒常性維持に寄与する可能性を提唱した。

2）非アルコール性脂肪肝炎（NASH）の病態における FAS の役割

炎症・線維化をきたした食餌誘導 NASH の病態における FAS の役割は明らかでない。そこで、ob/ob LKO を、トランス脂肪酸やフルクトースおよびコレステロールを多量に含む NASH 誘導食により飼育し、代謝表現型解析を行った。肝 FAS 欠損によって、通常食飼育では脂肪肝の著明な改善と肝機能障害の悪化を認めた。NASH 誘導食飼育では肝中性脂肪含量の軽度な低下と、肝機能障害の軽減、炎症関連遺伝子の発現低下や線維化の著明な抑制を認めた。FAS は NASH の病態形成の促進因子であり、その寄与は食餌内容によって異なると考えられた。

Ⅳ．性ステロイドの中枢作用（折笠千登世、勝又晴美）

性ステロイドは全身性に作用して、動物の生殖機能のみならず、生理機能を維持する役割を担っている。また、性ステロイドが周生期の脳に作用することによって性差を含む脳の機能的分化をもたらす。統合中枢である脳機能の分化および維持にどのように関与するのか、分子レベルで研究する。

1）ラットの養育行動の神経回路の解析

養育行動は、生存を脅かす様々な要因から仔をまもる行動であり、自然界ではもちろん、人工的に飼育する実験環境においても容易に認められる。本研究の目標は、養育行動関連の神経回路の特定を行い、その回路発現に関わる分子基盤を明らかにすることにある。養育行動の神経回路の組織化学的解析を行い、性的未経験雄の養育行動が単飼または群飼といった環境要因によって異なることを明らかにした（Orikasa et al. Physiol Behav 2015）。この行動を統御する遺伝子がメラニン凝集ホルモンであるか否か cfos 発現を指標にして検討した。

【研究業績】

〈原著〉

1. Orikasa C, Nagaoka K, Katsumata H, Sato M, Kondo Y, Minami S, Sakuma Y. Social isolation prompts maternal behavior in sexually naïve male ddN mice. Physiol Behav 151: 9-15, 2015

〈総説〉

〈学会発表〉

（国際学会）

1. Yuka Toyoshima, Reiko Tokita, Yusuke Taguchi, Fumiaki Yoshizawa, Shin-Ichiro Takahashi, Hisanori Kato, and Shiro Minami. Protein malnutrition increases the amount and phosphorylation of 4E-binding protein 1 (4E-BP1) to accumulate lipid in rat liver. 12th Asian Congress of Nutrition, May 2015, Yokohama

2. Taguchi Y, Toyoshima Y, Tokita R, Kato H, Takahashi S, Minami S. Insulin-induced acetyl-CoA carboxylase alpha is responsible for triglyceride accumulation in primary hepatocytes of low protein diet-fed rats. 12th Asian Congress of Nutrition, May 2015, Yokohama

（国内学会）

1. 八木　孝、酒井真志人、内田　亨、辻村－早川知子、山地大介、矢野宏行、満島　勝、長嶋洋治、南　史朗、春日雅人、松本道宏。肝臓特異的な脂肪酸合成酵素の欠損は ob/ob マウスの脂肪肝と耐糖能を改善するが随時高血糖を惹起する。第 52 回日本臨床分子医学会学術集会、2015 年 4 月、京都

2. 八木　孝、酒井真志人、辻村－早川知子、山地大介、矢野宏行、満島　勝、内田 亨、長嶋洋治、南　史朗、春日雅人、松本道宏。肝臓特異的な脂肪酸合成酵素の欠損は ob/ob マウスの脂肪肝と耐糖能を改善するが随時高血糖を惹起する。第 88 回日本内分泌学会学術総会、2015 年 4 月、東京

3. 八木　孝、酒井真志人、辻村－早川知子、山地大介、矢野宏行、満島　勝、内田　亨、長嶋洋治、南　史朗、春日雅人、松本道宏。肝臓特異的な脂肪酸合成酵素の欠損は ob/ob マウスの脂肪肝と耐糖能を改善するが随時高血糖を惹起する。第 58 回日本糖尿病学会年次学術集会、2015 年 4 月、下関

4. 村澤恒男、石川真由美、南　史朗。2 型糖尿病患者の alogliptin 無効例に対する sitagliptin 切り替え時の体重、推算 GFR を含めた有効性・安全性の検討。第 58 回日本糖尿病学会年次学術集会、2015 年 4 月、下関

5. 石川真由美、豊村順子、田口雄亮、中田朋子、豊島由香、南　史朗。成長ホルモンによる膵 β 細胞の小胞体ストレスの抑制。第 58 回日本糖尿病学会年次学術集会、2015 年 4 月　下関

6. Orikasa C, Nagaoka K, Katsumata H, Sato M, Kondo Y, Sakuma Y, Minami S. Social isolation prompts maternal behavior in sexually naïve male ddN mice. 第 42 回日本神経内分泌第 23 回日本行動神経内分泌合同学術集会、2015 年 9 月、仙台

7. 福永ヒトミ、望月留美、金子佳世、大槻昌子、八木　孝、石川真由美、南　史朗、立山尚子、米山剛一。妊娠糖尿病の反復例における患者の意識についての検討。第 31 回糖尿病・妊娠学会、2015 年 10 月、東京

8. 大槻昌子、八木　孝、南　史朗、石川真由美、金城忠志、田島廣之、山崎有人、笹野公伸。サブクリニカルクッシング症候群に合併した原発性アルドステロン症の 1 例。第 24 回内分泌臨床 Update、2015 年 11 月、大宮

9. 西　宏起、山中大介、亀井宏泰、森　友美、豊島由香、竹中麻子、潮　秀樹、千田和広、伯野史彦、高橋伸一郎．アミノ酸欠乏をシグナルとした肝臓特異的な脂質蓄積の新機構の解明．BMB2015（第 38 回日本分子生物学会年会／第 88 回日本生化学大会合同大会）、2015 年 12 月，神戸

10. 中田朋子、平野良隆、勝又晴美、時田玲子、南　史朗．成長ホルモンはラット肝臓において AKR1D1 の発現を抑制する。Growth hormone represses expression of AKR1D1 in the rat liver. 第 38 回日本分子生物学会年会　第 88 回日本生化学会大会　合同大会、2015 年 12 月、神戸

11. 八木　孝、酒井真志人、辻村－早川知子、矢野宏行、満島　勝、長嶋洋治、南　史朗、春日雅人、松本道宏。脂肪肝合併 2 型糖尿病の病態における肝臓の脂肪酸合成酵素の役割の解明。第 27 回分子糖尿病シンポジウム、2015 年 12 月、東京

12. 八木　孝、酒井真志人、辻村－早川知子、矢野宏行、満島　勝、飯田　智、長沼孝雄、高　峰英、長嶋洋二、南　史朗、春日雅人、松本道宏。肝臓特異的な脂肪酸合成酵素の欠損は食餌誘導性非アルコール性脂肪肝炎の進展を抑制する。第 19 回日本病態栄養学会年次学術集会、2016 年 1 月、横浜

Physiology & Behavior 151 (2015) 9–15

Contents lists available at ScienceDirect

Physiology & Behavior

journal homepage: www.elsevier.com/locate/phb

Social isolation prompts maternal behavior in sexually naïve male ddN mice

Chitose Orikasa [a,*], Kentaro Nagaoka [b], Harumi Katsumata [a], Manami Sato [c], Yasuhiko Kondo [c], Shiro Minami [a], Yasuo Sakuma [d]

[a] Institute for Advanced Medical Science, Nippon Medical School, Kanagawa 211-8533, Japan
[b] Department of Veterinary Medicine, Tokyo University of Agriculture and Technology, Tokyo 183-0054, Japan
[c] Department of Animal Sciences, Teikyo University of Science, Tokyo 120-0045, Japan
[d] University of Tokyo Health Science, Tokyo 206-0033, Japan

HIGHLIGHTS

- Social isolation in sexually naïve male mice promoted the onset of maternal behavior.
- Social isolation during either adolescence or young adulthood was effective.
- Partial isolation (exposure to conspecific signals) was not effective.

ARTICLE INFO

Article history:
Received 17 March 2015
Received in revised form 2 July 2015
Accepted 3 July 2015
Available online 10 July 2015

Keywords:
Maternal behavior
Social isolation
Chemosensory
ddN male mice
Puberty

ABSTRACT

Maternal behavior in mice is considered to be sexually dimorphic; that is, females show maternal care for their offspring, whereas this behavior is rarely shown in males. Here, we examined how social isolation affects the interaction of adult male mice with pups. Three weeks of isolation during puberty (5–8 weeks old) induced retrieving and crouching when exposed to pups, while males with 1 week isolation (7–8 weeks old) also showed such maternal care, but were less responsive to pups. We also examined the effect of isolation during young adulthood (8–11 weeks old), and found an induction of maternal behavior comparable to that in younger male mice. This effect was blocked by exposure to chemosensory and auditory social signals derived from males in an attached compartment separated by doubled opaque barriers. These results demonstrate that social isolation in both puberty and postpuberty facilitates male maternal behavior in sexually naïve mice. The results also indicate that airborne chemicals and/or sounds of male conspecifics, including ultrasonic vocalization and noise by their movement may be sufficient to interfere with the isolation effect on induction of maternal behavior in male mice.

1. Introduction

Maternal care is an indispensable aspect of mammalian reproduction, as offspring are fed by lactation. In rodents, parturient females build a nest as preparation for pups after delivery. After delivery, females immediately retrieve pups to the nest, licking around their anogenital area and crouching over them. In contrast, virgin females are less interested in pups and maternal care. However, such females may become maternal, provided they are exposed to pups for a few days (so-called priming) [1–3]. In contrast, maternal care is not spontaneous in most male rodents [3]. In laboratory mouse strains, sexually naïve males rarely show maternal behavior. When these males encounter pups, they sometimes engage in infanticide [4,5]. However, the experience of mating followed by cohabitation with gestating females has been reported to suppress infanticide and provoke males to show maternal behavior similar to lactating mothers [6,7]. This indicates that functional neural circuits regulating maternal-specific behaviors exist in the normal male mouse brain, but might not be activated in sexually naïve mice.

Social isolation exerts a variety of influences on a wide range of physiology and behaviors. In male mice, it induces inter-male aggression [8] and augmented emotionality [9]. In female mice, pubertal isolation disrupts sexual behavior despite the increased expression of estrogen receptors observed in the anteroventral periventricular nucleus and the ventromedial nucleus of the hypothalamus after pubertal isolation [10]. Social isolation can be a stressful event in mice and rats [11,12]. The effect of social stress during puberty can cause long-

* Corresponding author at: Institute for Advanced Medical Science, Nippon Medical School, Kosugi, Nakahara, Kanagawa 211-8533, Japan.
E-mail address: orikasa@nms.ac.jp (C. Orikasa).

http://dx.doi.org/10.1016/j.physbeh.2015.07.007
0031-9384/

lasting alterations in the brain and subsequently in adult behaviors. Therefore in this experiment, we examined the effect of social isolation starting at 5 weeks of age, when mice are just beginning to enter puberty. Interestingly, previous research has demonstrated that social isolation in adult mice can elevate play behavior [3] and parenting behavior in male mice [13]. Although typically 70–80% of adult male mice will attack a newborn pup [14], male mice showed decreased infanticide after isolation [13].

In this study, we examined whether lack of social signals during adolescence increases maternal behavior in sexually naïve male mice as well as during young adulthood. Pheromone signals may be involved in these physiological and behavioral responses [15–18]; therefore, we also examined the effect of modified social isolation that allowed male mice to smell and hear adjacent male conspecifics, but not to see or touch them.

2. Materials and methods

2.1. Animals

Two pairs of inbred strain ddN mice were purchased from the RIKEN Bio-Resource center (Wako, Japan) and bred in our laboratory. All male offspring were separated from female litter mates at weaning (21 days old) and kept in groups of three to five male siblings until the start of isolation. Mice were housed in 19 × 27 × 15 cm polypropylene cages with wood chip bedding. Throughout all experiments, mice were housed in our animal facility under controlled illumination (lights on from 6 a.m. to 8 p.m.), temperature (23 °C) and humidity (50.0 ± 10%). Food and water were given ad libitum.

2.2. Ethics statement

Experiments and animal housing adhered to the guidelines for the Care and Use of Laboratory Animals of Nippon Medical School, adopting NIH (National Institutes of Health) guidelines for the care and use of experimental animals. All procedures were approved by the Committee for Experimental Animal Ethics in Nippon Medical School.

2.3. Maternal behavior test

Each experimental male was placed in a clean cage with fresh bedding 2 days before testing. All behavioral tests were carried out during the day, 5–8 h after lights were turned on [19]. On each day of testing, cages containing experimental males were moved from shelves in the animal room to the observation setting, and acclimated there for 10 min. To test group-housed males' maternal behavior, each male was moved to a separate cage containing a mixture of fresh and soiled home-cage bedding 10 min before testing. We then followed a standard pup presentation paradigm [20] to obtain a measure of maternal behavior in virgin males. The observation began by placing three pups aged 4–7 days in the opposite corner farthest from the male or the corner occupied by the mouse's resting nest.

We recorded the distance between the males and the pups, and defined "close" as staying in close proximity (<1 cm) of pups and "far" as staying further away than 1 cm [21]. Maternal behavior was assessed over 10 min by recording retrieval (picking up a pup with its mouth and carrying it to the nest) and crouching (extending its limbs, assuming a nursing-like posture over the pups). Retrieval latencies, and time spent licking and crouching over the pups were recorded. In retrieval, the number of pups that they picked up was also recorded. For crouching, we recorded the number of pups they lay on top of.

We categorized males as "Maternal" when they displayed at least one of the above responses within 10 min, "Attack" if they attacked the pups (biting a pup, often accompanied by actual wounds on the pup), and "Ignore" when they showed no response to the pups. If a male appeared about to attack a pup, the pups were quickly removed and observation was terminated. Pups that had been attacked were not used in subsequent tests and experiments. Behavioral data of males that attacked pups were excluded from analysis of maternal behavior.

2.3.1. Experiment 1

Each male was assigned to one of three experimental groups during puberty. Mice were housed in isolation in two groups; one for 3 weeks beginning at age 5 weeks (P3I, n = 40), and one for 1 week beginning at age 7 weeks (P1I, n = 11). The third group (PG, n = 15) was continuously group-housed with siblings separated from female litter mates at weaning (Fig. 1). Each experimental group was made up of littermates. The sexually naïve P3I males at 5 weeks old and P1I males at 7 weeks old were displaced to cages and housed singly for 3 weeks or 1 week, respectively, prior to behavioral tests at 8 weeks of age. PG males remained in cages with siblings, and just before behavioral testing were displaced to cages alone for behavioral observation. All males were tested for maternal behavior at 8 weeks after the procedure described above.

2.3.2. Experiment 2

In Experiment 2, we examined the effect of modified social housing on the induction of maternal behavior by previous social isolation during adulthood. Sexually naïve male mice were assigned into three groups: isolation for 3 weeks (A3I: from 8 to 11 weeks old, n = 30), group-housing with barriers (A3G′: from 8 to 11 weeks old, n = 10)

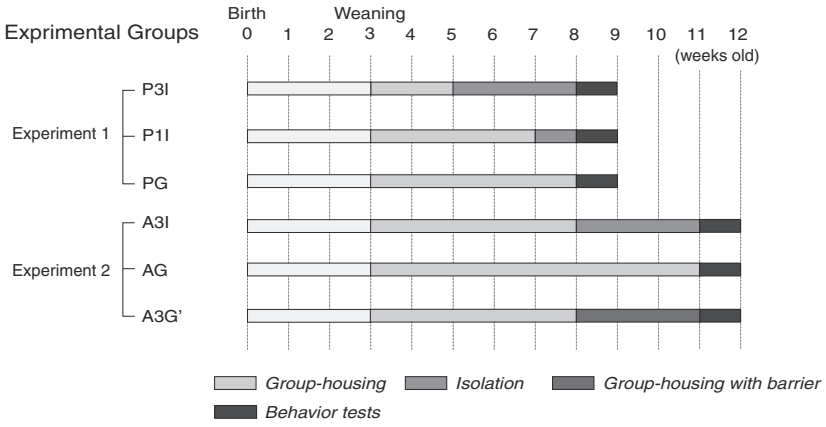

Fig. 1. Schematic representation of isolation and behavioral test schedules in each group.

or group-housing without barriers (AG: from 8 to 11 weeks old, n = 13) (see Fig. 1). In restrained social-housing (A3G′), a pair of litter mates was kept in the same cage (49 × 28.5 × 29 cm), but separated by a barrier made of two interstitial opaque acrylic boards containing six holes (2-cm diameter) at different levels. This barrier prevented physical, visual and involatile chemical interactions, but allowed airborne odors, audible and ultrasonic sounds (voice and noise) to pass through. The floors of both chambers were covered with wood chips, and food and water were freely available. Each pair was placed in this apparatus for 3 weeks (from 8 to 11 weeks old), which matched the isolation time of the A3I group. All mice were tested for maternal behaviors when they were 11 weeks old (Fig. 1).

2.4. Statistics

We used the Chi-squared test with Bonferroni post hoc tests to examine significant differences in incidences of the categories, maternal behaviors, and attacks toward pups. The duration of each behavior was analyzed by one-way analysis of variance (ANOVA), followed by Bonferroni post hoc tests to determine the significant differences among groups. The nonparametric Mann–Whitney U-test was applied for analysis of latencies, as a maximal latency (observation time) was allotted for mice that did not respond to the pups. All scoring was done blindly by two observers, and we checked for coherence between the parametric factors using Pearson's correlation (licking duration, $r = 0.908^{***}$; time spent close to pups, $r = 0.986^{***}$ of pubertal mice, $r = 0.994^{***}$ of young adults; crouching duration, $r = 0.993^{***}$ of pubertal mice, $r = 0.990$ of young adults), and the nonparametric using Spearman's correlation (latency to pup retrieval, $r = 0.996^{***}$ of one pup, $r = 0.964^{***}$ of three pups, $^{***}p < .001$).

3. Results

3.1. Experiment 1

Table 1 shows the number and percentage of males in each response category (see Materials and methods: Maternal behavior test). A significantly larger number of singly-housed male mice (P3I and P1I groups) displayed maternal behavior than PG mice did ($X^2 = 23.32$, df = 2, $p < .001$). Most group-housed males showed indifference toward pups. A significantly higher percentage of mice showed 'Ignore' in the PG group than in the P3I or P1I groups ($X^2 = 33.97$, df = 2, $p < .001$). No significant difference was found among groups in the number of attacked pups ($X^2 = 2.62$, df = 2, $p = .270$).

Isolated males from the P3I and P1I groups spent significantly more time in the vicinity of pups than did PG males ($F_{2,64} = 10.19$, $p < .001$, Bonferroni post hoc analysis, P3I: $p < .001$; P1I: $p < .05$) (Fig. 2).

Retrieval in each group was analyzed in terms of the number of retrieved pups: all pups, some pups, or no pups (Fig. 3A). Although the number of males that retrieved some pups was significantly higher in the P1I group than in the PG group ($X^2 = 10.75$, df = 2, $p < .05$), the number of males that retrieved all three pups was significantly higher in the P3I group than in the PG group ($X^2 = 13.28$, df = 2, $p < .05$). Additionally, latency of retrieval in P3I males was significantly shorter than that in PG males (Fig. 3B, one pup; all pups: $p < .05$). No significant difference in retrieval latency was observed between P1I and PG males (one pup: $p = .428$; all pups: $p = .643$), or between P3I and P1I males (one pup: $p = .215$; all pups: $p = .356$).

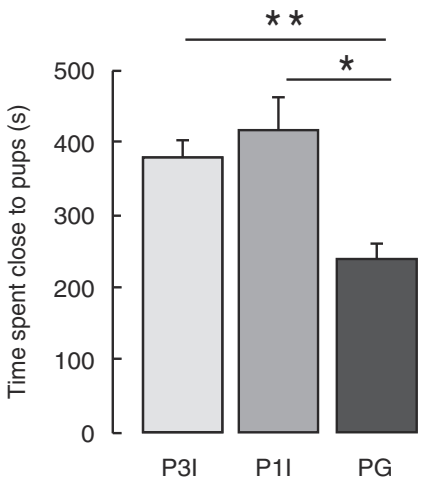

Fig. 2. Time spent being close to pups. Duration of time spent in close proximity (<1 cm) to pups was significantly longer in mice after social isolation for 3 weeks (P3I) or for 1 week (P1I) than in mice that were group-housed (PG). $^{**}p < .001$, $^{*}p < .05$, one-way ANOVA with Bonferroni post hoc analysis.

Fig. 4 shows data for time spent licking and crouching. While licking duration did not differ across groups (Fig. 4A: $F_{2,20} = 1.02$, $p = .38$), crouching duration was significantly longer in the P3I group than in the PG group (Fig. 4B: $F_{2,64} = 7.98$, $p < .05$, Bonferroni post hoc analysis, PG: $p < .05$). There was no significant difference in crouching duration between males in the P1I group compared with the other groups (Bonferroni post hoc analysis, P3I: $p = .356$; PG: $p = .380$). Crouching behavior in each group was analyzed in terms of the number of pups over which they crouched: all pups, some pups, or none (Fig. 4C). Although the number of males that crouched some pups was significantly higher in the P3I and P1I groups than in the PG group ($X^2 = 9.90$, df = 2, $p < .05$), the number of males that crouched all pups was significantly higher in the P3I group than in the PG group ($X^2 = 8.42$, df = 2, $p < .05$) (Fig. 4C).

3.2. Experiment 2

Table 1 includes the number and percentage of males in each response category for Experiment 2. Only A3I showed a significantly higher proportion of males displaying maternal behavior ($X^2 = 31.15$, df = 2, $p < .001$). The number of mice in the 'Ignore' category was higher in both the AG and A3G′ groups than in the A3I group ($X^2 = 22.90$, df = 2, $p < .001$), regardless of whether they were separated by a barrier. No significant difference was found among groups in the number of attacked pups ($X^2 = .73$, df = 2, $p = .70$).

Table 1
Number and percentage of males in each response category in Experiment 1 and Experiment 2.

Category	Experiment 1						Experiment 2					
	P3I (40)		P1I (11)		PG (15)		A3I (30)		AG (13)		A3G′ (10)	
	Number	%	Number	%	Number	%	Number	%	Number	%	Number	%
Maternal	27	67.5**	7	63.6**	0	0.0	22	73.3**	0	0.0	0	0.0
Ignored	7	17.5**	3	27.3**	15	100.0	5	16.7**	11	84.6	8	80.0
Attacked	6	15.0	1	9.1	0	0	3	10.0	2	15.4	2	20.0

Tests were interrupted when attacks occurred in order to avoid infanticide. Thus, males in the "Attack" category were excluded from further analyses. $^{**}p < .001$, Chi-square test with Bonferroni post hoc analysis, different from group-housed males.

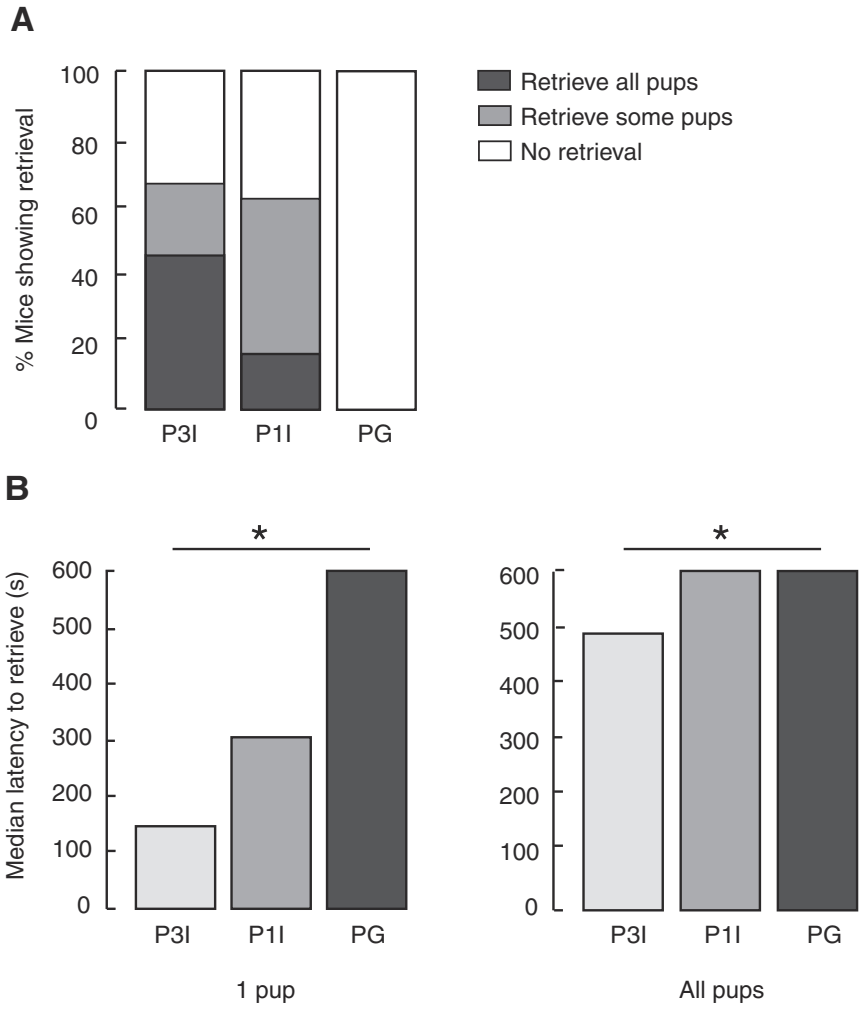

Fig. 3. Effect of social isolation on retrieving behavior. (A) Incidence of retrieval behavior in each group (carried all pups, some pups, or no pups). (B) Retrieval behavior was assessed by recording the latency to pup collection. Median times required to collect one pup (left panel), all pups (right panel) are shown for each group, $^{*}p < .05$, Mann–Whitney U-test.

Three week isolation after maturation also increased several male–pup interaction parameters. A3I males spent significantly more time in the vicinity of pups than did AG and A3G′ males ($F_{2,45} = 19.68$, $p < .001$, Bonferroni post hoc analysis, AG; A3G′: $p < .001$) (Fig. 5A). Approximately 73% of the A3I group retrieved pups, whereas few did so in the AG and A3G′ groups (Fig. 5B); this difference in incidence of retrieving all pups was significant (Fig. 5B: $X^2 = 17.57$, df = 2, $p < .001$). There was no significant difference between groups in incidence of retrieving some pups ($X^2 = 6.18$, df = 2, $p = .045$). Crouching duration for A3I males was also significantly longer than that for the AG or A3G′ groups (Fig. 6A: $F_{2,45} = 14.86$, $p < .001$, Bonferroni post hoc analysis, AG: $p < .001$; A3G′: $p < .05$), as was the number of all pups that they crouched over (Fig. 6B: $X^2 = 16.04$, df = 2, $p < .001$).

4. Discussion

The results of this study show that social isolation induced maternal behavior in male mice within 10 min, whereas group-housing did not. There is a large volume of literature demonstrating that social isolation usually results in various behavioral changes, such as depression-like behavior [22], enhanced aggressiveness [23], and higher levels of impulsivity [24]. It therefore seems paradoxical, at least outwardly, that social isolation enhances intermale aggression but reduces attacks on pups. These behaviors might be regulated by distinct neural circuits because of different biological signification in social behavior. One report found that social isolation during adolescence enhanced play and contact behaviors [25]. Our current results are also a case of isolation reinforcing sociality. Thus, the influence of social isolation may show a wide diversity depending on social context and behaviors examined.

Time spent with pups was significantly longer in mice that had been isolated for 3 weeks or for 1 week than in those that had been group housed. This resulted from the extended time they spent contacting and crouching over the pups. Three weeks of isolation also shortened the latency of pup retrieval, but did not affect time spent licking. This might be because the cues that trigger licking are different from those for other components of maternal behavior. First contact with pups and pup-licking have been suggested to be influenced by emotional arousal or anxiety in mice [26,27]. Thus, neural substrates underlying licking may be different from those underlying retrieval and crouching behavior. Although galanin neurons in the preoptic area (POA) have been reported to play an important role in male mouse maternal behavior, optogenetic activation of galanin neurons induced pup grooming but failed to increase crouching behavior in male mice [28].

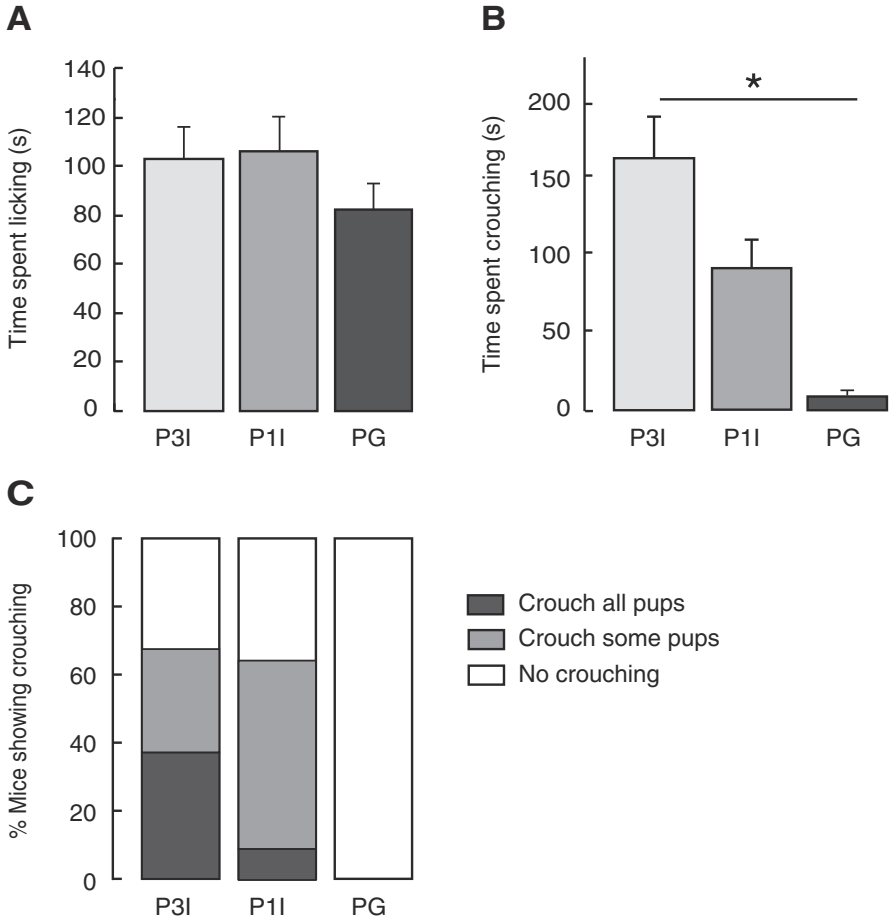

Fig. 4. Effect of social isolation on pup licking and crouching behavior. (A) Mean duration (s) that pups were licked in each group. Time spent licking pups was not significantly different across groups. (B) Mean duration (s) of crouching behavior (feeding posture) for each group. Males in the P3I group crouched longer than those in the PG group, $^{*}p < .05$, one-way ANOVA with Bonferroni post hoc analysis. (C) Incidence of crouching behavior in each group (over all pups, some pups, or no pups).

Although both P3I and P1I males were categorized as 'Maternal', the quality of maternal behavior was very different between them. A very high percentage of P3I males retrieved all pups and crouched over them, while most P1I males retrieved only one or two pups (Fig. 4). Thus, it seems that 3 weeks of isolation can induce robust maternal behavior, while 1 week of isolation is effective at slightly increasing

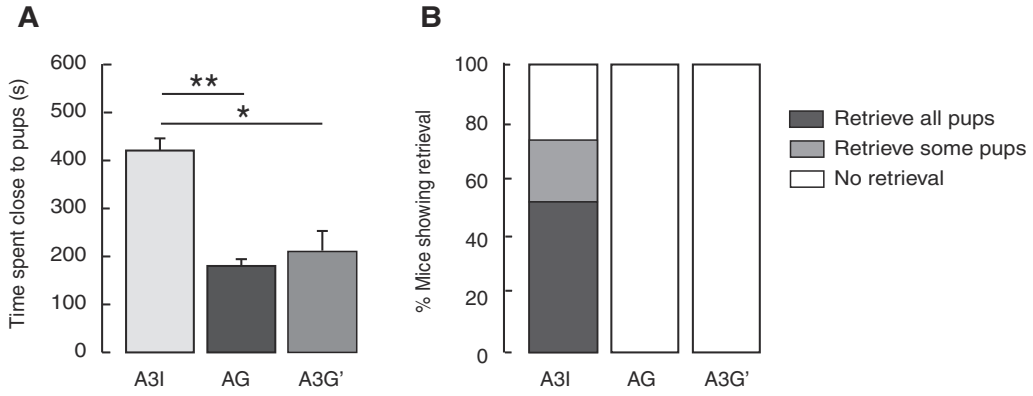

Fig. 5. Effects of social isolation after maturation on maternal behavior in male mice. (A) Mean duration (s) of time spent in the vicinity of pups was significantly longer in male mice after social isolation for 3 weeks (A3I) than group-housing males with barriers (A3G′) or without barriers (AG). $^{**}p < .001$, one-way ANOVA with Bonferroni post hoc analysis. (B) Incidence of retrieval behavior in each group (carried all pups, some pups, or no pups).

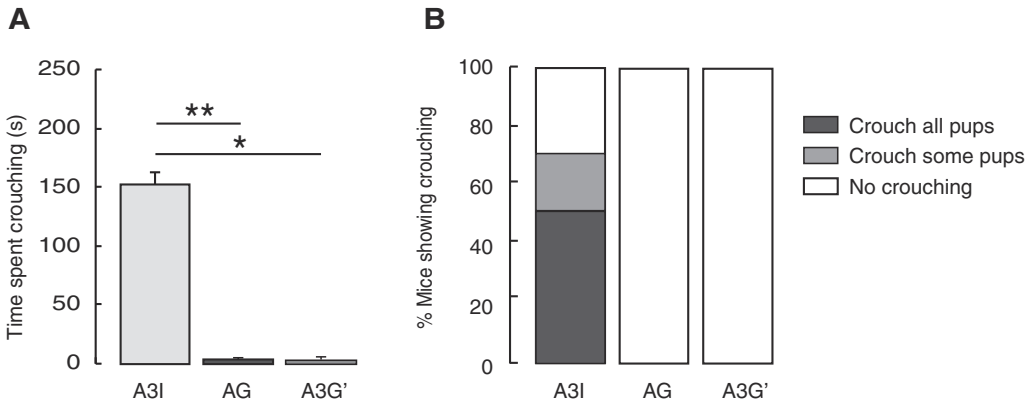

Fig. 6. Effect of social isolation after maturation on crouching behavior. (A) Crouching duration (s). A3I males spent more time crouching over pups than did group-housed male mice with or without barriers. $^{**}p < .001$, $^{*}p < .05$, one-way ANOVA with Bonferroni post hoc analysis. (B) Incidence of crouching behavior in each group (over all pups, some pups, or no pups).

maternal behavior but not to a sufficient level. We also examined the effect of isolation at different developmental stages, demonstrating that social isolation was not only effective in puberty (5–8 weeks old), but also post-puberty (8–11 weeks old). Therefore, the effect of social isolation on maternal care does not depend on hormonal conditions specific to puberty, but rather depends on neural and/or humoral conditions produced by the isolation. However, Ghiraldi and Svare [13] reported that long isolation from weaning to adult age failed to suppress attack of pups. Presumably, isolation for too long during development may disrupt socialization instead of inducing maternal behavior.

In non-monogamous rodents, maternal behavior is generally female specific (i.e. sexually dimorphic). In most strains of laboratory mice, males show indifference or attacking in response to pups [14]. Indeed, sexually naïve male laboratory mice rarely show maternal care, and sometimes commit infanticide [6]. Perinatal sex steroids masculinize the mouse brain, resulting in suppression of maternal behavior and facilitation of pup attack [29]. Sex steroids during the critical period of brain sex differentiation may produce inhibitory substrates for maternal behavior in male mice. However, a system that activates an inactive system of maternal behavior in the male mouse brain could be 'turned off' by social isolation, like a sensitization to pups for male rats [30,31].

What is the factor that activates maternal behavior in the male mouse brain through social isolation? In this study, we examined the effect of restricted social stimuli (A3G′) on maternal behavior, i.e., cohabiters were separated by double opaque barriers that prevented direct contact and visual cues but were permeable to airborne chemical and auditory signals. In most mammalian species, chemosensory signals derived from conspecifics may be the most important social stimulus. A lack of these chemosensory signals could hence be responsible for the isolation effect.

In male mice, copulation and subsequent cohabitation with a pregnant female lead to a transition in behavior from attacking (infanticide) to parenting [6,7]. The current study demonstrates that not only cohabitation but social isolation can cause male mice to be maternal. Currently, we do not have enough data to reveal whether these phenomena share the same neural substrates. It is noteworthy that the brain regions activated by pup exposure [6] are also activated during infanticide [7,32]. This might imply that the same or overlapped neural mechanisms underlie maternal responsiveness that appears after different social experiences. Future investigation into these drastic effects of social experience will be important to fully understand the neural circuitry controlling maternal behaviors.

Disclosure statement

The authors have nothing to disclose.

Acknowledgments

This work was founded by Grants-in-Aid for scientific research from the Ministry of Education, Science, Sports and Culture of Japan (C.O. 20590238).

References

[1] J.S. Lonstein, G.J. De Vries, Sex differences in the parental behavior of rodents, Neurosci. Biobehav. Rev. 24 (2000) 669–686.
[2] D.S. Stolzenberg, J.S. Stevens, E.F. Rissman, Experience-facilitated improvements in pup retrieval; evidence for an epigenetic effect, Horm. Behav. 62 (2012) 128–135.
[3] E. Noirot, The onset and development of maternal behavior in rats, hamsters and mice, in: D.S. Lehrman, R.A. Hinde, E. Shaw (Eds.), Advances in the Study of Behavior, Vol 4, Academic Press, New York 1972, pp. 107–145.
[4] E.D. Ketterson, V. Nolan, Hormones and life histories: an integrative approach, Am. Nat. 140 (Suppl. 1) (1992) S33–S62.
[5] J.A. Mennella, H. Moltz, Infanticide in rats: male strategy and female counter-strategy, Physiol. Behav. 42 (1988) 19–28.
[6] K.S. Tachikawa, Y. Yoshihara, K.O. Kuroda, Behavioral transition from attack to parenting in male mice: a crucial role of the vomeronasal system, J. Neurosci. 33 (2013) 5120–5126.
[7] L.C. Peters, M.B. Kristal, The suppression of infanticide in mother rats, J. Comp. Psychol. 97 (1983) 167–177.
[8] P. Corridi, F. Chiarotti, S. Bigi, E. Alleva, Familiarity with conspecific odor and isolation-induced aggressive behavior in male mice (*Mus domesticus*), J. Comp. Psychol. 107 (1993) 328–335.
[9] A.C. Matte, Growth hormone and isolation-induced aggression in wild male mice, Pharmacol. Biochem. Behav. 14 (Suppl 1) (1981) 85–87.
[10] J. Kercmar, S.A. Tobet, G. Majdic, Social isolation during puberty affects female sexual behavior in mice, Front. Behav. Neurosci. 66 (2014) 667–673.
[11] A.K. Dixon, The social behaviour of mice and its sensory control, in: H.J. Hedrich, G. Bullock (Eds.), The Laboratory Mouse: London, Elsevier Academic press, San Diego 2004, pp. 27–300.
[12] B. Buwalda, M. Geerdink, J. Vidal, J.M. Koolhaas, Social behavior and social stress in adolescence: a focus on animal models, Neurosci. Biobehav. Rev. 35 (2011) 1713–1721.
[13] L.L. Ghiraldi, B. Svare, Postpubertal isolation decreases infanticide and elevates parental care in C57BL/6J male mice, Physiol. Behav. 36 (1986) 59–62.
[14] J.S. Schneider, M.K. Stone, K.E. Wynne-Edwards, T.H. Horton, J. Lydon, B. O'Malley, J.E. Levine, Progesterone receptors mediate male aggression toward infants, Proc. Natl. Acad. Sci. U. S. A. 100 (2003) 2951–2956.
[15] P. Karlson, M. Luscher, 'Pheromones': a new term for a class of biologically active substances, Nature 183 (1959) 55–56.
[16] D.C. Blanchard, R.L. Spencer, S.M. Weiss, R.J. Blanchard, B. McEwen, R.R. Sakai, Visible burrow system as a model of chronic social stress: behavioral and neuroendocrine correlates, Psychoneuroendocrinology 20 (1995) 117–134.
[17] K.C. Fone, M.V. Porkess, Behavioural and neurochemical effects of post-weaning social isolation in rodents—relevance to developmental neuropsychiatric disorders, Neurosci. Biobehav. Rev. 32 (2008) 1087–1102.
[18] P.A. Brennan, F. Zufall, Pheromonal communication in vertebrates, Nature 444 (2006) 308–315.
[19] M.E. Timonin, K.E. Wynne-Edwards, Aromatase inhibition during adolescence reduces adult sexual and paternal behavior in the biparental dwarf hamster *Phodopus campbelli*, Horm. Behav. 54 (2008) 748–757.
[20] S. Okabe, M. Nagasawa, T. Kihara, M. Kato, T. Harada, N. Koshida, K. Mogi, T. Kikusui, The effects of social experience and gonadal hormones on retrieving behavior of

mice and their responses to pup ultrasonic vocalizations, Zoolog. Sci. 27 (2010) 790–795.
[21] M. Chauke, J.L. Malisch, C. Robinson, T.R. de Jong, W. Saltzman, Effects of reproductive status on behavioral and endocrine responses to acute stress in a biparental rodent, the California mouse (*Peromyscus californicus*), Horm. Behav. 60 (2011) 128–138.
[22] L.M. O'Keefe, S.J. Doran, L. Mwilambwe-Tshilobo, L.H. Conti, V.R. Venna, L.D. McCullough, Social isolation after stroke leads to depressive-like behavior and decreased BDNF levels in mice, Behav. Brain Res. 260 (2014) 162–170.
[23] A. Takeda, H. Tamano, F. Kan, T. Hanajima, K. Yamada, N. Oku, Enhancement of social isolation-induced aggressive behavior of young mice by zinc deficiency, Life Sci. 82 (2008) 909–914.
[24] H. Koike, D. Ibi, H. Mizoguchi, T. Nagai, A. Nitta, K. Takuma, T. Nabeshima, Y. Yoneda, K. Yamada, Behavioral abnormality and pharmacologic response in social isolation-reared mice, Behav. Brain Res. 202 (2009) 114–121.
[25] E.I. Varlinskaya, L.P. Spear, N.E. Spear, Social behavior and social motivation in adolescent rats: role of housing conditions and partner's activity, Physiol. Behav. 67 (1999) 475–482.
[26] C. Caldji, J. Diorio, M.J. Meaney, Variations in maternal care in infancy regulate the development of stress reactivity, Biol. Psychiatry 48 (2000) 1164–1174.
[27] D.D. Francis, K. Szegda, G. Campbell, W.D. Martin, T.R. Insel, Epigenetic sources of behavioral differences in mice, Nat. Neurosci. 6 (2003) 445–446.
[28] Z. Wu, A.E. Autry, J.F. Bergan, M. Watabe-Uchida, C.G. Dulac, Galanin neurons in the medial preoptic area govern parental behaviour, Nature 509 (2014) 325–332.
[29] M. Keller, J.L. Pawluski, O. Brock, Q. Douhard, J. Bakker, The alpha-fetoprotein knock-out mouse model suggests that parental behavior is sexually differentiated under the influence of prenatal estradiol, Horm. Behav. 57 (2010) 434–440.
[30] J.S. Lonstein, P.S. Quadros, C.K. Wagner, Effects of neonatal RU486 on adult sexual, parental, and fearful behaviors in rats, Behav. Neurosci. 115 (2001) 58–70.
[31] M. Numan, Hypothalamic neural circuits regulating maternal responsiveness toward infants, Behav. Cogn. Neurosci. Rev. 5 (2006) 163–190.
[32] D. Lin, M.P. Boyle, P. Dollar, H. Lee, E.S. Lein, P. Perona, D.J. Anderson, Functional identification of an aggression locus in the mouse hypothalamus, Nature 470 (2011) 221–226.

武蔵小杉地区動物実験室

運営委員会委員長　南　　史朗

【運営概要】

武蔵小杉地区動物実験室は、日本医科大学の共同利用研究設備として先端医学研究所と武蔵小杉病院が中心となって管理運営を行っている。

1．動物実験委員会の開催
日時：平成 27 年 4 月 1 日　午後 2 時 30 分より　場所：職員食堂　出席者数：12 名

2．動物実験講習会（教育訓練）の開催
日時：平成 27 年 4 月 30 日　午後 3 時より　場所：C 館 1 階会議室　出席者数：32 名

3．動物実験計画書の申請課題数　36 件

4．感染実験や発がん実験等の注意を要する実験の件数　10 件

5．年間延べ入室者数　4,261 名

6．日平均飼育数　　マウス　738 匹、ラット　164 匹

7．年間使用動物数　マウス　3,607 匹、ラット　513 匹

8．SPF 微生物モニタリングの実施
平成 27 年 4 月 20 日、平成 27 年 10 月 5 日

9．定期清掃の実施
SPF 飼育室　　平成 27 年 11 月 10－11 日、平成 28 年 3 月 29－30 日
マウス飼育室　平成 28 年 3 月 23－24 日
ラット飼育室　平成 28 年 3 月 22 日
小動物実験室　平成 28 年 3 月 2 日

10. 実験動物慰霊祭への参加
日時：平成 27 年 10 月 16 日午後 5 時より　場所：医学部教育棟講堂　出席者数：15 名

平成 27(2015)年度　先端医学研究所公開セミナー

（平成 27 年 4 月～平成 28 年 3 月）

4 月 30 日

アフリカツメガエルを用いた血管の形態形成機構の解析

藤原　正和（病態解析学部門）

血管は太い大動脈から細い毛細血管まで様々な大きさのものが存在する。また、分岐頻度や微細構造も様々で、血管は形態学的に極めて多様であることが分かっている。しかし、この多様な血管の形態がどのように形成されるのか、そのメカニズムについてはほとんど明らかになっていない。そこで、透明な体を持ち、血管の観察が容易に行えるアフリカツメガエルのオタマジャクシを用い、生体内の血管がいつ・どこで多様な形態を獲得するのかを解析し、血管の形態を制御するメカニズムを明らかにすることを目的とした。今回は、これまで用いてきた microangiography による血管の形態変化の解析結果や、現在作製中のトランスジェニックカエル Tg(Xl Flk-1:mCherry)についての経過報告を行いたい。

5 月 28 日

分子状水素は脂質のフリーラジカル連鎖反応に介入してシグナル伝達と遺伝子発現を制御する

井内　勝哉（細胞生物学部門）

新しい概念の抗酸化物質である水素（H_2）は、炎症が関与する様々な生活習慣病に対して効果を示すことから、H_2 の抗炎症作用の分子機構が注目されている。しかし、H_2 の抗炎症作用の正確な分子機構は明らかになっておらず、H_2 が最初に反応または結合する標的は未知である。そこで本研究では、炎症の引き金になる脂質過酸化に着目し、酸化ストレスによる過酸化脂質の生成や活性に対する H_2 の影響を調べた。その結果、酸化ストレスによる脂質過酸化が低濃度の H_2 によって調節されることが分かった。さらに、この過酸化脂質の調節を介して、H_2 は炎症性シグナルや遺伝子発現を制御することが分かった。

6 月 25 日

肺癌分子標的薬 crizotinib はオートファジーを誘導する

鈴木　淳也（遺伝子制御学部門）

オートファジーは飢餓などで誘導されオルガネラを分解しリサイクルすることで生存の為に働いている。いくつかの抗癌剤がアポトーシスとオートファジーを同時に誘導し、オートファジー阻害によりアポトーシスが増強して治療効果が上がることが現在数多く研究されている。一方で、オートファジーが細胞死を引き起こす事が報告されているが、反論も多くまだ実態は分かっていない。我々は肺がん治療薬の Crizotinib が、アポトーシスを全く誘導せずにオートファジーによって強力に細胞死を誘導する事、オートファジー阻害剤を併用してもアポトーシスが起こらない事を見出し、その機構を解析している。この解析から、オートファジー細胞死の実態解明が期待できる。

7月30日

翻訳抑制因子 4E－BP1 は肝臓で中性脂肪量を調節する

豊島　由香（生体機能制御学部門）

我々は、低タンパク質栄養状態の肝臓で、翻訳抑制因子 4E-BP1 の量が増加すると共に、中性脂肪量が増加することを見出してきた。一般的に、4E－BP1 は様々な組織においてタンパク質合成を調節することが知られているが、脂質代謝を調節しているかは不明であった。そこで、低タンパク質栄養状態の肝臓で起こる 4E－BP1 量の増加と中性脂肪量の増加に因果関係があるか明らかにするために、肝臓特異的に 4E－BP1 の発現を抑制させたラットを作出した。今回、このラットモデルを用いた解析で、肝臓において 4E－BP1 が中性脂肪量を調節することを明らかにしたので報告する。

9月24日

血管の多様な形態とその形成メカニズムについての研究

藤原　正和（病態解析学部門）

体の隅々まで張り巡らされた血管は、太さ･分岐頻度･有窓構造など、非常に多様な形態を持つ。しかし、これらの多様な形態がどのように構築されるのか、そのメカニズムについてはほとんど分かっていない。我々はヒト正常組織では観察することが困難な血管の形成過程を透明な体を持つアフリカツメガエルのオタマジャクシを用いて観察し、生体内の血管がいつ・どこで形態学的な多様性を獲得するのかを経時的に解析する実験系を開発した。今回は、これまでの microangiography の解析結果、作製中のトランスジェニックカエル Tg（Xl Flk-1:mCherry）、その他の計画などについて報告を行いたい。

10月29日

Applying Raman spectroscopy to biomedical studies

Liang-da Chiu　特任助教（東京大学　大学院理学系研究科　化学専攻　分析化学研究室）

Raman spectroscopy is an optical method that probes the molecular vibrations of a sample by detecting the energy shift of the scattered light from the incident light. It has a strong potential in biomedical research because of its non-destructive and label-free characteristics, which enables it to real-time analyse the chemical composition of a living specimen. In my talk, I will introduce my recent works on the Raman spectroscopic study of stem cell differentiation and bone formation. In the end, I will also quickly show how other research hospitals around the world are using Raman spectroscopy in medical practices, and how Raman spectroscopy can help the further progress in medical research and diagnosis.

11月26日

感音難聴の根治を目指して

～ウイルス感染時に内耳はどう応答するか、その分子メカニズムの解明～

林　裕史　講師（帝京大学）

突発性難聴、メニエール病、先天性難聴などウイルス感染の関与が示唆される内耳性難聴の存在は知られているものの、その病態はいまだ明らかではなく、ゆえに決定的な治療法は存在しない。内耳は血液脳関門の存在から、脳、網膜、精巣、毛根、胎盤などと同様、免疫特権部位と呼ばれる強い免疫抑制環境にあるとされてきた臓器であるが、我々はこれまでの研究において有毛細胞周囲に存在する支持細胞群のうち、ヘンゼン細胞・クラウディウス細胞が、ウイルス感染時にウイルスの genome RNA を認識

する細胞内受容体である retinoic acid-inducible gene-I(RIG-I)like receptor(RLR)family のシグナル伝達経路を介して type Ⅰ interferon(IFN)を発現することを示し、支持細胞が蝸牛における免疫担当細胞であることを見出している。本セミナーでは最新の知見も含めて内耳のウイルス感染応答について御紹介したい。

1月28日

成長ホルモン(GH)によって減少するタンパクの解析

中田　朋子（生体機能制御学部門）

GH の新たな生理機能を追跡する目的で次のような実験を行った。新生児期にグルタミン酸ナトリウム(MSG)を投与することによって下垂体の GH を枯渇させたラットを用いて GH の補充投与の効果を観察した。ラットの肝臓から抽出したタンパクを SDS 電気泳動後 CBB 染色したところ、MSG ラットで増加し、GH 投与で減少するタンパクを検出した。このタンパクは下垂体摘除手術によって増加した。このタンパクについて解析したので報告する。

2月25日

細胞はどのように力を感じているか？
ーメカノバイオロジーとメカノセラピーー

小川　令　大学院教授（形成再建再生医学分野）

メカノバイオロジーは、張力やせん断応力、静水圧や浸透圧といった物理的刺激が、生体にどのような影響を与えるかを解析する研究領域である。臨床医学の領域においては、常に物理的刺激が加わっている筋や骨格を扱う整形外科、心拍動、血圧や血流を扱う血液循環器内科などでは比較的なじみのある研究分野であるが、その他の領域ではまだ一般的ではない。われわれは、皮膚や軟部組織の形成過程また創傷の治癒過程においても細胞は常に物理的刺激を感受しながら遺伝子発現を調節していることを解明してきた。この物理的刺激の生体への作用機序を理解することによって、疾患の原因解明、創傷治癒の促進、再生医療、またがん治療などに応用できる可能性を考え、種々のメカノセラピーを臨床で実践している。今後の医工・医薬連携の必要性について報告する。

3月31日

アフリカツメガエルをモデルとした血管形成のイメージング解析

藤原　正和（病態解析学部門）

透明な体を持つアフリカツメガエルのオタマジャクシは発生や変態の過程で生じる様々な血管の形態変化を容易に観察できる優れた実験動物である。今回は Flk-1 プロモーター・エンハンサーによって蛍光タンパク質の発現が制御されたトランスジェニックカエル Tg(Xl Flk-1:TurboFP-C)を作製したのでそれについて報告をする。作製した F_0 個体は TurboFP-C を尾や頭部の血管で限定的に発現した。今後は血管の形態変化を長時間解析するために、全ての血管において TurboFP-C を発現する F_2 個体を作製し、血管の形態形成メカニズムを細胞レベルで解析し、触覚、後肢、尾などの特徴的な形態を持つ血管の形態機構を明らかにしていきたい。

平成27年度(2015)研究補助金、助成金受け入れ

細胞生物学部門

(1) 日本学術振興会科学研究費補助金　基盤研究（B）
「健康増進と疾病に寄与する分子状水素の多様な機能を発揮するメカニズムの解明」
太田　成男

(2) 日本学術振興会科学研究費助成事業（学術研究助成基金助成金）基盤研究（C）
「水素分子の糖尿病改善効果と遺伝子発現誘導における作用機序の解明」
上村　尚美

(3) 日本学術振興会科学研究費助成事業（学術研究助成基金助成金）基盤研究（C）
「水素分子による酸化ストレス防御機構と脳内レドックス動態の解析」
西槙貴代美

(4) 日本学術振興会科学研究費助成事業（学術研究助成基金助成金）若手研究（B）
「ミトコンドリア生体分子の化学修飾に着目した水素の抗炎症作用メカニズムの解明」
井内　勝哉

(5) 日本学術振興会科学研究費助成事業（学術研究助成基金助成金）若手研究（B）
「エピジェネティクス制御からみた水素の抗炎症作用のメカニズム」
Lee　Hyunjin

(6) 日本医療研究開発機構　難治性疾患実用化研究事業（分担）
「ミトコンドリア脳筋症 MELAS 脳卒中様発作に対するタウリン療法の開発」
太田　成男

(7) 日本学術振興会科学研究費助成事業（学術研究助成基金助成金）基盤研究（C）（分担）
「グルココルチコイドは高強度運動による海馬での神経新生の増加を引き起こす要因か否か」
太田　成男

(8) 日本学術振興会科学研究費助成事業（学術研究助成基金助成金）基盤研究（C）（分担）
「脂肪肝炎～肝発癌の病期に応じた最適な酸化ストレス介入療法の開発」
太田　成男

遺伝子制御学部門

(1) 私立大学等経常費補助金特別補助「戦略的研究基盤支援」
「Clinical Rebiopsy Bank Project を基盤とした包括的がん治療開発拠点形」（代表：弦間昭彦）
田中　信之

生体機能制御学部門

(1) 日本学術振興会科学研究費助成事業（学術研究助成基金助成金）・若手研究（B）
「低タンパク質栄養によるアディポネクチン増加機構の解明とその生理的意義」

鈴木（豊島）由香

(2) 文科省「オーダーメイド医療の実現プログラム（第３期)」

南　　史朗

先端医学研究所・教職員，研究者等氏名

平成 28 年 3 月 31 日現在

Ⅰ. 病態解析学部門

助　　教	藤原　正和
テクニカル・スタッフ	枝川　聖子
大学院研究生	村賀香名子
形成外科・講師	土佐眞美子
救命救急センター・助教	原　　義明
形成外科・助教	桑原　大彰
横浜中央看護専門学校・非常勤講師	清水　　一

Ⅱ. 細胞生物学部門

大学院教授	太田　成男
客員教授	鈴木　吉彦
准 教 授	上村　尚美
講　　師	Wolf Alexander Martin
助　　教	井内　勝哉
非常勤講師	森　　隆
マネジメントサポート・スタッフ	西槙貴代美
アシスタント・スタッフ	一宮　治美
ポスト・ドクター	李　　炫溱
大学院研究生	上家　明美
大学院研究生	中島　裕也
秘　　書	加藤　寸賀
実験補助	武田真由美
皮膚科・教授	船坂　陽子
スポーツ科学・准教授	三上　俊夫
形成外科・助教	渡邉　真泉
北里大学・助教	井本　明美
研 修 生	小田　文乃（皮膚科）

Ⅲ. 遺伝子制御学部門

大学院教授	田中　信之
講　　師	中嶋　　亘
助　　教	阿部　芳憲
助　　教	上原　郁野
助　　教	谷村　篤子
非常勤講師	川内　敬子

テクニカル・スタッフ	浅野　由ミ
ポスト・ドクター	清水　幹容
ポスト・ドクター	岩渕　千里
大学院生	松本　　優
大学院生	鈴木　淳也
実験補助	河越　美保
実験補助	高寺　俊美
帝京大学・講師	林　　裕史（帝京大学・講師）
研 修 生	中里　　茜（東京医科歯科大･大学院生）

Ⅳ．生体機能制御学部門

大学院教授	南　　史朗
准 教 授	折笠千登世
講　　師	豊島　由香
助　　教	中田　朋子
マネジメントサポート・スタッフ	勝又　晴美
テクニカル・スタッフ	時田　玲子
ポスト・ドクター	福島　　誠
ポスト・ドクター	田口　雄亮
大学院生	八木　　孝
大学院生	矢野　宏行
大学院研究生	大場るり子
パート事務員	大木佳菜子
内科・講師	石川真由美
東京大学・特任助教	鈴木　信周

Ⅴ．分子生物学部門

マネジメントサポート・スタッフ	横田　　隆
テクニカル・スタッフ	梶田　満子

Ⅵ．ゲノム医学部門

Ⅶ．アイソトープ実験室

室　　長	田中　信之
放射線取扱主任者	上原　郁野

Ⅷ. 組換え DNA 実験施設

安全主任者	中田　朋子

Ⅹ. 動物実験室

実験動物飼育員	金井祐美子
実験動物飼育員	田口　憲明

Ⅸ. 事務室

事務室長	里見　裕右
主　　任	小川　泰子
パート事務員	鈴木　弓子
パート事務員	山田　深雪

先端医学研究所紀要　第1巻

平成28年9月30日印刷
平成28年10月 1 日発行（非売品）
発 行　　日本医科大学
　　先端医学研究所　紀要委員会
〒211－8533　神奈川県川崎市中原区小杉町1－396
　　TEL （044）733－1821
　　FAX （044）733－1877

印刷所　栄和印刷株式会社